

# Computing the Intrinsic Delaunay Triangulation of a Closed Polyhedral Surface

Loïc Dubois  

Notre Dame, USA<sup>1</sup>

## 1 Abstract

Every surface that is intrinsically polyhedral can be represented by a portalgon: a collection of polygons in the Euclidean plane with some pairs of equally long edges abstractly identified. While this representation is arguably simpler than meshes (flat polygons in  $\mathbb{R}^3$  forming a surface), it has unbounded *happiness*: a shortest path in the surface may visit the same polygon arbitrarily many times. This pathological behavior is an obstacle towards efficient algorithms. On the other hand, Löffler, Ophelders, Staals, and Silveira [SoCG 2023] recently proved that the (intrinsic) Delaunay triangulations have bounded happiness.

In this paper, given a closed polyhedral surface  $S$ , represented by a triangular portalgon  $T$ , we provide an algorithm to compute the Delaunay triangulation of  $S$  whose vertices are the singularities of  $S$  (the points whose surrounding angle is distinct from  $2\pi$ ). The time complexity of our algorithm is polynomial in the number of triangles and in the logarithm of the aspect ratio  $r$  of  $T$ . Within our model of computation, we show that the dependency in  $\log r$  is unavoidable. Our algorithm can be used to pre-process a triangular portalgon before computing shortest paths on its surface, and to determine whether the surfaces of two triangular portalgons are isometric.

**2012 ACM Subject Classification** Theory of computation → Computational geometry

**Keywords and phrases** Polyhedral surface, intrinsic Delaunay triangulation, algorithmic complexity

## 1 Introduction

In one of its simplest forms a *triangulation* is a finite collection of disjoint triangles in the Euclidean plane, together with a partial matching of the sides of the triangles such that any two matched sides have the same length (Figure 1). This simple representation appears under different names in the literature (intrinsic triangulation [29, 30], portalgon [22]). Cutting out the triangles from the plane and identifying the matched sides isometrically, respecting the orientations of the triangles, provides a (compact, orientable) *polyhedral* surface. This surface is *closed* if, in addition, it is connected and without boundary.

In this paper we consider the *Delaunay* triangulation of a closed polyhedral surface whose vertex set consists of the singularities (the points surrounded by an angle distinct from  $2\pi$ ) of the surface (except for flat tori, see below). It is generically unique. Our main contribution is an algorithm to compute it from any triangulation of the surface, whose time complexity is polynomial in the number of triangles and in the logarithm of the aspect ratio of the input triangulation. Our second contribution is a lower bound showing that the dependency in the logarithm of the aspect ratio is unavoidable in our model of computation.

Before describing our contributions in more detail, we discuss related works.

### 1.1 Related works

Polyhedral surfaces can also be obtained from *meshes*, flat triangles in  $\mathbb{R}^3$  glued along their edges. Moreover, every mesh defines a triangulation of its surface. Yet triangulations are

<sup>1</sup> This work was done while the author was working at LIGM, CNRS, Univ Gustave Eiffel, F-77454 Marne-la-Vallée, France.



© Loïc Dubois;

licensed under Creative Commons License CC-BY 4.0

42nd International Symposium on Computational Geometry (SoCG 2026).

Editors: Hee-Kap Ahn, Michael Hoffmann, and Amir Nayyeri; Article No. XX; pp. XX:1–XX:45

Leibniz International Proceedings in Informatics



LIPIC Schloss Dagstuhl – Leibniz-Zentrum für Informatik, Dagstuhl Publishing, Germany



35 more general than meshes: most triangulations cannot be obtained from a mesh. Some recent  
 36 algorithms advantageously operate on triangulations of polyhedral surfaces without reference  
 37 to a mesh [28, 34, 19]. In this context the adjective “intrinsic” is sometimes placed before  
 38 the name “triangulation” to make the distinction with the particular triangulations arising  
 39 from a mesh. In the mathematical community, a prominent example is that of a translation  
 40 surface [23, 35, 16, 14], which arises naturally in the study of billiards in rational polygons.

41 Triangulations are so general that not all of them are suitable for computation, compared  
 42 to meshes. Prominently, a fundamental problem on polyhedral surfaces is to compute the  
 43 distance or a report a shortest path between two points. On a mesh, shortest paths can  
 44 be computed in time polynomial in the number of triangles. For example, an algorithm of  
 45 Mitchell, Mount, and Papadimitriou [25] propagates waves along the surface, starting from  
 46 the source, in a discrete manner. See also Chen and Han [5]. On a generic triangulation  
 47 however (not arising from a mesh), the number of times a shortest path visits a triangle is  
 48 not bounded by any function of the number of triangles, as noted for example almost 20  
 49 years ago by Erickson [10]. Recently, Löffler, Ophelders, Staals, and Silveira [22] coined the  
 50 term *happiness* of a triangulation, for the maximum number of times a shortest path visits a  
 51 triangle. They adapted the single-source shortest paths algorithm of Mitchell, Mount, and  
 52 Papadimitriou [25] from meshes to triangulations, whose time complexity now depends on  
 53 the happiness of the triangulation (it is more efficient on triangulations of *low* happiness).

54 This raises the problem of replacing any given triangulation by another triangulation of the  
 55 same surface whose happiness is “low”. Among the many remeshing algorithms [15, 31, 27, 32],  
 56 only few have been ported to the general context of intrinsic triangulations [29], and the only  
 57 solution we are aware of that compares to our main result (Theorem 1 below), by Löffler,  
 58 Ophelders, Staals, and Silveira [22, Section 5], is restricted to particular inputs whose surfaces  
 59 are all homeomorphic to an annulus; we will use it as a black box. Importantly, the same  
 60 authors also showed that Delaunay triangulations have bounded happiness [22, Section 4.2].

61 Delaunay triangulations are classical objects of computational geometry [6, 13, 2], closely  
 62 related to shortest paths. While mostly known in the plane, they generalize to closed  
 63 polyhedral surfaces, see for example the depiction of Bobenko and Springborn [4]. To  
 64 compute a Delaunay triangulation from an arbitrary intrinsic triangulation there are, to our  
 65 knowledge, only two approaches, and neither compares to our main result (Theorem 1). One  
 66 approach computes a Voronoi diagram with a suitably adapted multiple-source shortest path  
 67 algorithm, and then derives from it a Delaunay tessellation, see for example Mount [26], Liu,  
 68 Chen, and Tang [20], and Liu, Xu, Fan, and He [21]. Another approach starts from an initial  
 69 triangulation and flips its edges until it reaches a Delaunay triangulation; it was proved to  
 70 terminate by Indermitte, Liebling, Troyanov, and Cléménçon [4, 17].

## 71 1.2 Our results

72 In order to state our results precisely, it now matters to make the distinction between a  
 73 triangulation and the data structure representing it, and to allow for more general polygons  
 74 than triangles. Following Löffler, Ophelders, Staals, and Silveira [22], we call *portalgon* the  
 75 collection  $T$  of polygons in the Euclidean plane and the partial matching of their sides. We  
 76 denote by  $\mathcal{S}(T)$  the associated polyhedral surface. We say that the portalgon  $T$  is *triangular*  
 77 if all polygons are triangles. The sides of the polygons, once identified, constitute a graph  $T^1$   
 78 embedded on  $\mathcal{S}(T)$  (the polygons themselves correspond to the faces of  $T^1$ ): it is this graph  
 79  $T^1$  that we call *triangulation* if  $T$  is triangular, and we call  $T^1$  a *tessellation* in general.

82 We consider, on a closed polyhedral surface  $S$ , the unique Delaunay tessellation  $\mathcal{D}$  of  $S$   
 83 whose vertices are exactly the singularities of  $S$ , with a single very special exception: if  $S$  has

no singularity, then  $S$  is a flat torus and we let  $\mathcal{D}$  be any of the Delaunay tessellations of  $S$  that have exactly one vertex, for one can be mapped to the other via an orientation-preserving isometry of  $S$  anyway. In any case, we say that  $\mathcal{D}$  is *the* Delaunay tessellation of  $S$ , in a slight abuse.<sup>2</sup> It is “generically” a triangulation, but not always. If not, then triangulating the faces of  $\mathcal{D}$  along any vertex-to-vertex arcs provides a Delaunay triangulation. The *aspect ratio* of a triangular portalgon  $T$  is the maximum side length of a triangle of  $T$  divided by the smallest height of a triangle of  $T$  (possibly another triangle). Our main contribution is:

► **Theorem 1.** *Let  $T$  be a portalgon of  $n$  triangles, of aspect ratio  $r$ , whose surface  $\mathcal{S}(T)$  is closed. One can compute the portalgon of the Delaunay tessellation of  $\mathcal{S}(T)$  in  $O(n^3 \log^2(n) \cdot \log^4(r))$  time.*

As already mentioned, the only two methods we are aware of for computing a Delaunay tessellation from an arbitrary triangulation are the flip algorithm and the computation of the dual Voronoi diagram. The time complexities of these algorithms are not bounded by any polynomial in  $n$  and  $\log(r)$ .

Applications of Theorem 1 are provided in Appendix K. Briefly, on the portalgon returned by Theorem 1, shortest paths can be computed in  $O(n^2 \log^{O(1)} n)$  time. And Theorem 1 enables to test whether the surfaces of two given portalgons are isometric, simply by computing and comparing the portalgons of the associated Delaunay tessellations.

We analyze our algorithms within the real RAM model of computation described by Erickson, van der Hoog, and Miltzow [12]. It is an extension of the standard integer word RAM, with an additional memory array storing reals, and with additional instructions. On such a machine, we represent each polygon of a portalgon  $T$  by the list of its vertices, and each vertex is by its two coordinates, stored in the memory array dedicated to reals. So displacing (translating or rotating) the polygons in the plane provides different representations of  $T$ . When modifying a portalgon  $T$ , we actually modify our representation of  $T$ , using elementary operations that are easily seen to be achievable by a real RAM.

Within this model of computation, our second contribution is a lower bound that backs our main result, Theorem 1, by showing that the polynomial dependency in the logarithm of the aspect ratio is unavoidable:

► **Theorem 2.** *Let  $c \in (0, 1)$ . There are a flat torus  $S$ , and for every  $x \in (1, \infty)$ , a representation of a portalgon  $T_x$ , with two triangles, whose aspect ratio is  $O(x^2)$ , whose surface is  $S$ , that satisfy the following. There is no real RAM algorithm computing a representation of the portalgon of the Delaunay tessellation of  $S$  from  $T_x$  in  $O((\log x)^c)$  time.*

Altogether Theorem 1 and Theorem 2 show that, within our model of computation, the complexity of computing the Delaunay tessellation from an arbitrary triangulation of a (closed, orientable) polyhedral surface is polynomial in the number of triangles and in the logarithm of the aspect ratio of the input triangulation.

### 1.3 Overview of the proof of Theorem 1

The proof of Theorem 2 is deferred to Appendix H. The rest of the paper is dedicated to the proof of Theorem 1, of which we now provide an overview.

We introduce a slight variation of happiness, more suitable to our needs, which we call *segment-happiness*. To prove Theorem 1, the crux of the matter is to replace the input

<sup>2</sup> Given a set  $V$  of points of the surface, finite, non-empty, and containing all the singularities, our results easily extend to Delaunay triangulations whose vertex set is  $V$ , but this is incidental to us.

## XX:4 Computing the Intrinsic Delaunay Triangulation of a Closed Polyhedral Surface

126 triangular portalgon by another triangular portalgon of the same surface, whose segment-  
127 happiness is “low”. For this purpose, our approach is to first focus on portalgons  $T$  whose  
128 surface  $\mathcal{S}(T)$  is *flat*: the interior of  $\mathcal{S}(T)$  has no singularity. Note that here we allow  $\mathcal{S}(T)$  to  
129 have boundary, and this boundary may have singularities. The *systole* of  $\mathcal{S}(T)$  is the smallest  
130 length of a non-contractible geodesic closed curve in  $\mathcal{S}(T)$ . Our key technical result is:

131 ► **Proposition 3.** *Let  $T$  be a portalgon of  $n$  triangles, whose sides are all smaller than  $L > 0$ .  
132 Assume that  $\mathcal{S}(T)$  is flat. Let  $s > 0$  be smaller than the systole of  $\mathcal{S}(T)$ . One can compute in  
133  $O(n \log^2(n) \cdot \log^2(2 + L/s))$  time a portalgon of  $O(n \cdot \log(2 + L/s))$  triangles, whose surface  
134 is isometric to that of  $T$ , and whose segment-happiness is  $O(\log(n) \cdot \log^2(2 + L/s))$ .*

135 Sections 3–5 are devoted to the proof of Proposition 3. In Section 3 we focus on particular  
136 portalgons, whose surfaces are all homeomorphic to an annulus; the definitions and results of  
137 this section are used by the algorithm of Proposition 3. In Section 4 we describe the algorithm  
138 for Proposition 3. It is a finely tuned combination of elementary operations such as inserting  
139 and deleting edges and vertices in graphs. While the algorithm itself is relatively simple, its  
140 analysis is more involved, and is sketched in Section 5. In this section, we first provide a  
141 combinatorial analysis, and then we prepare for the geometric analysis by introducing a new  
142 parameter on the simple geodesic paths  $e$  of a flat surface, *enclosure*, possibly of independent  
143 interest. Informally,  $e$  is enclosed when a short non-contractible loop can be attached to a  
144 point of  $e$  not too close to the endpoints of  $e$ . We then use enclosure to analyze the algorithm  
145 from a geometric point of view, proving Proposition 3.

146 In Appendix G we extend Proposition 3 from flat surfaces to surfaces having singularities  
147 in their interior, essentially by cutting out caps around these singularities. To get a cleaner  
148 result, we also replace  $2 + L/s$  by the aspect ratio of  $T$ , and we replace segment-happiness  
149 by happiness, obtaining:

150 ► **Proposition 4.** *Let  $T$  be a portalgon of  $n$  triangles, of aspect ratio  $r$ . One can compute in  
151  $O(n \log^2(n) \cdot \log^2(r))$  time a portalgon of  $O(n \cdot \log(r))$  triangles, whose surface is  $\mathcal{S}(T)$ , and  
152 whose happiness is  $O(n \log(n) \cdot \log^2(r))$ .*

153 We have not discussed Delaunay tessellations yet. Still, we are almost ready to prove  
154 Theorem 1. Indeed, once we have a portalgon of low happiness, we can compute shortest  
155 paths on the surface. And, as already mentioned, shortest path algorithms classically extend  
156 to construct Voronoi diagrams and then Delaunay tessellations. Formally:

157 ► **Proposition 5.** *Let  $T$  be a portalgon of  $n$  triangles, of happiness  $h$ , such that  $\mathcal{S}(T)$  is closed.  
158 One can compute the portalgon of the Delaunay tessellation of  $\mathcal{S}(T)$  in  $O(n^2 h \log(nh))$  time.*

159 We could not find a statement equivalent to Proposition 5 in the literature, so we provide  
160 a proof in Appendix J for completeness. We insist that the proof of Proposition 5 is incidental  
161 to us, and Proposition 5 is not surprising at all. Our contribution is really the proof of  
162 Proposition 4. Theorem 1 is immediate from Proposition 4 and Proposition 5:

163 **Proof of Theorem 1.** Proposition 4 computes in  $O(n \log^2(n) \cdot \log^2(r))$  time a portalgon  $T'$  of  
164  $O(n \cdot \log(r))$  triangles, whose happiness is  $O(n \log(n) \cdot \log^2(r))$ . Proposition 5 then computes  
165 the portalgon of the Delaunay tessellation from  $T'$  in  $O(n^3 \log^2(n) \cdot \log^4(r))$  time. ◀

## 166 2 Preliminaries

167 We use without review standard notions of graph theory and low dimensional topology and  
168 geometry, referring to textbooks for details [7, 1, 33, 8]. We only mention that on a surface

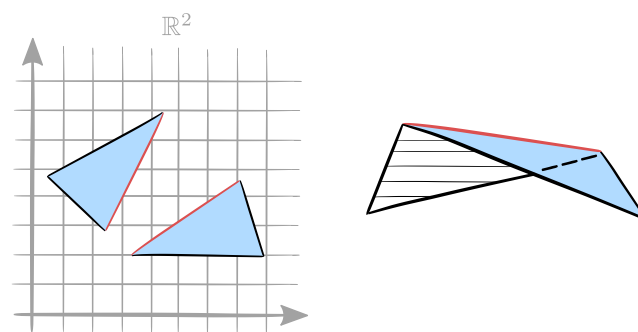
169  $S$ , a path  $p : [0, 1] \rightarrow S$  is **simple** if its restriction to the interval  $(0, 1)$  is injective, in which  
 170 case the image of  $(0, 1)$  by  $p$  is the **relative interior** of  $p$ . We denote by  $\ell(p)$  the length of a  
 171 geodesic path  $p$ . Throughout the paper, logarithms are in base two.

172 The definition of Delaunay tessellation given by Bobenko and Springborn [4, Section 2] is  
 173 not used in the core of the paper, but only in Appendix J for proving Proposition 5. We  
 174 collect details on this definition in Appendix I for completeness.

## 175 2.1 Portalgons, tessellations, and polyhedral surfaces

176 A **portalgon**  $T$  is a disjoint collection of oriented polygons in the Euclidean plane, together  
 177 with a partial matching of the sides of the polygons such that any two matched sides have the  
 178 same length. It is **triangular** if all polygons are triangles. See Figure 1. Any subset of the  
 179 polygons defines a **sub-portalgon**  $T'$  of  $T$ : two sides of polygons are matched in  $T'$  if and  
 180 only if they are matched in  $T$ . In a portalgon  $T$ , identifying the matched sides, isometrically,  
 181 and respecting the orientations of the polygons, provides **the surface of  $T$** , denoted  $\mathcal{S}(T)$ ;  
 182 it is a 2-dimensional Riemannian manifold whose metric may have singularities. The sides of  
 183 the polygons of  $T$  correspond to a graph  $T^1$  embedded on  $\mathcal{S}(T)$ , the **1-skeleton** of  $T$ .

184 A **polyhedral surface** is any Riemannian manifold  $S$  (possibly with singularities)  
 185 isometric to the surface of a portalgon. And when we say that a portalgon  $T$  is a **portalgon**  
 186 **of  $S$** , we implicitly fix an isometry between  $\mathcal{S}(T)$  and  $S$ . A **tessellation** of  $S$  is any 1-skeleton  
 187 of a portalgon of  $S$ , it is a **triangulation** if the portalgon is triangular.



188 ■ **Figure 1** (Left) A triangular portalgon  $T$ : two triangles in the Euclidean plane, with two sides  
 189 matched in red. (Right) The surface  $\mathcal{S}(T)$ , and the 1-skeleton  $T^1$ .

190 Consider a polyhedral surface  $S$ , a triangulation  $T^1$  of  $S$ , a vertex  $x$  of  $T^1$ , and the sum  $a$   
 191 of the angles of faces of  $T^1$  around  $x$ . The point  $x$  is a **singularity** if  $x$  lies in the boundary  
 192 of  $S$  and  $a \neq \pi$ , or if  $x$  lies in the interior of  $S$  and  $a \neq 2\pi$ . Every other point of  $S$  is **flat**.  
 193 This does not depend on any particular triangulation of  $S$ . A surface  $S$  is **flat** if its interior  
 194 has no singularity (although its boundary may have singularities). The closed flat surfaces  
 195 are called **flat tori**.

## 196 2.2 Aspect ratio, systole, happiness, and segment-happiness

197 The **aspect ratio** of a triangular portalgon  $T$  is the maximum side length of a triangle of  $T$   
 198 divided by the smallest height of a triangle of  $T$  (possibly another triangle). Note that the  
 199 aspect ratio is always greater than or equal to  $2/\sqrt{3} > 1$ , because the maximum side length  
 200 of a triangle is always greater than or equal to  $2/\sqrt{3}$  times its smallest height.

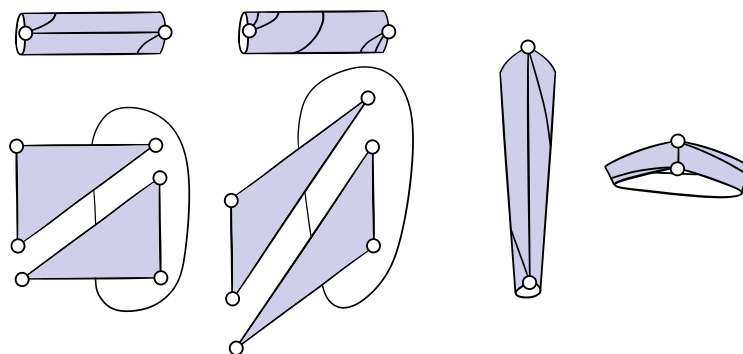
201 The **systole** of a polyhedral surface  $S$  is the smallest length of a non-contractible geodesic  
 202 closed curve in  $S$ , except in the particular case where every closed curve in  $S$  is contractible,

203 in which case the systole is  $\infty$ . The important thing is that for every positive real  $s$  smaller  
 204 than the systole of  $S$ , any non-contractible closed curve in  $S$  is longer than  $s$ .

205 The **happiness** of a portalgon  $T$  is the maximum number of times a shortest path in  
 206  $\mathcal{S}(T)$  visits the image of a polygon of  $T$ , maximized over all the shortest paths of  $\mathcal{S}(T)$  and all  
 207 the polygons of  $T$  (see [22, Section 3]). We introduce a variation, more suitable to our needs.  
 208 In a polyhedral surface  $S$ , a **segment** is a simple geodesic path  $e$  whose relative interior  
 209 is disjoint from any singularity of  $S$ . The **segment-happiness** of  $e$  in  $S$ , denoted  $h_S(e)$ ,  
 210 is the maximum number of intersections between  $e$  and a shortest path of  $S$ , maximized  
 211 over all the shortest paths of  $S$ . The **segment-happiness** of a portalgon  $T$  is then the  
 212 maximum segment-happiness  $h_{\mathcal{S}(T)}(e)$ , maximized over the edges  $e$  of its 1-skeleton  $T^1$ . A  
 213 priori, the segment-happiness of a portalgon  $T$  differs from the happiness of  $T$ . Indeed a  
 214 path in  $\mathcal{S}(T)$  may visit many times a face of  $T^1$  without intersecting any edge of  $T^1$  more  
 215 than once, if the face has high degree. However, if  $T$  is triangular, then the happiness and  
 216 the segment-happiness of  $T$  do not differ by more than a constant factor.

217 **3 Tubes and bifaces**

218 In this section we focus on particular triangular portalgons. See Figure 2. A **tube** is a  
 219 triangular portalgon  $X$  whose surface  $\mathcal{S}(X)$  is homeomorphic to an annulus and has no  
 220 singularity in its interior, and whose 1-skeleton  $X^1$  has exactly one vertex on each boundary  
 221 component of  $\mathcal{S}(X)$ . Among tubes, a **biface** is a portalgon  $B$  of two triangles whose respective  
 222 sides  $s_0, s_1, s_2$  and  $s'_0, s'_1, s'_2$ , in order (clockwise say), are such that  $s_0$  is matched with  $s'_0$   
 223 and  $s_1$  is matched with  $s'_1$ . Its 1-skeleton  $B^1$  has four edges: two loop edges forming the  
 224 two boundary components of  $\mathcal{S}(B)$ , which we call **boundary edges**, and two edges whose  
 225 relative interiors are included in the interior of  $\mathcal{S}(B)$ , which we call **interior edges**.



226 **Figure 2** (From left to right) A good biface, a biface not good, a thin biface, a thick biface.

227 We say that a biface  $B$  is **good** if the two interior edges  $e$  and  $f$  of  $B^1$  satisfy both of the  
 228 following up to possibly exchanging  $e$  and  $f$ . First,  $e$  is a shortest path in  $\mathcal{S}(B)$ . Second, cut  
 229  $\mathcal{S}(B)$  along  $e$ , and consider the resulting quadrilateral. If this quadrilateral has two diagonals  
 230 then  $f$  is shortest among the two diagonals. We will distinguish good bifaces. A good biface  
 231  $B$  is **thin** if every interior edge of  $B^1$  is longer than every boundary edge of  $B^1$ . Otherwise  
 232  $B$  is **thick**. While tubes and bifaces have unbounded happiness, good bifaces on the other  
 233 hand satisfy the following (Appendix A):

234 **► Lemma 6.** *Given a good biface  $B$ , let  $e$  be an interior edge of  $B^1$ . Then  $h_{\mathcal{S}(B)}(e) \leq 6$ .*

235 We will use the elementary operation of replacing a tube by a good biface (Appendix A):

236 ► **Proposition 7.** *Let  $X$  be a tube with  $n$  triangles, whose sides are smaller than  $L > 0$ . Let*  
 237  *$s > 0$  be smaller than the systole of  $\mathcal{S}(X)$ . One can compute a good biface whose surface is*  
 238  *$\mathcal{S}(X)$  in  $O(n \log n \cdot \log(2 + L/s))$  time.*

239 Proposition 7 is similar to a result described by Löffler, Ophelders, Silveira, and Staals [22,  
 240 Theorem 45], building upon a ray shooting algorithm of Erickson and Nayyeri [11].

## 241 4 Description of the algorithm

242 In this section we describe our algorithm for Proposition 3. We first describe the elementary  
 243 operations and the data structure, before giving the algorithm itself. Along the way, we  
 244 provide informal explanations of our choices. We do not prove anything, as the analysis of  
 245 the algorithm is deferred to Section 5.

### 246 4.1 Inserting vertices and edges

247 Informally, our goal is to “improve the geometry” of a triangular portalgon  $T$ . We will  
 248 make this precise in Section 5. Roughly, the issue is that, without any condition on  $T$ , the  
 249 edges of  $T^1$  that lie in the interior of  $\mathcal{S}(T)$  can be arbitrarily long, so one of them may  
 250 intersect some shortest path arbitrarily many times by wrapping around the surface, and so  
 251 the segment-happiness of  $T$  can be arbitrarily large. A naive way of shortening an edge is to  
 252 cut the edge in two at its middle point.

253 **InsertVertices.** Given a triangular portalgon  $T$ , consider every edge  $e$  of  $T^1$  that lies in  
 254 the interior of  $\mathcal{S}(T)$ , and insert the middle point of  $e$  as a vertex in  $T^1$ .

255 Appendix B details how to modify the portalgon  $T$  to perform **InsertVertices**. Applying  
 256 **InsertVertices** to a *triangular* portalgon  $T$  produces a portalgon  $T'$  whose polygons are  
 257 usually not triangles. We now consider transforming  $T'$  into a triangular portalgon. To do  
 258 that we repeatedly cut the polygons of  $T'$ . We need a definition. In the plane consider a  
 259 polygon  $P$ , two vertices  $u \neq v$  of  $P$ , and the rectilinear segment  $a$  between  $u$  and  $v$ . If the  
 260 relative interior of  $a$  is included in the interior of  $P$  then  $a$  is called a vertex-to-vertex arc  
 261 of  $P$ . It is easily seen that if  $P$  is not a triangle then  $P$  has at least one vertex-to-vertex  
 262 arc. Among the vertex-to-vertex arcs of  $P$ , the shortest ones are the **shortcuts** of  $P$ . We  
 263 emphasize that we consider the shortest ones among all the vertex-to-vertex arcs, without  
 264 fixing the endpoints, but the endpoints are chosen among the vertices of  $P$ . In a portalgon  
 265  $T$  every polygon  $P$  corresponds to a face  $F$  of  $T^1$ , and every shortcut of  $P$  corresponds to a  
 266 path whose relative interior is included in  $F$ : we say of this path that it is a shortcut of  $F$ .

267 **InsertEdges.** Given a portalgon  $T$ , as long as there is a face of  $T^1$  that is not a triangle,  
 268 insert a shortcut of this face as an edge in  $T^1$ .

269 Appendix B details how to modify the portalgon  $T$  to perform **InsertEdges**. We shall  
 270 apply **InsertVertices** followed by **InsertEdges** to a triangular portalgon  $T$  in order to  
 271 produce another triangular portalgon  $T'$ , hopefully with a “nicer geometry”. The problem  
 272 is now that  $T'^1$  has more vertices than  $T^1$ . All the other operations of the algorithm are  
 273 devoted to keeping the number of vertices low.

274 **4.2 Deleting vertices**

275 From now on it is important that every surface considered is flat, there is no singularity  
 276 in its interior. Given a triangular portalgon  $T$ , assuming that the surface  $\mathcal{S}(T)$  is flat, we  
 277 consider decreasing the number of vertices of  $T^1$ . To do that we naturally consider deleting  
 278 some vertices. Not all vertices can be deleted. For example a vertex incident to a loop edge  
 279 cannot be deleted. Also we will not delete vertices that lie on the boundary of the surface  
 280  $\mathcal{S}(T)$ . A vertex of  $T^1$  is **weak** if it lies in the interior of  $\mathcal{S}(T)$  and is not incident to any loop  
 281 edge in  $T^1$ . It is **strong** otherwise.

282 **DeleteVertices.** Given a triangular portalgon  $T$  whose surface  $\mathcal{S}(T)$  is flat, construct a  
 283 maximal independent set  $V$  of weak vertices of  $T^1$  that have degree smaller than or equal to  
 284 six. For every vertex  $v \in V$  delete  $v$  and its incident edges from  $T^1$ .

285 Appendix B details how to modify the portalgon  $T$  to perform **DeleteVertices**. Afterward  
 286 the polygons of  $T$  are usually not triangles anymore, but this will be solved by applying  
 287 **InsertEdges** after each application of **DeleteVertices**. Observe that in **DeleteVertices**  
 288 we delete only vertices of degree smaller than or equal to six. Informally, the reason is that  
 289 deleting a weak vertex of degree  $d \geq 3$  creates a face of degree  $d$  around it. We then insert  
 290  $d - 3$  edges in this face when applying **InsertEdges**. The problem is that only a constant  
 291 number of edges can be inserted in each face without risking to destroy our improvements on  
 292 the geometry of the tessellation. This is why we make sure that  $d = O(1)$  beforehand. The  
 293 exact bound on  $d$  is not really important (although changing it would change some constants  
 294 of the algorithm), but it must be at least six so that we can still remove a fraction of the  
 295 excess vertices this way, at least when most of them are strong. Similar ideas can be found  
 296 in the literature, see for example Kirkpatrick [18, Lemma 3.2].

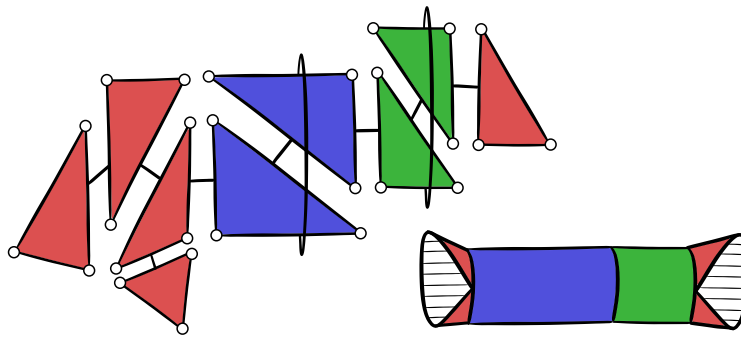
297 **4.3 Simplifying tubes**

298 The operation **DeleteVertices** cannot delete strong vertices, and among them the vertices  
 299 that lie the interior of the surface and are incident to a loop edge. In this section we describe  
 300 an operation for deleting such vertices.

301 In order to grasp the intuition, observe, informally, that it is possible that almost all the  
 302 vertices of  $T^1$  lie in the interior of  $\mathcal{S}(T)$  and are incident to a loop edge. Fortunately, it turns  
 303 out that in this case there must be a sub-portalgon  $X$  of  $T$  such that  $X$  is a tube and the  
 304 interior of  $\mathcal{S}(X)$  contains loop edges of  $X^1$ . We delete such loop edges by replacing  $X$  by a  
 305 good biface with Proposition 7. There is one subtlety: we must choose  $X$  carefully so that  
 306 we replace any concatenation of tubes by a single biface when possible, in order to delete the  
 307 loops in-between the tubes, instead of replacing each tube individually. That leads to:

308 **SimplifyTubes.** In a triangular portalgon  $T$  whose surface  $\mathcal{S}(T)$  is flat, do the following:

- 309 **1.** In  $T^1$  build a set  $J$  of loop edges that lie in the interior of  $\mathcal{S}(T)$  and are pairwise disjoint,  
 310 as follows. There are two cases:
  - 311 **a.** If  $\mathcal{S}(T)$  is homeomorphic to a torus, do the following. Let  $J$  contain two disjoint loop  
 312 edges of  $T^1$  if there exist two such edges, otherwise let  $J = \emptyset$ .
  - 313 **b.** Otherwise do the following. Construct a set  $J'$  of loop edges by considering every  
 314 vertex  $v$  of  $T^1$  that lies in the interior of  $\mathcal{S}(T)$  and is incident to a loop edge, and  
 315 by putting one of the loop edges incident to  $v$  in  $J'$ . Then build a subset  $J \subseteq J'$  by  
 316 removing from  $J'$  every  $e \in J'$  satisfying both of the following. First, cutting  $\mathcal{S}(T)$   
 317 along the loops in  $J'$ , and considering the resulting connected components, two such



329 **Figure 3** Data structure for **Algorithm**: a portalgon whose polygons are partitioned, here by  
 330 color, inducing sub-portalgons called regions, and a region singularized as active, here in red.

318 components are adjacent to  $e$  (instead of one), say  $S_0$  and  $S_1$ . Second, each one of the  
 319 two sub-portalgons of  $T$  whose surfaces are  $S_0$  and  $S_1$  is a tube.

320 2. Cut the surface  $\mathcal{S}(T)$  along the loops in  $J$ . Each resulting component is the surface of a  
 321 sub-portalgon  $X$  of  $T$ . If  $X$  is a tube replace  $X$  by a good biface  $B$ .

322 The idea behind step 1b is to remove loops from  $J'$  so that step 2 replaces a concatenation  
 323 of tubes by a single good biface when possible, instead of replacing the tubes individually.

#### 324 4.4 Data structure for marking bifaces as inactive

325 We are almost ready to give the algorithm, but there is still one important thing to describe.  
 326 In step 2 of **SimplifyTubes**, if the good biface  $B$  is *thin* we will not just replace  $X$  by  $B$ ,  
 327 but we will also make sure to not modify  $B$  ever again. In this sense  $B$  becomes inactive.  
 328 Doing so requires a data structure remembering which parts of the portalgon are inactive.

331 See Figure 3. The data structure maintains a portalgon  $R$  together with a partition of  
 332 the polygons of  $R$ . Each set  $X$  of polygons in the partition defines a sub-portalgon of  $R$   
 333 which we call **region**. One region is singularized as the **active** region  $R_A$ . The other regions  
 334 are **inactive**. Note that the surface of the active region may be disconnected, and that the  
 335 surfaces of distinct inactive regions may be adjacent.

336 The data structure will be initialized by setting  $R_A = R$ , without inactive region. Then  
 337 the algorithm will apply the routines **InsertVertices**, **InsertEdges**, **DeleteVertices**, and  
 338 **SimplifyTubes** to the active region  $R_A$ , and mark as inactive every thin biface encountered  
 339 in step 2 of **SimplifyTubes**. The surface of  $R_A$  will diminish over time as more and more  
 340 regions are marked inactive. This may increase the numbers of connected components and  
 341 boundary components of  $\mathcal{S}(R_A)$ , ruining our efforts to keep the combinatorial complexity of  
 342  $R_A$  bounded. To counteract this, we introduce:

343 **Gardening.** Every connected component of  $\mathcal{S}(R_A)$  is the surface of a sub-portalgon  $X$  of  
 344  $R_A$ . If  $X$  is a tube replace  $X$  by a good biface  $B$ , and mark  $B$  as inactive.

345 We described everything that the algorithm can do to the data structure. This immediately  
 346 implies three invariants maintained by the algorithm. First, 1) Every polygon of the active  
 347 region has degree at most six, and 2) Every inactive region is a good biface. For the last  
 348 invariant we need a definition. Recall that in  $R$  if two sides  $s$  and  $s'$  of polygons are matched  
 349 then  $s$  and  $s'$  correspond to an edge  $e$  of  $R^1$ . If moreover  $s$  and  $s'$  belong to different polygons,

## XX:10 Computing the Intrinsic Delaunay Triangulation of a Closed Polyhedral Surface

350 and if their respective polygons belong to different regions, we say that  $e$  is **separating**.  
351 Then  $e$  is a loop, for it is a boundary edge of a biface by 2), and  $e$  belongs to the interior of  
352  $\mathcal{S}(R)$ . The third invariant is that 3) The separating loops are pairwise disjoint (no two of  
353 them are based at the same vertex of  $R^1$ ).

### 354 4.5 Algorithm

355 The algorithm repeatedly applies two parts. The first part “improves the geometry” by  
356 applying **InsertVertices** and then **InsertEdges**. However this increases the number of  
357 vertices. So the second part applies **SimplifyTubes**, **DeleteVertices**, and **InsertEdges**,  
358 together with **Gardening**. The second part can only remove a fraction of the vertices at  
359 once, so it is repeated several times. It turns out that 350 repetitions suffice.

360 **Algorithm.** Given a triangular portalgon  $T$  whose surface  $\mathcal{S}(T)$  is flat, and  $N \geq 1$ , do the  
361 following. Initialize the data structure by letting  $R$  be the input portalgon  $T$ , and by letting  
362 the active region  $R_A$  be  $R$  itself, without inactive region. Repeat  $N$  times the following:

- 363 1. Apply **InsertVertices** to  $R_A$ . Then apply **InsertEdges** to  $R_A$ .
- 364 2. Repeat 350 times the following:
  - 365 a. Apply **Gardening**. Then apply **SimplifyTubes** to  $R_A$  but in step 2 of **Simpli-**  
366 **fyTubes**, whenever  $B$  is thin, mark  $B$  as inactive. Apply **Gardening** again.
  - 367 b. Apply **DeleteVertices** to  $R_A$ . Then apply **InsertEdges** to  $R_A$ .

368 In the end return  $R$ .

369 When proving Proposition 3, we will apply **Algorithm** with  $N = \lceil \log(2 + L/s) \rceil$ .

## 370 5 Analysis of the algorithm

371 In this section, we sketch the analysis of **Algorithm** (Section 4) to prove Proposition 3.

### 372 5.1 Combinatorial analysis

373 ► **Proposition 8.** *Apply **Algorithm** to a portalgon  $T$  of  $n$  triangles, whose surface  $\mathcal{S}(T)$  is*  
374 *flat. During the execution the number of polygons of the active region  $R_A$  is  $O(n)$ .*

375 We only sketch the proof of Proposition 8, the complete proof is deferred to Appendix C.

376 **Sketch of proof.** We consider  $R_A^1$ , the 1-skeleton of the active region  $R_A$ , and we show that  
377 the number  $m_A$  of vertices of  $R_A^1$  remains  $O(n)$  throughout the execution. There are two  
378 loops in the algorithm: the main loop, which repeats  $N$  times, and the interior loop, which  
379 repeats 350 times within each iteration of the main loop. To prove the lemma, we consider a  
380 single iteration of the main loop, we assume that  $m_A$  exceeds  $n$  by at least a constant factor  
381 at the beginning of the iteration, and we prove that  $m_A$  has decreased after the iteration.

382 The iteration starts with **InsertVertices**. This is the only moment where  $m_A$  may  
383 increase, and we prove that  $m_A$  is multiplied by at most a constant factor. Then the iteration  
384 applies the interior loop, and we claim that, as long as  $m_A$  exceeds  $n$  by a constant factor,  
385  $m_A$  is divided by at least a constant factor by each iteration of the interior loop. We show  
386 that this claim implies the lemma as the interior loop is applied sufficiently many times to  
387 counteract the initial increase of  $m_A$ . To prove the claim, we show that for **DeleteVertices**  
388 to remove a fraction of the vertices of  $R_A^1$ , it suffices that  $m_A$  vastly exceeds the genus and  
389 the number of boundary components of  $\mathcal{S}(R_A)$ , and that almost all of the vertices of  $R_A^1$  are  
390 weak. We show that this is ensured by first applying **Gardening** and **SimplifyTubes**. ◀

## 5.2 Enclosure

To analyze **Algorithm** from a geometric point of view, we introduce, on the segments of a flat surface  $S$ , a parameter that we call *enclosure*. So consider a segment  $e$  of  $S$ . See Figure 4.

Informally,  $e$  is “enclosed” in  $S$  when a short non-contractible loop can be attached to a point of  $e$  not too close to the endpoints of  $e$ . Formally, consider a point  $x$  in the relative interior of  $e$ . We denote by  $\langle x \rangle_e$  the minimum length of the two sub-segments of  $e$  separated by  $x$ . Assume that there exists a loop  $\gamma$  based at  $x$  in  $S$ , such that  $\gamma$  is geodesic except possibly at its basepoint. Further assume that its length satisfies  $\ell(\gamma) < \langle x \rangle_e$ . In this case  $\gamma$  and  $e$  are necessarily in *general position*: informally, they do not overlap, more formally, every sufficiently short sub-path of  $\gamma$  is either disjoint from  $e$  or its intersection with  $e$  is a single point. There are two cases: either  $\gamma$  crosses  $e$  at  $x$ , or  $\gamma$  meets  $x$  on only one side of  $e$ . If  $\gamma$  crosses  $e$  at  $x$ , then we say that  $\gamma$  **encloses**  $e$  in  $S$ . Also we say that  $\gamma$  encloses  $e$  **by a factor of**  $\langle x \rangle_e / \ell(\gamma)$  in  $S$ . The **enclosure**  $c_S(e) \geq 1$  is the supremum of the ratios  $\langle x \rangle_e / \ell(\gamma)$  over all the basepoints  $x$  in the relative interior of  $e$ , and over all the loops  $\gamma$  based at  $x$  that enclose  $e$  in  $S$ . It is conventionally set to one if there is no loop enclosing  $e$  in  $S$ .

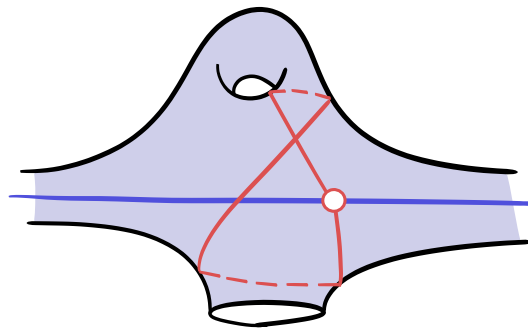


Figure 4 The red loop encloses the blue segment in the surface.

The segment-happiness  $h_S(e)$  and the length  $\ell(e)$  can be bounded from above using the enclosure  $c_S(e)$ . Our bound depends on the surface  $S$ . More precisely, on the systole of  $S$  and the diameter of  $S$ . But instead of the diameter of  $S$ , we consider a triangulation of  $S$ , and we use its number  $n$  of triangles together with the maximum length  $L$  of its edges. This will be more convenient to us when analyzing **Algorithm**. We prove (Appendix D):

► **Proposition 9.** *Let  $e$  be a segment of  $S$ . Let  $s > 0$  be smaller than the systole of  $S$ . Assume that there is a triangulation of  $S$  with  $n \geq 1$  triangles, whose edges are all smaller than  $L > 0$ . Then  $h_S(e) = O(c_S(e) \cdot (1 + \log c_S(e) + \log n + \log \lceil L/s \rceil))$  and  $\ell(e)/s = O(c_S(e) \cdot n \cdot \lceil L/s \rceil^2)$ .*

In Proposition 9 the  $O()$  notation does not depend on  $S$ , it involves a universal constant. In the second inequality of Proposition 9 the exact powers above  $\lceil L/s \rceil$  and  $n$ , here 2 and 1, do not matter to us. We need only a polynomial in  $\lceil L/s \rceil$  and  $n$ .

## 5.3 Geometric analysis

The geometric analysis of **Algorithm** consists in two properties on the enclosure and the length of the edges involved in any execution: Lemma 10 and Proposition 12 below, whose proofs we sketch in Section 5.3.1 and Section 5.3.2. Each proof relies on properties of enclosure that are independent of **Algorithm**, or of any portalgon, and can be seen as independent mathematical contributions of us. In this extended abstract we only explain how these properties of enclosure serve to analyse **Algorithm**, deferring their proof to Appendix D.

## XX:12 Computing the Intrinsic Delaunay Triangulation of a Closed Polyhedral Surface

425 In this section, we fix a portalgon  $T$  of  $n$  triangles, whose sides are smaller than some  
426 positive real  $L$ , and whose surface  $\mathcal{S}(T)$  is flat. We abbreviate  $S = \mathcal{S}(T)$ . We apply the  
427 algorithm **Algorithm** to  $T$ , and we discuss the execution of the algorithm.

### 428 5.3.1 The separating loops are not very enclosed

429 ► **Lemma 10.** *Any time during the execution every separating loop  $e$  satisfies  $c_S(e) \leq 2$ .*

430 Lemma 10 follows from the following property of enclosure (Appendix D):

431 ► **Proposition 11.** *Assume that  $S$  contains the surface of a thin biface  $B$ , and let  $e$  be one  
432 of the two boundary edges of  $B^1$ . Then  $c_S(e) \leq 2$ .*

433 **Proof of Lemma 10.** Only step 2 of **SimplifyTubes** may create a separating loop, by  
434 marking a *thin* biface  $B$  as inactive. Then  $B$  is never touched again by the algorithm. So  
435 the algorithm maintains the invariant that every separating loop  $e$  is adjacent to the surface  
436 of at least one inactive region that is a *thin* biface. So  $c_S(e) \leq 2$  by Proposition 11. ◀

### 437 5.3.2 The very enclosed edges shorten exponentially fast

438 ► **Proposition 12.** *After  $i \geq 1$  iterations of the main loop, let  $e$  be an edge of  $R_A^1$ . If  
439  $c_S(e) > 22000 \cdot i$  then  $\ell(e) < 2^{1-i}L$ .*

440 To prove Proposition 12, we analyze each routine applied. Informally, each application of  
441 **InsertVertices** “improves the geometry” of the active region, and the rest of the algorithm  
442 does not deteriorate this improvement too much. Formally:

443 ► **Lemma 13.** *Consider the active regions  $R_A$  and  $R'_A$  respectively before and after some  
444 application of **InsertVertices**. Assume that there is an edge  $e'$  of  $R'_A$  such that  $c_S(e') > 2$ .  
445 Then there is an edge  $e$  of  $R_A^1$  such that  $c_S(e) \geq c_S(e')$  and  $\ell(e) \geq 2\ell(e')$ .*

446 Lemma 13 follows from the following (easy) property of enclosure (Appendix D):

447 ► **Lemma 14.** *Let  $f \subseteq e$  be segments in  $S$ . Then  $c_S(e) \geq c_S(f)$ .*

448 **Proof of Lemma 13.** First observe that  $e'$  is not included in the boundary of  $\mathcal{S}(R'_A)$  because  
449  $e'$  is enclosed and thus not included in the boundary of  $S$ , and because  $e'$  is not a separating  
450 loop by Lemma 10. So there is an edge  $e$  of  $R_A^1$  such that  $e'$  is one of the two half-segments  
451 obtained after the insertion of the middle point of  $e$  as a vertex. Then  $\ell(e) = 2\ell(e')$ . And  
452  $c_S(e) \geq c_S(e')$  by Lemma 14. ◀

453 ► **Lemma 15.** *Consider the active regions  $R_A$  and  $R'_A$  respectively before and after some  
454 application of **InsertEdges**. Assume that there is an edge  $e'$  of  $R'_A$  such that  $c_S(e') > 14$ .  
455 Then there is an edge  $e$  of  $R_A^1$  such that  $c_S(e) \geq c_S(e') - 12$  and  $\ell(e) \geq (1 - 12/c_S(e')) \cdot \ell(e')$ .*

456 Lemma 15 follows from the following (key) property of enclosure (Appendix D):

457 ► **Proposition 16.** *Let  $F$  be a face of a tessellation of  $S$ . Assume that  $F$  has a shortcut  $e$  such  
458 that  $c_S(e) > 6$ . Then  $F$  has a side  $f$  such that  $c_S(f) \geq c_S(e) - 4$  and  $\ell(f) \geq (1 - 4/c_S(e)) \cdot \ell(e)$ .*

459 **Proof of Lemma 15.** Here we crucially use the fact that every polygon of  $R_A$  has degree at  
460 most six. so that at most three edges are inserted within the polygon. Indeed either  $e'$  was  
461 already an edge of  $R_A^1$  and there is nothing to do, or  $e'$  has been inserted in some face  $F$  of  $R_A^1$ .  
462 At most three edges were inserted in  $F$ , and Proposition 16 applied at most three times gives  
463 a boundary edge  $e$  of  $F$  such that  $c_S(e) \geq c_S(e') - 12$  and  $\ell(e) \geq (1 - 12/c_S(e'))\ell(e')$ . ◀

464 ► **Lemma 17.** Consider the active regions  $R_A$  and  $R'_A$  respectively before and after some  
 465 application of **SimplifyTubes**. Assume that there is an edge  $e'$  of  $R'_A$  such that  $c_S(e') > 6$ .  
 466 Then there is an edge  $e$  of  $R_A$  such that  $c_S(e) \geq c_S(e') - 5$  and  $\ell(e) \geq (1 - 4/c_S(e')) \cdot \ell(e')$ .

467 Lemma 17 is similar to Lemma 15, its proof is deferred to Appendix E.

468 **Proof of Proposition 12.** Consider the active regions  $R_A$  and  $R'_A$  respectively at the be-  
 469 ginning of the algorithm, and after  $i$  iterations of the main loop. Assume that there is  
 470 an edge  $e'$  in  $R'_A$  such that  $c_S(e') > 22000 \cdot i$ . During those  $i$  iterations there has been  $i$   
 471 applications of **InsertVertices**,  $351i$  applications of **InsertEdges**, and  $350i$  applications of  
 472 **SimplifyTubes**. Also  $12 \cdot 351i + 5 \cdot 350i < 11000i$ . So Lemma 13, Lemma 15, and Lemma 17  
 473 imply that there is an edge  $e$  in  $R_A$  such that  $\ell(e) \geq 2^i(1 - 11000i/c_S(e'))\ell(e') > 2^{i-1}\ell(e')$ .  
 474 And  $\ell(e) \leq L$  because  $e$  belongs to the input triangulation  $T^1$ . ◀

## 475 5.4 Proof of Proposition 3

476 We need a last (easy) lemma (Appendix F):

477 ► **Lemma 18.** Let  $S$  be a flat surface. Assume that  $S$  contains the surface of a tube  $X$ . Then  
 478 the systole of  $\mathcal{S}(X)$  is greater than or equal to the systole of  $S$ .

479 **Proof of Proposition 3.** Apply **Algorithm** to  $T$  with  $N = \lceil \log(2 + L/s) \rceil$ , resulting in a  
 480 triangular portalgon  $R$ . By Proposition 8 the number of polygons of the active region is  $O(n)$   
 481 throughout the execution. So in the end  $R$  has  $O(n \cdot \log(2 + L/s))$  triangles; Indeed each  
 482 iteration of the main loop marks  $O(n)$  triangles as inactive, and there are  $\lceil \log(2 + L/s) \rceil$   
 483 iterations of the main loop. We have two claims that immediately imply the proposition.

484 Our first claim is that the algorithm takes  $O(n \log^2(n) \cdot \log^2(2 + L/s))$  time. Let us prove  
 485 this first claim. Each application of **InsertVertices** or **InsertEdges** takes  $O(n)$  time. And  
 486 each application of **SimplifyTubes** or **Gardening** takes  $O(n \log(n) \cdot \log(2 + \Lambda/s))$  time by  
 487 Proposition 7 and Lemma 18, where  $\Lambda$  is the maximum length reached by an edge of the  
 488 1-skeleton of the active region during the execution. Now let us bound  $\Lambda$ . If at some point  
 489 an edge  $e$  of the 1-skeleton of the active region is longer than  $L$  then  $c_S(e) = O(\log(2 + L/s))$   
 490 by Proposition 12. Moreover  $\ell(e)/s = O(c_S(e) \cdot n \lceil L/s \rceil^2)$  by Proposition 9. This proves  
 491  $\log(2 + \Lambda/s) = O(\log(n) + \log(2 + L/s))$ , which proves the claim.

492 Our second claim is that in the end every edge  $e$  of  $R^1$  satisfies  $h_S(e) = O(\log(n) \cdot$   
 493  $\log^2(2 + L/s))$ . Let us prove this second claim. First observe that if  $e$  is in  $R_A$  then  $c_S(e) <$   
 494  $22000 \log(2 + L/s)$ , for otherwise Proposition 12 would imply  $\ell(e) < 2s$ , implying that no loop  
 495 encloses  $e$  in  $S$ , a contradiction. In this case  $h_S(e) = O(\log(2 + L/s) \cdot (\log(n) + \log(2 + L/s)))$   
 496 by Proposition 9, and we are done. Every other edge of  $R^1$  belongs to the 1-skeleton of an  
 497 inactive good biface  $B$ . Every boundary edge  $e$  of  $B^1$  is either a boundary component of  $S$   
 498 or a separating loop, so  $c_S(e) \leq 2$  by Lemma 10, and so  $h_S(e) = O(\log(n) + \log(2 + L/s))$  by  
 499 Proposition 9. Every interior edge  $f$  of  $B^1$  then satisfies  $h_S(f) = O(\log(n) + \log(2 + L/s))$   
 500 by Lemma 6. This proves the second claim, and the proposition. ◀

## 501 ——— References ———

- 502 1 Mark Anthony Armstrong. *Basic Topology*. Springer Science & Business Media, 2013.  
 503 2 Franz Aurenhammer, Rolf Klein, and Der-Tsai Lee. *Voronoi diagrams and Delaunay triangulations*. World Scientific Publishing Company, 2013.  
 504

## XX:14 Computing the Intrinsic Delaunay Triangulation of a Closed Polyhedral Surface

- 505 3 Lenore Blum, Mike Shub, and Steve Smale. On a theory of computation and complexity over  
506 the real numbers: NP-completeness, recursive functions and universal machines. *Bulletin of*  
507 *the American Mathematical Society*, 21(1):1–46, 1989.
- 508 4 Alexander I. Bobenko and Boris A. Springborn. A discrete Laplace–Beltrami operator for  
509 simplicial surfaces. *Discrete & Computational Geometry*, 38(4):740–756, 2007.
- 510 5 Jindong Chen and Yijie Han. Shortest paths on a polyhedron, part I: Computing shortest  
511 paths. *International Journal of Computational Geometry & Applications*, 6(02):127–144, 1996.
- 512 6 Mark De Berg. *Computational geometry: algorithms and applications*. Springer Science &  
513 Business Media, 2000.
- 514 7 Reinhard Diestel. *Graph Theory*. Springer-Verlag, 2000.
- 515 8 Manfredo Perdigao Do Carmo. *Riemannian Geometry*, volume 2. Springer, 1992.
- 516 9 David B. A. Epstein. Curves on 2-manifolds and isotopies. *Acta Mathematica*, 115:83–107,  
517 1966.
- 518 10 Jeff Erickson. Ernie’s 3D pancakes: Shortest paths on PL surfaces. [https://3dpancakes.  
519 typepad.com/ernie/2006/03/shortest\\_paths\\_.html](https://3dpancakes.typepad.com/ernie/2006/03/shortest_paths_.html), 2006.
- 520 11 Jeff Erickson and Amir Nayyeri. Tracing compressed curves in triangulated surfaces. In  
521 *Proceedings of the twenty-eighth annual symposium on Computational geometry*, pages 131–140,  
522 2012.
- 523 12 Jeff Erickson, Ivor Van Der Hoog, and Tillmann Miltzow. Smoothing the gap between NP  
524 and ER. *SIAM Journal on Computing*, pages FOCS20–102, 2022.
- 525 13 Steven Fortune. Voronoi diagrams and delaunay triangulations. In *Handbook of discrete and*  
526 *computational geometry*, pages 705–721. Chapman and Hall/CRC, 2017.
- 527 14 Eugene Gutkin and Chris Judge. Affine mappings of translation surfaces: geometry and  
528 arithmetic. *Duke Mathematical Journal*, 2000.
- 529 15 Paul S Heckbert and Michael Garland. Survey of polygonal surface simplification algorithms.  
530 In *Proceedings of the 24th annual conference on Computer graphics and interactive techniques*.  
531 Siggraph, 1997.
- 532 16 Pascal Hubert and Thomas A Schmidt. An introduction to veech surfaces. *Handbook of*  
533 *dynamical systems*, 1(200601), 2006.
- 534 17 Claude Indermitte, Th M Liebling, Marc Troyanov, and Heinz Cléménçon. Voronoi diagrams  
535 on piecewise flat surfaces and an application to biological growth. *Theoretical Computer*  
536 *Science*, 263(1-2):263–274, 2001.
- 537 18 David Kirkpatrick. Optimal search in planar subdivisions. *SIAM Journal on Computing*,  
538 12(1):28–35, 1983.
- 539 19 Hsueh-Ti Derek Liu, Mark Gillespie, Benjamin Chislett, Nicholas Sharp, Alec Jacobson, and  
540 Keenan Crane. Surface simplification using intrinsic error metrics. *ACM Transactions on*  
541 *Graphics*, 42(4), 2023.
- 542 20 Yong-Jin Liu, Zhanqing Chen, and Kai Tang. Construction of iso-contours, bisectors, and  
543 voronoi diagrams on triangulated surfaces. *IEEE Transactions on Pattern Analysis and*  
544 *Machine Intelligence*, 33(8):1502–1517, 2010.
- 545 21 Yong-Jin Liu, Chun-Xu Xu, Dian Fan, and Ying He. Efficient construction and simplification  
546 of delaunay meshes. *ACM Transactions on Graphics (TOG)*, 34(6):1–13, 2015.
- 547 22 Maarten Löffler, Tim Ophelders, Rodrigo I. Silveira, and Frank Staals. Shortest paths in  
548 portalgons. In *39th International Symposium on Computational Geometry (SoCG 2023)*,  
549 volume 258, pages 48:1–48:16, 2023. doi:10.4230/LIPIcs.SocG.2023.48.
- 550 23 Howard Masur. Ergodic theory of translation surfaces. *Handbook of dynamical systems*,  
551 1:527–547, 2006.
- 552 24 John Milnor. On the betti numbers of real varieties. *Proceedings of the American Mathematical*  
553 *Society*, 15(2):275–280, 1964.
- 554 25 Joseph S.B. Mitchell, David M. Mount, and Christos H. Papadimitriou. The discrete geodesic  
555 problem. *SIAM Journal on Computing*, 16(4):647–668, 1987.

- 556 26 David M. Mount. *Voronoi Diagrams on the Surface of a Polyhedron*. University of Maryland,  
557 1985.
- 558 27 Jim Ruppert. A delaunay refinement algorithm for quality 2-dimensional mesh generation.  
559 *Journal of algorithms*, 18(3):548–585, 1995.
- 560 28 Nicholas Sharp and Keenan Crane. You can find geodesic paths in triangle meshes by just  
561 flipping edges. *ACM Transactions on Graphics (TOG)*, 39(6):1–15, 2020.
- 562 29 Nicholas Sharp, Mark Gillespie, and Keenan Crane. Geometry processing with intrinsic  
563 triangulations. *SIGGRAPH'21: ACM SIGGRAPH 2021 Courses*, 2021.
- 564 30 Nicholas Sharp, Yousuf Soliman, and Keenan Crane. Navigating intrinsic triangulations. *ACM*  
565 *Transactions on Graphics (TOG)*, 38(4):1–16, 2019.
- 566 31 Jonathan Richard Shewchuk. *Delaunay refinement mesh generation*. Carnegie Mellon Univer-  
567 sity, 1997.
- 568 32 Jonathan Richard Shewchuk. Delaunay refinement algorithms for triangular mesh generation.  
569 *Computational geometry*, 22(1-3):21–74, 2002.
- 570 33 John Stillwell. *Classical topology and combinatorial group theory*. Springer-Verlag, New York,  
571 second edition, 1993.
- 572 34 Kenshi Takayama. Compatible intrinsic triangulations. *ACM Transactions on Graphics*  
573 *(TOG)*, 41(4):1–12, 2022.
- 574 35 Anton Zorich. Flat surfaces. *arXiv preprint math/0609392*, 2006.

## 575 **A** Appendix of Section 3

576 **Proof of Lemma 6.** Among the two interior edges of  $B^1$ , let  $f$  be a shortest one. Let  $g \neq f$   
577 be the other interior edge of  $B^1$ . Let  $p$  be a shortest path in  $\mathcal{S}(B)$ . The relative interior  $\mathring{p}$  of  
578  $p$  cannot intersect the relative interior of  $f$  twice for those intersections would be crossings  
579 and  $p$  and  $f$  are both shortest paths because  $B$  is good. So  $\mathring{p}$  intersects  $f$  less than four  
580 times. Then  $\mathring{p}$  cannot intersect the relative interior of  $g$  five times, for those intersections  
581 would be crossings, and  $\mathring{p}$  would intersect  $f$  in-between any two consecutive crossings with  
582 the relative interior of  $g$ . Altogether  $p$  intersects  $f$  and  $g$  at most six times each. ◀

583 The rest of this section is dedicated to the proof of Proposition 7, which we restate for  
584 convenience:

585 ▶ **Proposition 7.** *Let  $X$  be a tube with  $n$  triangles, whose sides are smaller than  $L > 0$ . Let*  
586  *$s > 0$  be smaller than the systole of  $\mathcal{S}(X)$ . One can compute a good biface whose surface is*  
587  *$\mathcal{S}(X)$  in  $O(n \log n \cdot \log(2 + L/s))$  time.*

588 Proposition 7 is similar to but different from a result of Löffler, Ophelders, Silveira, and  
589 Staals [22, Theorem 45] (building upon a ray shooting algorithm of Erickson and Nayyeri [11]),  
590 in which the authors provide an algorithm to transform a biface into a portalgon of bounded  
591 happiness, and of bounded combinatorial complexity. They extend their result from bifaces  
592 to portalgons  $X$  such that the dual graph of  $X^1$  in  $\mathcal{S}(X)$  has at most one simple cycle,  
593 but unfortunately this does not include tubes. We extend their result to tubes to prove  
594 Proposition 7, reusing some of ideas developed in the core of the paper.

595 We need a few lemmas. The following is a corollary of [22, Theorem 45]:

596 ▶ **Lemma 19.** *Let  $B$  be a biface of happiness  $h$ . One can compute in  $O(1 + \log h)$  time a*  
597 *good biface whose surface is that of  $B$ .*

598 **Proof.** By the result of Löffler, Ophelders, Silveira, and Staals [22, Theorem 45] we can  
599 compute in  $O(1 + \log h)$  time a portalgon  $T$ , whose surface is  $\mathcal{S}(B)$ , whose happiness is  $O(1)$ ,  
600 and whose 1-skeleton  $T^1$  has  $O(1)$  edges. Without loss of generality the two vertices  $b_0$  and

## XX:16 Computing the Intrinsic Delaunay Triangulation of a Closed Polyhedral Surface

601  $b_1$  of  $B^1$  are also vertices of  $T^1$ , and we know which vertices of the polygons of  $T$  correspond  
602 to  $b_0$  and  $b_1$ .

603 We now describe how to compute, in constant time, from  $T$ , a good biface of  $\mathcal{S}(T)$ . The  
604 key thing is that we can exploit the fact that  $T$  has  $O(1)$  combinatorial complexity and  
605 happiness to compute by exhaustive search. First compute, in constant time, by exhaustive  
606 search, a shortest path  $q$  between  $b_0$  and  $b_1$  in  $\mathcal{S}(T)$ : represent  $q$  by its pre-image in the  
607 polygons of  $T$ . Then cut the polygons of  $T$  along the pre-image of  $q$ : every time a polygon  
608 is cut in two along a segment  $a$ , the two edges issued of  $a$  are not matched in the resulting  
609 portalgon (the goal is to cut the surface of  $T$ , not just changing  $T$ ). Consider the resulting  
610 portalgon  $D$ . Then  $\mathcal{S}(D)$  is homeomorphic to a closed disk. The two endpoints  $b_0$  and  $b_1$  of  
611  $q$  become a set  $V$  of four vertices of  $D^1$  that lie on the boundary of  $\mathcal{S}(D)$ . Every singularity  
612 of  $\mathcal{S}(D)$  lies on the boundary of  $\mathcal{S}(D)$  and belongs to  $V$ . Now replace  $D$  by a triangular  
613 portalgon  $D'$ , of the same surface, and such that the vertex set of  $D'^1$  is exactly  $V$ . This can  
614 be done for example by iteratively inserting vertex-to-vertex arcs in the faces of  $D^1$  to make  
615  $D^1$  a triangulation, and by deleting a vertex  $v$  of  $D^1$  and its incident edges. When  $v$  lies on  
616 the boundary of  $\mathcal{S}(D)$ , only the edges whose relative interior is included in the interior of  
617  $\mathcal{S}(D)$  are deleted. In the end, identify back the occurrences of  $q$  on the boundary of  $\mathcal{S}(D')$ ,  
618 by matching the two corresponding sides of polygons in  $D'$ , thereby obtaining a biface  $B'$  of  
619  $\mathcal{S}(B)$  such that  $q$  is an interior edge of  $B'$ . Change the other interior edge of  $B'$  if necessary  
620 so that  $B'$  is good. ◀

621 Consider  $k \geq 1$  bifaces  $B_1, \dots, B_k$ . For every  $1 \leq i \leq k$  let  $e_i$  and  $f_i$  be the two sides of  
622 triangles of  $B_i$  that correspond to the boundary of  $\mathcal{S}(B_i)$ . If  $i < k$ , assume  $\ell(e_i) = \ell(f_{i+1})$ ,  
623 and match  $e_i$  with  $f_{i+1}$ . The resulting triangular portalgon  $T$  is a **concatenation** of the  
624 bifaces  $B_1, \dots, B_k$ . Note that  $T$  is not necessarily a tube, for the vertices of  $T^1$  in the interior  
625 of  $\mathcal{S}(T)$  may be singularities.

626 ▶ **Lemma 20.** *Let  $T$  be the concatenation of two good bifaces. If  $T$  is a tube, then one can  
627 compute in constant time a good biface whose surface is that of  $T$ .*

628 **Proof.** Consider a shortest path  $p$  in  $\mathcal{S}(T)$ , and the loop edge  $e$  of  $T^1$  that lies in the interior  
629 of  $\mathcal{S}(T)$ , in-between the surfaces of the two bifaces. We claim that the relative interior of  $p$   
630 does not cross the relative interior of  $e$  more than twice. By contradiction assume that  $p$   
631 crosses the relative interior of  $e$  three times. There is a connected component  $S_0$  of  $\mathcal{S}(T) \setminus e$   
632 whose angle at the base vertex of  $e$  is greater than or equal to  $\pi$ . Some portion  $p'$  of  $p$   
633 enters  $S_0$  and then leaves  $S_0$  by two of the three crossings between  $p$  and  $e$ . One of the two  
634 connected components of  $S_0 \setminus p'$ , say  $S_1$ , is homeomorphic to an open disk. By construction  
635  $S_1$  has at most three angles distinct from  $\pi$ : at the two points where  $p$  crosses  $e$ , and possibly  
636 at the base vertex of  $e$ . By the Gauss-Bonnet theorem, there are exactly three such angles,  
637 not less, and they are all smaller than  $\pi$ . One of them is the incidence of  $S_0$  and the base  
638 vertex of  $e$ . This is a contradiction. This proves the claim.

639 Using the claim immediately the intersection of  $p$  and  $e$  has  $O(1)$  connected components,  
640 so  $p$  writes as a concatenation of  $k = O(1)$  paths  $p_1, \dots, p_k$  such that for every  $1 \leq i \leq k$  the  
641 path  $p_i$  is either included in  $e$  or its relative interior is disjoint from  $e$ . Every edge  $f \neq e$  of  $T^1$   
642 intersects  $p_i$  less than 7 times: if  $f$  is included in the boundary of  $\mathcal{S}(T)$  then  $f$  intersects  $p_i$   
643 at most once, otherwise Lemma 6 applies. So  $f$  intersects  $p$  less than  $O(1)$  times. We proved  
644 that the segment-happiness of  $T$  is  $O(1)$ . Then the happiness of  $T$  is also  $O(1)$  because the  
645 polygons of  $T$  are all triangles. So we can compute a good biface whose surface is that of  $T$   
646 in constant time, exactly as in the proof of Lemma 19. ◀

647 We will use the following simple consequence of Euler's formula, similar to Lemma 26:

648 ► **Lemma 21.** *Let  $S$  be the topological annulus. Let  $Y$  be a topological triangulation of  $S$*   
 649 *that has only one vertex on each boundary component of  $S$ . Among the vertices of  $Y$  that lie*  
 650 *in the interior of  $S$  and are not incident to any loop edge, at least half have degree smaller*  
 651 *than or equal to ten.*

652 **Proof.** We may assume without loss of generality that no vertex of  $Y$  in the interior of  $S$   
 653 is incident to a loop edge, by cutting  $S$  open at an interior loop edge and recursing on the  
 654 resulting two triangulations otherwise. Euler's formula gives  $m - m_1 + m_2 = 0$ , where  $m$ ,  
 655  $m_1$ , and  $m_2$  count respectively the vertices, edges, and faces of  $Y^1$ . Double counting gives  
 656  $3m_2 = 2m_1 - 2$  and  $\sum_v \deg v = 2m_1$ , where the sum is over the vertices  $v$  of  $Y$ . Then  
 657  $\sum_v (6 - \deg v) = 4$ . The two vertices of  $Y$  on the boundary of  $S$  have degree greater than  
 658 or equal to four. So in the interior of  $S$  every vertex of degree greater than ten must be  
 659 compensated by a vertex of degree smaller than or equal to ten. ◀

660 Now we start proving Proposition 7. In particular we fix a tube  $X$  with  $n$  triangles, whose  
 661 sides are all smaller than some  $L > 0$ .

662 ► **Lemma 22.** *One can compute in  $O(n \log n)$  time a concatenation of less than  $3n$  bifaces,*  
 663 *whose surface is that of  $X$ , whose edges are all shorter than  $(3n)^c L$  with  $c = \log_{14/13}(3) < 15$ .*

664 **Proof.** Let us first describe the algorithm before analyzing it. As long as there are vertices  
 665 of  $X^1$  in the interior of  $\mathcal{S}(X)$  that are not incident to any loop edge and have degree smaller  
 666 than or equal to ten, we consider a maximal independent set  $V$  of such vertices, and we do  
 667 the following. First we delete all the vertices in  $V$  along with their incident edges. Then we  
 668 insert arbitrary vertex-to-vertex arcs in the faces of  $X^1$  to make  $X^1$  a triangulation again.

669 The algorithm terminates because the number of vertices of  $X^1$  decreases at each iteration.  
 670 In the end every vertex in the interior of  $\mathcal{S}(X)$  is incident to a loop edge by Lemma 21, so  $X$   
 671 is a concatenation of less than  $m$  bifaces, where  $m \leq 3n$  is the initial number of vertices of  $X^1$ .  
 672 Each iteration can be performed in  $O(n)$  time by maintaining a bucket with the vertices of  
 673 degree smaller than or equal to ten. And we claim that there less than  $\log_{14/13} m$  iterations.  
 674 Before proving the claim, observe that it implies the lemma. Indeed the algorithm then  
 675 terminates in  $O(n \log n)$  time. Also no edge can get longer than  $3^{\log_{14/13} m} L = m^c L$  because  
 676 the maximum edge length of  $X^1$  cannot be multiplied by more than 3 at each iteration.

677 Let us now prove the claim. Consider the number  $m'$  of vertices of  $X^1$  not incident to  
 678 any loop edge that lie in the interior of  $\mathcal{S}(X)$ . By Lemma 21, if  $m' > 0$  before an iteration  
 679 of the algorithm, then at least  $m'/2$  such vertices have degree smaller than or equal to ten.  
 680 So  $V$  contains at least  $m'/14$  vertices, which are deleted. Every non-deleted vertex that  
 681 was incident to a loop edge before the iteration remains incident to a loop edge after the  
 682 iteration. We proved that  $m'$  is divided by at least  $14/13$  during the iteration, which proves  
 683 the claim. ◀

684 **Proof of Proposition 7.** Apply Lemma 22, and replace  $X$  in  $O(n \log n)$  time by a concatena-  
 685 tion of less than  $3n$  bifaces whose edges are smaller than  $(3n)^c L$  for some constant  $c > 0$ . Each  
 686 biface  $B$  has segment-happiness  $O(1 + (3n)^c L/s)$ ; indeed the systole of  $\mathcal{S}(B)$  is greater than  
 687 or equal to the systole of  $X$ , so every segment  $e$  in  $\mathcal{S}(B)$  satisfies  $h_{\mathcal{S}(B)}(e) = O(1 + \ell(e)/s)$ .  
 688 Replace  $B$  by a good biface whose surface is that of  $B$  in  $O(\log(n) + \log(2 + L/s))$  time with  
 689 Lemma 19. Doing so for all bifaces takes  $O(n \cdot (\log(n) + \log(2 + L/s)))$  time in total. We  
 690 crudely bound this running time from above by  $O(n \log(n) \cdot \log(2 + L/s))$ . In the end apply  
 691 Lemma 20 repeatedly to merge those  $O(n)$  good bifaces into a single good biface, in  $O(n)$   
 692 total time. ◀

693 **B Appendix of Section 4**

694 In this section, we detail how to modify a portalgon  $T$  to perform the routines **InsertVertices**,  
695 **InsertEdges**, and **DeleteVertices**.

696 To perform **InsertVertices**, recall that  $T$  is given as a disjoint collection of triangles in  
697 the plane, together with a partial matching of their sides: we consider every triangle  $P$  of  $T$ ,  
698 and every side  $s$  of  $P$  that is matched in  $T$ , and we make the middle point of  $s$  a new vertex  
699 of  $P$ .

700 We perform **InsertEdges** as follows: as long as there is a polygon  $P$  of  $T$  that is not a  
701 triangle, we cut  $P$  into two polygons along a shortcut. This creates two new polygon sides,  
702 which we match in  $T$ .

703 We perform **DeleteVertices** as follows. To delete a vertex  $v$  of  $T^1$ , we consider the  
704 triangle vertices of  $T$  that correspond to  $v$ . No two of them belong to the same triangle for  
705 otherwise there would be a loop of  $T^1$  based at  $v$ , contradicting the assumption that  $v$  is  
706 weak. We move their triangles in the plane so that these vertices are now placed at the same  
707 point of the plane, and so that the triangles are placed in the correct cyclic order around  
708 this point, without overlapping. This is possible because  $v$  lies in the interior of  $\mathcal{S}(T)$ , and  
709 because we assumed that every point in the interior of  $\mathcal{S}(T)$  is flat: it is surrounded by an  
710 angle of  $2\pi$ . Now the union of the triangles is a polygon. In  $T$ , we replace all the triangles  
711 by this single polygon.

712 **C Appendix of Section 5.1: proof of Proposition 8**

713 In this section we prove Proposition 8, which we restate for convenience:

714 ► **Proposition 8.** *Apply **Algorithm** to a portalgon  $T$  of  $n$  triangles, whose surface  $\mathcal{S}(T)$  is*  
715 *flat. During the execution the number of polygons of the active region  $R_A$  is  $O(n)$ .*

716 We analyze each operation independently before proving Proposition 8. Our analysis  
717 is on the number vertices of  $R_A^1$ , not the number of polygons of  $R_A$ , but bounding one  
718 immediately bounds the other, as we shall see, and we find it more convenient to reason  
719 about the vertices of  $R_A^1$ .

720 **C.1 Analysis of InsertVertices**

721 We start by bounding the increase in vertices of **InsertVertices**:

722 ► **Lemma 23.** *Let  $T$  be a triangular portalgon. Let  $g$  be the genus of  $\mathcal{S}(T)$ . Let  $m$  be the*  
723 *number of vertices of  $T^1$ . Apply **InsertVertices** to  $T$  and consider the resulting portalgon*  
724  *$T'$ . Then  $T'^1$  has less than  $7(g + m)$  vertices.*

725 Lemma 23 relies on the following classical consequence of Euler's formula:

726 ► **Lemma 24.** *There are less than  $6(g + m)$  edges in  $T^1$ .*

727 **Proof.** Let  $m_1$  and  $m_2$  count respectively the edges and the faces of  $T^1$ , and let  $b$  count the  
728 boundary components of  $\mathcal{S}(T)$ . Double counting gives  $3m_2 \leq 2m_1$ . Euler's formula gives  
729  $m_1 - m_2 = m + 2g + b - 2$ . And we have  $b \leq m$ . Therefore  $m_1 \leq 3m_1 - 3m_2 < 6(m + g)$ . ◀

730 **Proof of Lemma 23.** There are no more vertices inserted than there are edges in  $T^1$ , and  
731 there are less than  $6(g + m)$  edges in  $T^1$  by Lemma 24. ◀

## 732 C.2 Analysis of DeleteVertices

733 For **DeleteVertices** to remove a fraction of the vertices, it suffices that the number of  
 734 vertices vastly exceeds the topology of the surface, and that almost all of the vertices are  
 735 weak:

736 ► **Lemma 25.** *Let  $T$  be triangular portalgon whose surface  $\mathcal{S}(T)$  is flat. Let  $m$  be the number  
 737 of vertices of  $T^1$ . Let  $g$  be the genus of  $\mathcal{S}(T)$ , and let  $\bar{m}$  be the number of strong vertices of  
 738  $T^1$ . Apply **DeleteVertices** to  $T$  and consider the resulting portalgon  $T'$ . If  $m > 24(g + \bar{m})$   
 739 then  $T'^1$  has less than  $167m/168$  vertices.*

740 Lemma 25 relies on the following classical consequence of Euler's formula:

741 ► **Lemma 26.** *Let  $S$  a topological surface of genus  $g$  with  $b$  boundary components. Let  $Y$  be  
 742 a topological triangulation of  $S$  with  $m$  vertices. If  $m > 24(g + b)$  then at least  $m/12$  vertices  
 743 of  $Y$  have degree smaller than or equal to 6.*

744 **Proof.** Let  $m_1$  and  $m_2$  count respectively the edges and the faces of  $Y$ . Euler's formula gives  
 745  $6m - 6m_1 + 6m_2 = 12 - 12g - 6b$ . Double counting gives  $3m_2 \leq 2m_1 - b$  and  $2m_1 = \sum_v \deg v$ ,  
 746 where the sum is over the vertices, and where  $\deg v$  denotes the degree of a vertex  $v$ . Then  
 747  $\sum_v 6 - \deg v = 6m - 2m_1 \geq 6m - 6m_1 + 6m_2 + 2b \geq 12 - 12g - 4b > -m/2$ . Let  $a$  and  $b$   
 748 count the number of vertices whose degree is respectively smaller than or equal to six, and  
 749 greater than six. Then  $b < 5a + m/2$ . Assuming  $a < m/12$ , we get  $b < 11m/12$ , and so  
 750  $a + b < m$ . This is a contradiction. This proves the lemma. ◀

751 **Proof of Lemma 25.** Let  $b$  be the number of boundary components of  $\mathcal{S}(T)$ . We have  
 752  $m > 24(g + b)$ . Indeed we assumed  $m > 24(g + \bar{m})$ , and we have  $\bar{m} \geq b$  as every boundary  
 753 component of  $\mathcal{S}(T)$  contains a strong vertex of  $T^1$ . So by Lemma 26 at least  $m/12$  vertices  
 754 of  $T^1$  have degree smaller than or equal to six. Moreover less than  $m/24$  vertices of  $T^1$  are  
 755 strong by assumption. So more than  $m/24$  vertices of  $T^1$  are weak and have degree smaller  
 756 than or equal to six. Any maximal independent set of such vertices contains more than  
 757  $m/(24 \times 7) = m/168$  vertices, so **DeleteVertices** deletes more than  $m/168$  vertices. ◀

## 758 C.3 Analysis of SimplifyTubes

759 Right after applying **SimplifyTubes** the number of vertices that lie in the interior of the  
 760 surface and are incident to a loop is bounded by the topology of the surface:

761 ► **Lemma 27.** *Let  $T$  be a triangular portalgon whose surface  $\mathcal{S}(T)$  is flat. Let  $g$  and  $b$  be  
 762 the genus and the number of boundary components of  $\mathcal{S}(T)$ . Apply **SimplifyTubes** to  $T$ ,  
 763 and consider the resulting portalgon  $T'$ . At most  $9(g + b)$  vertices of  $T'^1$  lie in the interior of  
 764  $\mathcal{S}(T')$  and are incident to a loop in  $T'^1$ .*

765 Lemma 27 relies on the following:

766 ► **Lemma 28.** *Let  $I$  be a set of loop edges of  $T^1$  that lie in the interior of  $\mathcal{S}(T)$  and are  
 767 pairwise disjoint. In  $I$  all but at most  $9(g + b)$  loops  $e$  satisfy the following: there are  
 768 two connected components of  $\mathcal{S}(T) \setminus I$  incident to  $e$ , and each of them is the surface of a  
 769 sub-portalgon of  $T$  that is a tube.*

770 **Proof.** Cut  $\mathcal{S}(T)$  along  $I$ , and consider the resulting connected components. Those com-  
 771 ponents are the surfaces of sub-portalgons of  $T$ . Let  $Z$  contain those sub-portalgons of  $T$ .  
 772 Let  $Z' \subseteq Z$  contain the sub-portalgons that are not tubes. Without loss of generality  $I \neq \emptyset$ .

## XX:20 Computing the Intrinsic Delaunay Triangulation of a Closed Polyhedral Surface

773 Then every  $T_0 \in Z$  is such that  $\partial\mathcal{S}(T_0) \neq \emptyset$  because  $\mathcal{S}(T)$  is connected. Let  $\chi(T_0)$  and  $d(T_0)$   
774 be respectively the Euler characteristic of  $\mathcal{S}(T_0)$  and the number of boundary components of  
775  $\mathcal{S}(T)$  that belong to  $\mathcal{S}(T_0)$ . Let  $\lambda(T_0) = 2d(T_0) - \chi(T_0)$ .

776 We claim that every  $T_0 \in Z$  satisfies  $\lambda(T_0) \geq 0$ , and that if  $T_0 \in Z'$  then  $\lambda(T_0) > 0$ .  
777 Indeed we have  $\chi(T_0) \leq 1$  because  $\mathcal{S}(T_0)$  is not homeomorphic to a sphere. So assuming  
778  $\lambda(T_0) \leq 0$ , we get  $d(T_0) = 0$ . Then  $\chi(T_0) \neq 1$  for otherwise  $\mathcal{S}(T_0)$  would be homeomorphic to  
779 a disk, would have no curved point in its interior, and would be bounded by a single geodesic  
780 loop issued of  $I$ , contradicting the formula of Gauss–Bonnet. So  $\chi(T_0) = 0$ . Then  $T_0$  is a  
781 tube because  $\mathcal{S}(T_0)$  is not homeomorphic to a torus. This proves the claim.

782 Now for every  $T_0 \in Z'$  let  $b(T_0)$  be the number of boundary components of  $\mathcal{S}(T_0)$ . The  
783 claim implies  $b(T_0) \leq 2 - \chi(T_0) \leq 2 + \lambda(T_0) \leq 3\lambda(T_0)$ . So  $\sum_{T_0 \in Z'} b(T_0) \leq 3 \sum_{T_0 \in Z'} \lambda(T_0) \leq$   
784  $3 \sum_{T_0 \in Z} \lambda(T_0) \leq 9(g + b)$ . Therefore at most  $9(g + b)$  loops in  $I$  are incident to the surface  
785 of some  $T_0 \in Z'$ . If every other loop in  $I$  is incident to the surfaces of two distinct  $T_0, T_1 \in Z$   
786 then we are done. Otherwise there is a loop  $e \in I$  incident to the surface of only one  $T_0 \in Z$ .  
787 Because  $T_0$  is a tube,  $\mathcal{S}(T)$  is a homeomorphic to a torus, and  $e$  is the only loop in  $I$ , so we  
788 are done. This proves the lemma. ◀

789 **Proof of Lemma 27.** We claim that in the application of **SimplifyTubes** the set  $J$  contains  
790 at most  $9(g + b)$  loops. This is true if step 1a is applied, for in this case  $g = 1$  and  $J$  contains  
791 either zero or two loops. And if step 1b is applied all but  $9(g + b)$  loops in  $J'$  are incident to  
792 two distinct connected component of  $\mathcal{S}(T) \setminus J'$  whose corresponding sub-portalgons of  $T$  are  
793 tubes, by Lemma 28. Those loops are not retained in  $J$ . This proves the claim.

794 In the particular case where the surface  $\mathcal{S}(T)$  is homeomorphic to a torus, and where  $T^1$   
795 contains exactly one vertex incident to loop a edge, the application of **SimplifyTubes** does  
796 nothing and  $T = T'$ . In this case the lemma is proved. In all other cases if a vertex  $v$  of  $T'^1$   
797 lies in the interior of  $\mathcal{S}(T')$  and is incident to a loop edge in  $T'^1$ , then  $v$  is the base vertex  
798 of some loop in  $J$ . Indeed  $v$  would otherwise have been deleted by **SimplifyTubes** when  
799 replacing a tube by a biface. There are at most  $9(g + b)$  such vertices by our claim. This  
800 proves the lemma. ◀

### 801 C.4 Analysis of Gardening

802 Right after applying **Gardening** the topology of  $\mathcal{S}(R_A)$ , the surface of the active region, is  
803 bounded by the topology of  $\mathcal{S}(R)$ , the whole surface:

804 ▶ **Lemma 29.** *Let  $g$  and  $b$  be the genus and the number of boundary components of  $\mathcal{S}(R)$ .  
805 The genus of  $\mathcal{S}(R_A)$  is smaller than or equal to  $g$ . And right after applying **Gardening**  
806  $\mathcal{S}(R_A)$  has at most  $10(g + b)$  boundary components.*

807 **Proof.** The genus of  $\mathcal{S}(R_A)$  is smaller than or equal to  $g$ . It is the number of boundary  
808 components of  $\mathcal{S}(R_A)$  that we must handle. Each boundary component of  $\mathcal{S}(R_A)$  is either a  
809 boundary component of  $\mathcal{S}(R)$ , and there are  $b$  of them, or it is a separating loop. We bound  
810 the the number of separating loops adjacent to  $\mathcal{S}(R_A)$ , so let  $I$  contain those loops. Each  
811  $e \in I$  is incident to two connected components of  $\mathcal{S}(R) \setminus I$ : one of them is in  $\mathcal{S}(R_A)$ , the  
812 other is not. The component in  $\mathcal{S}(R_A)$  is not the surface of a tube because **Gardening** was  
813 just applied. So  $I$  contains at most  $9(g + b)$  loops by Lemma 28. We proved that  $\mathcal{S}(R_A)$  has  
814 at most  $10(g + b)$  boundary components. ◀

## 815 C.5 Proof of Proposition 8

816 **Proof of Proposition 8.** We will prove that the number of vertices of  $R_A^1$  is  $O(n)$  throughout  
 817 the execution. This will prove the lemma for then the number of edges of  $R_A^1$  is also  $O(n)$  by  
 818 Lemma 24, because the genus of  $\mathcal{S}(R_A)$  is  $O(n)$ , and so the number of polygons of  $R_A$  is  
 819 also  $O(n)$ .

820 Consider the input triangular portalgon  $T$ . Let  $m$  be the number of vertices of  $T^1$ . Let  $g$   
 821 and  $b$  be the genus and the number of boundary components of  $\mathcal{S}(T)$ . Observe that  $m \leq 3n$ ,  
 822  $g \leq n$ , and  $b \leq n$ . We will argue using  $m$ ,  $g$ , and  $b$  instead of  $n$ . There are two loops in the  
 823 algorithm: the main loop, which repeats  $N$  times, and the interior loop, which repeats 350  
 824 times within each iteration of the main loop.

825 First we consider a single iteration of the interior loop. Let  $m_A$  be the number of vertices  
 826 of  $R_A^1$  at the beginning of this iteration. Observe that the iteration does not insert any new  
 827 vertex in  $R_A^1$ . We claim that if  $m_A > 3000(g + b + m)$  then less than  $167m_A/168$  vertices  
 828 are in  $R_A^1$  at the end of the loop. To prove the claim first observe that after each application  
 829 of **Gardening**  $\mathcal{S}(R_A)$  has at most  $10(g + b)$  boundary components by Lemma 29. And the  
 830 genus of  $\mathcal{S}(R_A)$  is smaller than or equal to  $g$ . Now after the application of **SimplifyTubes** at  
 831 most  $9(g + 10(g + b)) \leq 99(g + b)$  vertices of  $R_A^1$  lie in the interior of  $\mathcal{S}(R_A)$  and are incident  
 832 to a loop by Lemma 27. This is still the case just before the application of **DeleteVertices**.  
 833 Moreover, at this point, at most  $m + 10(g + b)$  vertices of  $R_A^1$  lie on the boundary of  $\mathcal{S}(R_A)$ ;  
 834 indeed every such vertex is either a vertex of  $T^1$ , and there are at most  $m$ , or it is the  
 835 base vertex of a separating loop, in which case it is the unique vertex in its boundary  
 836 component of  $\mathcal{S}(R_A)$ , and there are at most  $10(g + b)$ . Altogether, just before the application  
 837 of **DeleteVertices**, the number  $\bar{m}_A$  of strong vertices of  $R_A^1$  satisfies  $\bar{m}_A \leq m + 109(g + b)$ . If  
 838 at this point  $R_A^1$  has at most  $24(g + \bar{m}_A)$  vertices then it already has less than  $167m_A/168$   
 839 vertices because we assumed  $m_A > 3000(g + b + m)$ . Otherwise less than  $167m_A/168$  vertices  
 840 remain after **DeleteVertices** by Lemma 25. In any case the claim is proved.

841 Now we prove the lemma by considering a single iteration of the main loop. Assuming  
 842 that  $R_A^1$  has more than  $3000(g + b + m)$  vertices at the beginning of the iteration, we shall  
 843 prove that in the end of the iteration the number of vertices of  $R_A^1$  has decreased. To do so  
 844 first observe that the iteration starts with **InsertVertices**, and this is the only moment where  
 845 vertices are inserted. At this point the number of vertices of  $R_A^1$  is multiplied by less than 8  
 846 by Lemma 23. And by our claim, as long as the number of vertices exceeds  $3000(g + b + m)$   
 847 it is divided by more than  $168/167$  by each iteration of the interior loop. There are 350  
 848 iterations of the interior loop, and  $8 < (168/167)^{350}$ . This proves the lemma. ◀

## 849 **D** Appendix of Sections 5.2 and 5.3: enclosure

### 850 D.1 Proof Lemma 14

851 In this section we prove Lemma 14, which we restate for convenience:

852 ▶ **Lemma 14.** *Let  $f \subseteq e$  be segments in  $S$ . Then  $c_S(e) \geq c_S(f)$ .*

853 **Proof of Lemma 14.** Let  $t > 1$ . Assume that there is a loop  $\gamma$ , based at a point  $x$ , that  
 854 encloses  $f$  by a factor of  $t$ . Then  $\gamma$  encloses  $e$  by a factor of  $t$  because  $\langle x \rangle_f \leq \langle x \rangle_e$ . ◀

### 855 D.2 Proof of Proposition 16

856 In this section we prove Proposition 16, which we restate for convenience:

## XX:22 Computing the Intrinsic Delaunay Triangulation of a Closed Polyhedral Surface

857 ► **Proposition 16.** *Let  $F$  be a face of a tessellation of  $S$ . Assume that  $F$  has a shortcut  $e$  such*  
 858 *that  $c_S(e) > 6$ . Then  $F$  has a side  $f$  such that  $c_S(f) \geq c_S(e) - 4$  and  $\ell(f) \geq (1 - 4/c_S(e)) \cdot \ell(e)$ .*

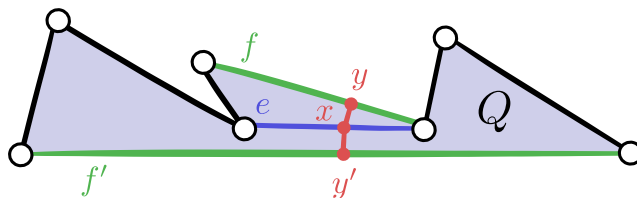
859 First we need a lemma:

860 ► **Lemma 30.** *In  $S$ , let  $e$  and  $f$  be two segments whose relative interiors are disjoint, and let*  
 861  *$\gamma$  be a geodesic loop. Assume that  $\gamma$  encloses  $e$  by a factor of  $t > 2$ , and that  $\gamma$  intersects  $f$*   
 862 *at a point  $y$  such that  $\langle y \rangle_f > \ell(\gamma)$ . Rebase  $\gamma$  at  $y$ , and let  $\gamma'$  be the geodesic loop homotopic*  
 863 *to it. Then  $\gamma'$  meets  $y$  on both sides of  $f$ .*

864 We emphasize that, in Lemma 30, the loops  $\gamma$  and  $\gamma'$  have distinct basepoints, and that  
 865 they may not be geodesic at their basepoints.

866 **Proof.** We have  $\ell(\gamma') \leq \ell(\gamma)$  so  $\ell(\gamma') < \langle y \rangle_f$ , and so  $\gamma'$  is in general position with  $f$ . We  
 867 prove the lemma by contradiction, so assume that  $\gamma'$  meets  $y$  only on the right side of  $f$ ,  
 868 for some direction of  $f$ . In the universal covering space  $\tilde{S}$  of  $S$ , consider a lift  $\tilde{f}$  of  $f$ . Let  
 869  $\tilde{y}$  be the lift of  $y$  that belongs to  $\tilde{f}$ . Because the interior of  $\tilde{S}$  is flat, there is a geodesic  $\tilde{L}$ ,  
 870 containing  $\tilde{f}$ , such that on both ends  $\tilde{L}$  is either infinite or reaches the boundary of  $\tilde{S}$ . Then  
 871  $\tilde{L}$  separates  $\tilde{S}$  in two connected components. The two lifts of  $\gamma'$  incident to  $\tilde{y}$  meet  $\tilde{y}$  on the  
 872 right side of  $\tilde{f}$  by assumption, and they are otherwise disjoint from  $\tilde{L}$ . In particular, their  
 873 other endpoints lie on the right side of  $\tilde{L}$ .

874 We have  $\ell(\gamma) < \langle y \rangle_f$  so  $\gamma$  is in general position with  $f$ . Direct  $\gamma$  so that  $\gamma$  crosses  $f$  from  
 875 right to left at  $y$ , and write  $\gamma$  as the concatenation of two paths  $\gamma_0$  and  $\gamma_1$  respectively before  
 876 and after its crossing at  $y$ . There is a lift  $\tilde{\gamma}_1$  of  $\gamma_1$  that leaves  $\tilde{y}$  on the left of  $\tilde{f}$ . And  $\tilde{\gamma}_1$   
 877 is otherwise disjoint from  $\tilde{L}$ , because the interior of  $\tilde{S}$  is flat. Thus the endpoint  $\tilde{x}$  of  $\tilde{\gamma}_1$   
 878 lies on the left of  $\tilde{L}$ . There is a lift  $\tilde{\gamma}_0$  of  $\gamma_0$  that starts at  $\tilde{x}$ . And  $\tilde{\gamma}_0$  is otherwise disjoint  
 879 from  $\tilde{\gamma}_1$  because  $\gamma$  meets  $x$  on both sides of  $e$ , and because the interior of  $\tilde{S}$  is flat. By the  
 880 previous paragraph, the endpoint of  $\tilde{\gamma}_0$  lies on the right side of  $\tilde{L}$ , so  $\tilde{\gamma}_0$  intersects  $\tilde{L}$ . Cut  
 881  $\tilde{\gamma}_0$  at its first intersection point  $\tilde{z}$  with  $\tilde{L}$ . Let  $\tilde{I}$  be the sub-segment of  $\tilde{L}$  between  $\tilde{y}$  and  $\tilde{z}$ .  
 882 The concatenation of the prefix of  $\tilde{\gamma}_0$  ending at  $\tilde{z}$ , of  $\tilde{I}$ , and of  $\tilde{\gamma}_1$  is a simple closed curve  $\tilde{C}$ .  
 883 At  $\tilde{x}$ , there is a portion of  $\tilde{e}$  that enters the bounded side of  $\tilde{C}$ , because  $\gamma$  meets  $x$  on both  
 884 sides of  $e$ . This portion of  $\tilde{e}$  can be extended into a geodesic  $\tilde{p}$  that meets  $\tilde{C}$  at some point  $\tilde{v}$ ,  
 885 because the interior of  $\tilde{S}$  is flat. Then  $\tilde{v}$  belongs to the relative interior of  $\tilde{I}$ . We claim that  $\tilde{v}$   
 886 belongs to the relative interiors of both  $\tilde{e}$  and  $\tilde{f}$ , which is a contradiction because the relative  
 887 interiors of  $e$  and  $f$  are disjoint. To prove the claim, first observe that the distance between  $\tilde{y}$   
 888 and  $\tilde{z}$  in  $\tilde{S}$  is at most  $\ell(\gamma)$ , and this distance is equal to the length of  $\tilde{I}$ , because the interior  
 889 of  $\tilde{S}$  is flat. So the sub-segment of  $\tilde{I}$  between  $\tilde{y}$  and  $\tilde{v}$  is no longer than  $\ell(\gamma) < \langle y \rangle_f$ , and is  
 890 thus included in the relative interior of  $\tilde{f}$ . Also, the distance between  $\tilde{v}$  and  $\tilde{x}$  is smaller than  
 891 or equal to  $2\ell(\gamma) \leq 2\langle x \rangle_e/t < \langle x \rangle_e$ , so  $\tilde{p}$  is included in the relative interior of  $\tilde{e}$ . ◀



892 ■ **Figure 5** The setting of Lemma 31.

893 The proof of Proposition 16 also relies on the following construction. See Figure 5. In the  
 894 Euclidean plane  $\mathbb{R}^2$  let  $Q$  be a polygon with more than three vertices. Let  $e$  be a shortcut of

895  $Q$ . Let  $f$  and  $f'$  be sides of  $Q$  separated by  $e$  along the boundary of  $Q$ . Let  $x$  be a point in  
 896 the relative interior of  $e$ . Let  $y$  and  $y'$  be points that lie on respectively  $f$  and  $f'$  (possibly  
 897 vertices of  $Q$ ), and do not lie on  $e$ . Consider the segments  $p$  and  $p'$  between  $x$  and respectively  
 898  $y$  and  $y'$ . Assume that the relative interiors  $p$  and  $p'$  are included in the interior of  $Q$ . Then:

899 ► **Lemma 31.** *Let  $t > 6$ . If  $\ell(p) \leq \langle x \rangle_e/t$  and  $\ell(p') \leq \langle x \rangle_e/t$ , then at least one of  $f$  and  $f'$ ,  
 900 say  $f$ , is such that  $\langle y \rangle_f \geq (1 - 4/t) \cdot \langle x \rangle_e$  and  $\ell(f) \geq (1 - 4/t) \cdot \ell(e)$ .*

901 **Proof.** Assume without loss of generality that  $e$  is horizontal, that  $f$  lies above  $e$ , and that  
 902  $x$  is the origin  $(0, 0) \in \mathbb{R}^2$ . Then  $x$  cuts  $e$  into two segments  $e_0$  and  $e_1$ , respectively the right  
 903 and left one. Let  $v_0$  and  $v_1$  be respectively the right and left endpoints of  $e$ . Consider the  
 904 following algorithm in three phases. In the first phase consider the point  $z = x$  and move  $z$   
 905 along  $p$ . Doing so, consider the segments from  $z$  to  $v_0$  and  $v_1$ . If moving  $z$  makes the relative  
 906 interior of one of those two segments intersect  $\partial Q$ , then stop: this is a break condition. Also  
 907 break if  $z$  reached  $y$  and  $y$  is a vertex of  $Q$ . Otherwise the algorithm enters its second phase.  
 908 Then  $y$  cuts  $f$  in two segments  $f_0$  and  $f_1$ , where  $f_0$  is on the right of  $y$  as seen from the path  
 909  $p$  directed from  $x$  to  $y$ . In phase two move  $z$  along  $f_0$  or  $f_1$ , choosing carefully which segment  
 910 to move along so that the second coordinate of  $z$  does not increase. We assume without loss  
 911 of generality that  $z$  moves along  $f_0$ , by flipping the figure horizontally otherwise. Move along  
 912  $f_0$  by a distance of  $(1 - 4/t)\ell(e_0)$ , but break if  $z$  reaches the right end-vertex of  $f$ , or if the  
 913 relative interior of the segment between  $z$  and  $v_0$  intersects  $\partial Q$ . If the algorithm did not  
 914 break, it enters its third and final phase. In this phase put  $z$  back on  $y$ , and move it along  
 915 the other sub-segment of  $f$ , here  $f_1$ , by a distance of  $(1 - 4/t)\ell(e_1)$ , breaking if  $z$  reaches the  
 916 left end-vertex of  $f$ , or if the relative interior of the segment between  $z$  and  $v_1$  intersects  $\partial Q$ .

917 If the algorithm did not break then  $\ell(f) \geq (1 - 4/t)\ell(e)$  and  $\langle y \rangle_f \geq (1 - 4/t)\langle x \rangle_e$  and we  
 918 are done. Otherwise, if the algorithm broke, consider the triangle  $\Delta$  between  $v_0$ ,  $v_1$ , and  $z$ .  
 919 The break conditions ensure that the interior of  $\Delta$  is included in the interior of  $Q$ , and that  
 920 there is a vertex  $w$  of  $Q$  that lies on  $\partial\Delta$  and not on  $e$ . We claim that the inner-angles of  
 921  $\Delta$  at  $v_0$  and  $v_1$  are both strictly smaller than  $\pi/4$ . We prove this claim by considering the  
 922 coordinates  $(\alpha, \beta) \in \mathbb{R} \times [0, +\infty[$  of  $z$ , and the coordinates  $(\ell(e_0), 0)$  and  $(-\ell(e_1), 0)$  of  $v_0$  and  
 923  $v_1$  respectively, and by proving that the invariants  $\ell(e_0) - \alpha > \beta$  and  $\alpha + \ell(e_1) > \beta$  hold at any  
 924 time during the algorithm. Let  $m = \min(\ell(e_0), \ell(e_1)) = \langle x \rangle_e$ . In the first phase  $|\alpha| \leq m/t$   
 925 and  $0 \leq \beta \leq m/t$ , so the invariants hold because  $t > 2$ . In the second phase  $\beta$  does not  
 926 increase and  $\alpha$  does not decrease. Moreover  $\alpha$  does not increase by more than  $\ell(e_0)(1 - 4/t)$   
 927 so the invariants hold. If the second phase ends without breaking then the absolute slope  
 928  $\lambda$  of the line supporting  $f$  is smaller than or equal to  $1/(t - 5)$ . Indeed during the second  
 929 phase  $\beta$  decreased by at most  $m/t$  while  $z$  moved a distance  $\ell(e_0)(1 - 4/t)$ , so  $\alpha$  increased  
 930 by at least  $\ell(e_0)(1 - 4/t) - m/t$ , and so  $1/\lambda \geq \ell(e_0)(1 - 4/t)t/m - 1 \geq t - 5$ . In the third  
 931 phase  $\alpha \geq -m/t - \ell(e_1)(1 - 4/t)$  and  $\beta \leq m/t + \lambda\ell(e_1)(1 - 4/t)$  so  $\alpha + \ell(e_1) \geq 3\ell(e_1)/t > \beta$   
 932 because  $t > 6$ . Also  $\beta$  increases less than  $\alpha$  decreases because  $\lambda < 1/2$ , so  $\ell(e_0) - \alpha > \beta$   
 933 remains true. This proves the claim.

934 Applying the algorithm to  $p'$  and  $f'$  on the other side of  $e$ , either the algorithm does  
 935 not break in which case  $\ell(f') \geq (1 - 4/t)\ell(e)$ ,  $\langle y' \rangle_{f'} \geq (1 - 4/t)\langle x \rangle_e$ , and we are done. Or  
 936 the algorithm breaks and we get similarly a triangle  $\Delta'$  and a vertex  $w'$  of  $P$ . The inner  
 937 angles of  $\Delta'$  at  $v_0$  and  $v_1$  are also both strictly smaller than  $\pi/4$ , so the relative interior of  
 938 the segment between  $w$  and  $w'$  is included in the interior of the quadrilateral formed by  $\Delta$   
 939 and  $\Delta'$ , and is strictly shorter than  $e$ . This segment is a vertex-to-vertex arc of  $Q$  shorter  
 940 than  $e$ , a contradiction. ◀

941 **Proof of Proposition 16.** Let  $t > 6$ . Assume that there is a geodesic loop  $\gamma$  that encloses

## XX:24 Computing the Intrinsic Delaunay Triangulation of a Closed Polyhedral Surface

942  $e$  by a factor of  $t$ . Let  $x$  be the basepoint of  $\gamma$ . In the Euclidean plane, consider the  
 943 polygon  $Q$  corresponding to  $F$ . Let  $\widehat{e}$  and  $\widehat{x}$  be the pre-images of  $e$  and  $x$  in  $Q$ . Consider  
 944 the prefix and the suffix of  $\gamma$  that leave  $x$  on both sides of  $e$  to meet  $\partial F$ , and their pre-  
 945 image paths in  $Q$  that meet two boundary edges  $\widehat{f}$  and  $\widehat{f}'$  of  $Q$ , at respective points  $\widehat{y}$  and  
 946  $\widehat{y}'$ . By Lemma 31, one of those two points, say  $\widehat{y}$  without loss of generality, is such that  
 947  $\langle \widehat{y} \rangle_{\widehat{f}} \geq (1 - 4/t)\langle \widehat{x} \rangle_{\widehat{e}}$  and  $\ell(\widehat{f}) \geq (1 - 4/t)\ell(\widehat{e})$ . Also  $\widehat{f}$  projects to a boundary edge  $f$  of  $F$ ,  
 948 and  $\widehat{y}$  projects to a point  $y$  in the relative interior of  $f$ . Now rebase  $\gamma$  at  $y$ , and consider the  
 949 geodesic loop  $\gamma'$  homotopic to it (where the basepoint at  $y$  is fixed by the homotopy). Then  
 950  $\ell(\gamma') \leq \ell(\gamma) = \langle x \rangle_e/t < \langle y \rangle_f/(t - 4)$ . In particular  $\ell(\gamma') < \langle y \rangle_f$  because  $t > 5$ . And  $\gamma'$  meets  
 951  $y$  on both sides of  $f$  by Lemma 30, because  $t > 2$ . ◀

### 952 D.3 Interior of a thick biface

953 In this section we prove the following:

954 ▶ **Proposition 32.** *Assume that  $S$  contains the surface of a thick biface  $B$ , and let  $e$  be one*  
 955 *of the two interior edges of  $B^1$ . Assume that  $c_S(e) > 6$ . Then there is a boundary edge  $f$  of*  
 956  *$B^1$  such that  $c_S(f) \geq c_S(e) - 5$  and  $\ell(f) \geq (1 - 4/c_S(e)) \cdot \ell(e)$ .*

957 First we need a lemma:

958 ▶ **Lemma 33.** *Let  $B$  be a good biface. Among the two interior edges of  $B^1$  let  $f$  be a longest*  
 959 *one. Let  $F$  be the face of  $B^1$  adjacent to  $f$ . Each corner of  $F$  incident to  $f$  has angle smaller*  
 960 *than or equal to  $\pi/2$ .*

961 **Proof.** Among the two interior edges of  $B^1$  let  $e$  be a shortest one, and let  $g \neq e$  be the  
 962 other one. Then  $e$ ,  $g$ , and  $f$  are the sides of  $F$ . The angle at the corner of  $F$  between  $f$  and  
 963  $g$  is smaller than  $\pi/2$  because  $\ell(e) \leq \ell(g)$ . Now consider the corner  $c$  between  $f$  and  $e$ . Cut  
 964  $\mathcal{S}(B)$  open along  $e$  and consider the resulting quadrilateral  $Q$  in the plane. The edge  $f$  of  $B^1$   
 965 corresponds to a side  $\widehat{f}$  of  $Q$ , the edge  $e$  corresponds to two opposite sides  $\widehat{e}$  and  $\widehat{e}'$ , and the  
 966 edge  $g$  corresponds to a vertex-to-vertex arc  $\widehat{g}$  of  $Q$ . Also the other boundary edge  $f' \neq f$   
 967 of  $B^1$  corresponds to the side  $\widehat{f}'$  of  $Q$  opposite to  $\widehat{f}$ . And the corner  $c$  corresponds to the  
 968 corner  $\widehat{c}$  of  $Q$  between  $\widehat{e}$  and  $\widehat{f}$ . Let  $\widehat{d}$  be the corner of  $Q$  opposite to  $\widehat{c}$ , between  $\widehat{e}'$  and  $\widehat{f}'$ .  
 969 Assume by contradiction that the angle at  $\widehat{c}$  is greater than  $\pi/2$ . We have  $\ell(\widehat{e}) = \ell(\widehat{e}')$  and  
 970  $\ell(\widehat{f}) \geq \ell(\widehat{f}')$  so the angle at  $\widehat{d}$  is greater than or equal to the angle at  $\widehat{c}$ , and in particular is  
 971 also greater than  $\pi/2$ . The two other angles of  $Q$  are smaller than  $\pi$ , so  $Q$  is convex and  
 972 admits a diagonal  $p \neq \widehat{g}$ . Consider the unique circle  $C$  that admits  $\widehat{g}$  as a diameter. Then  
 973 the two endpoints of  $p$  lie in the interior of  $C$ . So  $p$  is shorter than  $\widehat{g}$ . This contradicts the  
 974 assumption that  $B$  is good. ◀

975 **Proof of Proposition 32.** Among the two interior edges of  $B^1$  let  $g$  be a shortest one. Among  
 976 the two boundary edges of  $B^1$  let  $g'$  be a longest one. Then  $\ell(g) \leq \ell(g')$  because  $B$  is thick.  
 977 We claim that if  $c_S(g) > 2$ , then  $c_S(g') \geq c_S(g) - 1$ . To prove the claim let  $t > 2$  and assume  
 978 that there is a loop  $\gamma$  that encloses  $g$  by a factor of  $t$  in  $S$ . Let  $x$  be the basepoint of  $\gamma$ . Let  $F$   
 979 be the face of  $B^1$  adjacent to  $g'$ . Around  $x$  there is a portion of  $\gamma$  that enters  $F$ . This portion  
 980 of  $\gamma$  must leave  $F$  by a point  $y$  of  $g'$  because the angle of  $F$  between  $g$  and  $g'$  is smaller than  
 981 or equal to  $\pi/2$  by Lemma 33, because  $\ell(g) \leq \ell(g')$ , and because  $\ell(\gamma) = \langle x \rangle_g/t < \langle x \rangle_{g'}/\sqrt{2}$ .  
 982 Then  $\langle y \rangle_{g'} \geq \langle x \rangle_g - \ell(\gamma) = (1 - 1/t)\langle x \rangle_g$  by triangular inequality and because  $\ell(g) \leq \ell(g')$ .  
 983 Rebase  $\gamma$  at  $y$ , and consider the geodesic loop  $\gamma'$  homotopic to it (where the homotopy fixes  
 984 the basepoint at  $y$ ). Then  $\ell(\gamma') \leq \ell(\gamma) = \langle x \rangle_g/t \leq \langle y \rangle_{g'}/(t - 1)$ . And  $\gamma'$  encloses  $g'$  by  
 985 Lemma 30, because  $t > 2$ . This proves the claim.

986 If  $e = g$  we are done by our claim, so assume that  $e$  is a longest interior edge of  $B^1$ .  
 987 Deleting  $e$  merges the two faces of  $B^1$  into a single face  $F'$  of which  $e$  is a shortcut, because  $B$   
 988 is good. So Proposition 16 applies because  $c_S(e) > 6$ : there is a boundary edge  $f$  of  $F'$  such  
 989 that  $c_S(f) \geq c_S(e) - 4$  and  $\ell(f) \geq (1 - 4/c_S(e))\ell(e)$ . If  $f$  is a boundary edge of  $B^1$  we are  
 990 done. Otherwise  $f = g$  so  $\ell(g') \geq \ell(f) \geq (1 - 4/c_S(e))\ell(e)$  and  $c_S(g') \geq c_S(f) - 1 \geq c_S(e) - 5$   
 991 by our claim because  $c_S(e) > 6$ . This proves the proposition. ◀

## 992 D.4 Proof of Proposition 11

993 In this section we prove Proposition 11, which we restate for convenience:

994 ▶ **Proposition 11.** *Assume that  $S$  contains the surface of a thin biface  $B$ , and let  $e$  be one*  
 995 *of the two boundary edges of  $B^1$ . Then  $c_S(e) \leq 2$ .*

996 First we need two lemmas:

997 ▶ **Lemma 34.** *Let  $B$  be a thin biface. Among the two interior edges of  $B^1$  let  $e$  be a shortest*  
 998 *one. Each of the four corners between  $e$  and the boundary of  $S(B)$  has angle greater than*  
 999  *$\pi/4$ .*

1000 **Proof.** Assume by contradiction that there is a corner  $c$  between  $e$  and a boundary edge  
 1001  $f$  of  $B^1$  whose angle is smaller than or equal to  $\pi/4$ . Cut  $S(B)$  open along  $e$  and embed  
 1002 the resulting quadrilateral  $Q$  in the plane, isometrically. The edge  $e$  corresponds to two  
 1003 opposite sides  $\widehat{e}$  and  $\widehat{e}'$  of  $Q$ . The edge  $f$  corresponds to one of the other two sides of  $Q$ , that  
 1004 we call  $\widehat{f}$ . The vertex  $v$  of the corner  $c$  corresponds to the two end-vertices of  $\widehat{f}$ : let  $\widehat{v}$  be  
 1005 the one incident to  $\widehat{e}$ , and let  $\widehat{v}'$  be the one incident to  $\widehat{e}'$ . Without loss of generality the  
 1006 corner  $c$  corresponds to the corner of  $Q$  at  $\widehat{v}$ , whose angle is thus smaller than or equal to  
 1007  $\pi/4$ . Consider the orthogonal projection  $x$  of  $\widehat{v}'$  on the line containing  $\widehat{e}$ . Then  $x$  belongs to  
 1008  $\widehat{e}$  because  $\widehat{e}$  is longer than  $\widehat{f}$ , as  $B$  is thin. The segment  $p$  between  $x$  and  $\widehat{v}$  is shorter than  
 1009 the portion of  $\widehat{e}$  between  $x$  and  $\widehat{v}$ . Also  $p$  is included in  $Q$  because  $\widehat{e}$  and  $\widehat{e}'$  are longer than  $\widehat{f}$ .  
 1010 Thus  $p$  projects to a path that shortcuts  $e$ , contradicting the fact that  $B$  is a good biface. ◀

1011 ▶ **Lemma 35.** *In  $S(B)$  every path  $p$  between the two boundary components of  $S(B)$  is such*  
 1012 *that  $\ell(p) \geq \ell(e)/2$ .*

1013 **Proof.** Without loss of generality one of the two endpoints of  $p$  (at least) is a vertex  $v$  of  $B^1$ .  
 1014 Consider the other endpoint  $x$  of  $p$ , and the vertex  $w \neq v$  of  $B^1$ . There is a path  $q$  from  $x$  to  
 1015  $w$  in the boundary of  $S(B)$ . Without loss of generality  $\ell(q) \leq \ell(e)/2$  because  $B$  is thin. Also  
 1016  $e$  is a shortest path because  $B$  is good. So  $\ell(p) + \ell(q) \geq \ell(e)$ . We proved  $\ell(p) \geq \ell(e)/2$ . ◀

1017 **Proof of Proposition 11.** Among the two interior edges of  $B^1$  let  $e$  be a shortest one. Let  $f$   
 1018 be any one of the two boundary edges of  $B^1$ . We have  $\ell(e) \geq \ell(f)$  because  $B$  is thin. Assume  
 1019 by contradiction that there is in  $S$  a loop  $\gamma$  that encloses  $f$  by a factor of  $t > 2$ . Let  $x$  be  
 1020 the basepoint of  $\gamma$ . There is a portion of  $\gamma$  that leaves  $x$  and enters the interior of  $S(B)$ .  
 1021 This portion of  $\gamma$  cannot leave  $S(B)$  via the other boundary edge of  $S(B)$ , for otherwise  
 1022  $\ell(\gamma) \geq \ell(e)/2$  by Lemma 35, so  $\ell(\gamma) > \langle x \rangle_f/t$ , a contradiction. Then  $\gamma$  intersects  $e$ . And  $f$   
 1023 and  $e$  have a corner whose angle is smaller than  $\pi/4$  because  $\ell(\gamma) < \langle x \rangle_f/2$ . This contradicts  
 1024 Lemma 34. ◀

1025 **D.5 Proof of Proposition 9**

1026 In this section we prove Proposition 9, which we restate for convenience:

1027 **► Proposition 9.** *Let  $e$  be a segment of  $S$ . Let  $s > 0$  be smaller than the systole of  $S$ . Assume*  
 1028 *that there is a triangulation of  $S$  with  $n \geq 1$  triangles, whose edges are all smaller than  $L > 0$ .*  
 1029 *Then  $h_S(e) = O(c_S(e) \cdot (1 + \log c_S(e) + \log n + \log \lceil L/s \rceil))$  and  $\ell(e)/s = O(c_S(e) \cdot n \cdot \lceil L/s \rceil^2)$ .*

1030 First we need a few lemmas.

1031 **► Lemma 36.** *Let  $t > 1$ . Assume that there is a shortest path whose relative interior crosses*  
 1032 *the relative interior of  $e$  twice in the same direction, at points  $x$  and  $y$ . If the sub-segment of*  
 1033  *$e$  between  $x$  and  $y$  is shorter than  $\langle x \rangle_e / 2t$  then  $c_S(e) > t$ .*

1034 **Proof.** Consider the portion  $p$  of the shortest path that starts just before its crossing at  $x$ ,  
 1035 and ends just before its crossing at  $y$ . Consider also the geodesic path  $q$  that runs parallel  
 1036 to the sub-segment of  $e$  from  $y$  to  $x$ , such that the concatenation of  $p$  and  $q$  forms a loop  
 1037  $\gamma$ . Base  $\gamma$  at  $x$ . There is a unique geodesic loop  $\gamma'$  homotopic to  $\gamma$  (where the base-point  
 1038 at  $x$  is fixed in the homotopy) because the interior of  $S$  is flat. We have that  $\gamma'$  is not the  
 1039 constant loop based at  $x$ ; for otherwise  $\gamma$  would be contractible, so  $p$  would be homotopic to  
 1040 the reversal of  $q$ , and so  $p$  would actually be equal to the reversal of  $q$  because the interior of  
 1041  $S$  is flat, a contradiction. Moreover  $\gamma'$  is shorter than  $\langle x \rangle_e / t$ ; indeed  $\gamma'$  is not longer than  $\gamma$ ,  
 1042  $q$  is shorter than  $\langle x \rangle_e / 2t$  by assumption, and  $p$  is not longer than  $q$  because  $p$  is a shortest  
 1043 path. Then  $\gamma'$  is in general position with  $e$ . We shall prove that  $\gamma'$  meets  $x$  on both sides of  
 1044  $e$ . This will prove the lemma for then  $\gamma'$  will enclose  $e$  by a factor of  $\langle x \rangle_e / \ell(\gamma') > t$ .

1045 Let us prove that. Orient  $e$  so that  $\gamma$  crosses  $e$  from right to left. Consider the universal  
 1046 covering space  $\tilde{S}$  of  $S$ , and a lift  $\tilde{e}$  of  $e$  in  $\tilde{S}$ . The interior of  $\tilde{S}$  being flat, there is a geodesic  
 1047  $\tilde{L}$ , containing  $\tilde{e}$ , such that on both ends  $\tilde{L}$  is either infinite or reaches the boundary of  $\tilde{S}$ .  
 1048 And  $\tilde{L}$  separates  $\tilde{S}$  in two connected components. Now let  $\tilde{x}$  be the lift of  $x$  in  $\tilde{e}$ . There are  
 1049 two lifts of  $\gamma'$  incident to  $\tilde{x}$ : one lift  $\tilde{\gamma}'_0$  starts at  $\tilde{x}$ , the other lift  $\tilde{\gamma}'_1$  ends at  $\tilde{x}$ . Let  $\tilde{a}_0$  be the  
 1050 endpoint of  $\tilde{\gamma}'_0$ , and let  $\tilde{a}_1$  be the startpoint of  $\tilde{\gamma}'_1$ . We claim that  $\tilde{a}_0$  lies strictly to the left of  
 1051  $\tilde{L}$ , and that  $\tilde{a}_1$  lies strictly to the right of  $\tilde{L}$ . This claim implies that  $\tilde{\gamma}'_0$  meets  $\tilde{x}$  on the left  
 1052 of  $\tilde{e}$ , and that  $\tilde{\gamma}'_1$  meets  $\tilde{x}$  on the right of  $\tilde{e}$ , which implies that  $\gamma'$  meets  $x$  on both sides of  $e$ .

1053 Let us prove the claim. First we prove that  $\tilde{a}_0$  lies strictly to the left of  $\tilde{L}$ . To do so  
 1054 consider also the lift  $\tilde{p}$  of  $p$  that starts at  $\tilde{x}$ , and the lift  $\tilde{q}$  of  $q$  that starts at the endpoint of  
 1055  $\tilde{p}$ . The endpoint of  $\tilde{q}$  is  $\tilde{a}_0$  because the concatenation of  $\tilde{p}$  and  $\tilde{q}$  is a lift of  $\gamma$ , and because  
 1056  $\gamma$  is homotopic to  $\gamma'$ . By definition  $\tilde{p}$  leaves  $\tilde{x}$  on the left of  $\tilde{L}$ . Also  $\tilde{p}$  is disjoint from  $\tilde{L}$   
 1057 except for its startpoint at  $\tilde{x}$ , the interior of  $S$  being flat. Moreover  $\tilde{q}$  is disjoint from  $\tilde{L}$ .  
 1058 For otherwise  $\tilde{q}$  would intersect  $\tilde{L}$  at a point  $\tilde{z}$  whose distance to  $\tilde{x}$  would be smaller than  
 1059  $\langle x \rangle_e / t$ . But then the sub-segment of  $\tilde{L}$  between  $\tilde{z}$  and  $\tilde{x}$  would be no longer, and so would  
 1060 be included in  $\tilde{e}$ . In particular  $\tilde{q}$  and  $\tilde{e}$  would intersect, a contradiction. This proves that  $\tilde{a}_0$   
 1061 lies strictly to the left of  $\tilde{L}$ .

1062 To prove that  $\tilde{a}_1$  lies strictly to the right of  $\tilde{L}$ , consider the lift  $\tilde{y}$  of  $y$  in  $\tilde{e}$ , and the lift  
 1063  $\tilde{p}_1$  of  $p$  that ends at  $\tilde{y}$ . Then the startpoint of  $\tilde{p}_1$  is  $\tilde{a}_1$ , and it lies strictly to the right of  
 1064  $\tilde{L}$  because  $\tilde{p}_1$  meets  $\tilde{y}$  on the right of  $\tilde{L}$ , and because  $\tilde{p}_1$  is otherwise disjoint from  $\tilde{L}$ . This  
 1065 proves the claim, and the lemma. ◀

1066 **► Lemma 37.** *We have  $h_S(e) = O(c_S(e) \cdot (1 + \log \lceil \ell(e)/s \rceil))$ .*

1067 **Proof.** Let  $t > 1$ . Assume  $h_S(e) > 12t \cdot (3 + \log \lceil \ell(e)/s \rceil)$ . We will prove  $c_S(e) \geq t$ , and  
 1068 this will prove the lemma. In  $S$  there is a shortest path  $p$  that intersects  $e$  more than  
 1069  $12t \cdot (3 + \log \lceil \ell(e)/s \rceil)$  times. Cut  $e$  at its middle point. One of the two resulting sub-segments

1070 of  $e$ , say  $f$ , intersects  $p$  more than  $6t \cdot (3 + \log\lceil\ell(e)/s\rceil)$  times. Partition  $f$  into sub-segments  
 1071  $f_0, f_1, \dots, f_n$  with  $n \leq 2 + \log\lceil\ell(e)/s\rceil$ , where the sub-segment  $f_0$  contains the points  $x \in f$   
 1072 such that  $\langle x \rangle_e \leq s/4$ , and where for every  $1 \leq i \leq n$  the sub-segment  $f_i$  contains the  
 1073 points  $x \in f$  such that  $2^{i-3}s \leq \langle x \rangle_e \leq 2^{i-2}s$ . There is  $0 \leq i \leq n$  such that  $p$  intersects  $f_i$   
 1074 more than  $6t$  times. Then the relative interior of  $p$  crosses  $f_i$  twice (at least) in the same  
 1075 direction at points  $x$  and  $y$ , such that the sub-segment of  $f_i$  between  $x$  and  $y$  is shorter than  
 1076  $2^{i-4}s/t$ , because  $\ell(f_i) \leq 2^{i-3}s$ . Also  $i \geq 1$  as no shortest path crosses  $f_0$  twice, because  
 1077  $\ell(f_0) < s/2$ , and because the interior of  $S$  is flat. In particular  $\langle x \rangle_e \geq 2^{i-3}s$ . Then  $c_S(e) \geq t$   
 1078 by Lemma 36. ◀

1079 ▶ **Lemma 38.** *We have  $\ell(e) = O(c_S(e) \cdot n\lceil L/s \rceil L)$ .*

1080 **Proof.** Let  $t > 1$ . Assume  $\ell(e) \geq 600t \cdot n\lceil L/s \rceil L$ . We will prove that  $c_S(e) \geq t$ , and this will  
 1081 prove the proposition. To do so let  $d = 120n\lceil L/s \rceil L$ . Cut  $e$  into three segments, a middle  
 1082 segment  $e_0$  of length  $d$ , and two peripheral segments each longer than  $2t \cdot d$ . We claim that  
 1083 there is in  $S$  a shortest path crossing the relative interior of  $e_0$  twice in the same direction.  
 1084 This claim implies  $c_S(e) \geq t$  by Lemma 36, which proves the proposition.

1085 Let us prove the claim. Consider a triangulation  $T$  of  $S$  with  $n$  triangles, whose edges  
 1086 are all smaller than  $L > 0$ . Cut each edge of  $T$  into  $2\lceil L/s \rceil$  equal-length segments, that we  
 1087 shall call *doors*. Each door is smaller than or equal to half the systole of  $S$  so it is a shortest  
 1088 path. There are at most  $6n\lceil L/s \rceil$  doors because  $T$  has at most  $3n$  edges. Each sub-segment  
 1089  $e_1$  of length  $4L$  of  $e_0$  contains in its relative interior three points  $x_0, x_1, x_2$  in this order such  
 1090 that  $x_0 \notin p$ ,  $x_1 \in p$ , and  $x_2 \notin p$  for some door  $p$ . The relative interior of  $e_0$  intersects at  
 1091 least  $30n\lceil L/s \rceil$  times this way, so there is a door  $p$  intersected at least 5 times by the  
 1092 relative interior of  $e_0$ . Then each intersection is a single point ( $p$  and  $e_0$  do not overlap).  
 1093 Two of those intersection points may be endpoints of  $p$ , but otherwise the relative interior of  
 1094  $p$  crosses the relative interior of  $e_0$  at least three times. So  $p$  crosses  $e_0$  twice in the same  
 1095 direction, which proves the claim, and the proposition. ◀

1096 **Proof of Proposition 9.** We have  $h_S(e) = O(c_S(e) \cdot (1 + \log\lceil\ell(e)/s\rceil))$  by Lemma 37. Also  
 1097  $\ell(e)/s = O(c_S(e) \cdot n \cdot \lceil L/s \rceil^2)$  by Lemma 38. So  $\log(\lceil\ell(e)/s\rceil) = O(1 + \log c_S(e) + \log(n) +$   
 1098  $\log\lceil L/s \rceil)$ . This proves the proposition. ◀

## 1099 **E Appendix of Section 5.3: proof of Lemma 17**

1100 **Proof of Lemma 17.** Assume that  $e'$  was not already an edge of  $R_A^1$  for otherwise there is  
 1101 nothing to do. Then there is a good biface  $B$  computed by step 2 of **SimplifyTubes** such  
 1102 that  $e$  is one of the two interior edges of  $B^1$ . Also  $B$  is thick, for  $B$  has not been marked as  
 1103 inactive. So by Proposition 32 there is a boundary edge  $e$  of  $B^1$  such that  $c_S(e) \geq c_S(e') - 5$   
 1104 and  $\ell(e) \geq (1 - 4/c_S(e'))\ell(e')$ . ◀

## 1105 **F Appendix of Section 5.4: proof of Lemma 18**

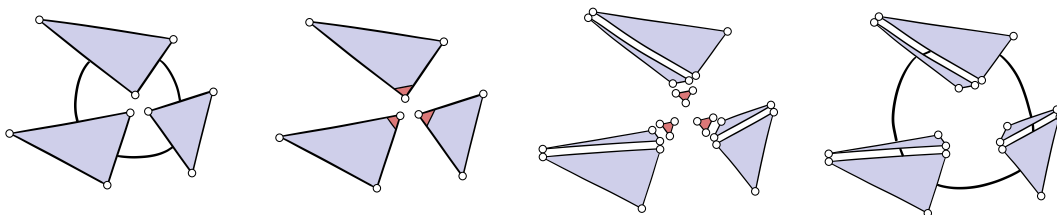
1106 **Proof of Lemma 18.** Otherwise one of the two loops of  $X^1$  that constitute the boundary  
 1107 of  $\mathcal{S}(X)$  is contractible in  $S$ . So this loop bounds a topological disk in  $S$  by a result of  
 1108 Epstein [9, Theorem 1.7]. The interior of the disk is flat, and its boundary is geodesic except  
 1109 possibly at the basepoint of the loop. This contradicts the formula of Gauss–Bonnet. ◀

1110 **G Appendix: proof of Proposition 4**

1111 In this section we prove Proposition 4, which we restate for convenience:

1112 ► **Proposition 4.** *Let  $T$  be a portalgon of  $n$  triangles, of aspect ratio  $r$ . One can compute in*  
 1113  *$O(n \log^2(n) \cdot \log^2(r))$  time a portalgon of  $O(n \cdot \log(r))$  triangles, whose surface is  $\mathcal{S}(T)$ , and*  
 1114 *whose happiness is  $O(n \log(n) \cdot \log^2(r))$ .*

1115 We deduce Proposition 4 from Proposition 3, essentially by cutting out caps around the  
 1116 singularities in the interior of the surface, by applying Proposition 3 to the truncated surface,  
 1117 and by putting the caps back afterward. See Figure 6.



1118 ■ **Figure 6** Cutting out a cap in the proof of Proposition 4.

1119 **Proof of Proposition 4.** Let  $S := \mathcal{S}(T)$  be the surface of  $T$ . Let  $d$  be the minimum height of  
 1120 the triangles of  $T$ . Given a vertex  $v$  of  $T^1$  in the interior of  $S$ , we define a region around  $v$  in  $S$ ,  
 1121 as follows. On every directed edge  $e$  of  $T^1$  whose tail is  $v$ , place a point at distance  $d/6$  from  
 1122 the tail of  $e$  along  $e$ . Link those  $k \geq 1$  points in order (clockwise say, but counter-clockwise  
 1123 would do to) around  $v$ , using geodesic segments within the faces of  $T^1$  incident to  $v$ . In each  
 1124 corner of  $T^1$  incident to  $v$  there is a newly created triangle incident to  $v$ . Those  $k$  triangles  
 1125 define a region  $C$  around  $v$ , which we call *cap* of  $v$ . Importantly, every point in the cap  
 1126 of  $v$  is at distance smaller than or equal to  $d/6$  from  $v$  in  $S$ . Also every segment  $p$  tracing  
 1127 the boundary of  $C$  satisfies  $\ell(p) \geq d/6r$ . To see that consider the face  $F$  of  $T^1$  containing  
 1128  $p$ , and the two sides  $e_0$  and  $e_1$  of  $F$  incident to  $v$ . For each  $i$  consider the point on  $e_i$  at  
 1129 distance  $m := \min(\ell(e_0), \ell(e_1))$  from  $v$  along  $e_i$ . Join those two points by a geodesic segment  
 1130  $q$  in  $F$ . Then  $q$  is at least as long as the minimum height of the triangle corresponding to  
 1131  $F$ , so  $\ell(q) \geq m/r$ . Moreover  $\ell(p)/\ell(q) = d/(6m)$  by the theorem of Thales. This proves  
 1132  $\ell(p) \geq d/6r$ .

1133 For the sake of analysis, given an arbitrary vertex  $v$  of  $T^1$  (possibly on the boundary of  
 1134  $S$ ), we define another kind of region around  $v$ . Link the middle points of the edges around  
 1135  $v$  in order around  $v$ . The resulting triangles around  $v$  constitute the *protected region* of  $v$ .  
 1136 Importantly, every path smaller than  $d/2$  starting from  $v$  must lie in the protected region  
 1137 of  $v$ . Indeed the relative interior of every geodesic path  $p$  smaller than  $d$  starting from  $v$  is  
 1138 included in a single face or edge of  $T^1$ . Then every prefix of  $p$  smaller than  $\ell(p)/2$  lies in the  
 1139 protected region of  $v$ .

1140 First construct in  $O(n)$  time a triangular portalgon  $T_0$  whose surface is  $S$ , as follows.  
 1141 Consider every singularity in the interior of  $S$  (if any). This singularity is a vertex  $v$  of  
 1142  $T^1$ . Trace the boundary of the cap around  $v$  in the faces of  $T^1$ . Then cut those faces along  
 1143 the trace, as in Figure 6. Afterward some polygons of  $T_0$  may not be triangles, so cut each  
 1144 polygon of  $T_0$  into triangles along shortcuts. Now remove the triangles corresponding to the  
 1145 caps from  $T_0$ , and let  $T_1$  be the resulting triangular portalgon. The surface  $\mathcal{S}(T_1)$  is flat.

1146 Our first claim is that the systole of  $\mathcal{S}(T_1)$  is greater than or equal to  $d/6r$ . By contradiction  
 1147 assume that there is a non-contractible closed curve  $\gamma$  in  $\mathcal{S}(T_1)$  smaller than  $d/6r$ . Without

1148 loss of generality  $\gamma$  intersects a vertex  $w$  of  $T_1^1$ ; indeed if such a  $\gamma$  has minimum length  
 1149 and does not intersect any vertex of  $T_1^1$  then it can be slid along the surface, without  
 1150 changing its length, until it intersects a vertex of  $T_1^1$ . If  $w$  is a vertex of  $T_1^1$ , then  $\gamma$  lies in  
 1151 the protected region around  $w$ , and so  $\gamma$  is contractible in  $\mathcal{S}(T_1)$ , a contradiction. If  $w$  is a  
 1152 vertex on the boundary of some cap  $C$  removed, then  $\gamma$  lies in the protected region around  
 1153 the central vertex of  $C$ . In that case  $\gamma$  is at least as long as any edge of the boundary of  $C$ ,  
 1154 so  $\ell(\gamma) \geq d/6r$ . This proves the first claim.

1155 The number of triangles and the maximum side length of a triangle of  $T_1$  may be greater  
 1156 than those of  $T$ , but only by a constant factor. Using the first claim and Proposition 3,  
 1157 replace  $T_1$  by a portalgon of  $O(n \log(r))$  triangles, whose surface is that of  $T_1$ , and whose  
 1158 segment-happiness is  $O(\log(n) \log^2(r))$ , all in  $O(n \log^2(n) \log^2(r))$  time. Place back the caps  
 1159 on  $\mathcal{S}(T_1)$ , and return the resulting triangular portalgon  $T'$ .

1160 The segment-happiness of  $T'$  and the happiness of  $T'$  do not differ by more than a constant  
 1161 factor because the polygons of  $T'$  are all triangles. Our second claim is that the segment-  
 1162 happiness of  $T'$ , and thus the happiness of  $T'$ , is bounded by  $O(n \log(n) \log^2(r))$ . To prove  
 1163 the second claim, we call *cap path* any shortest path in  $S$  that lies in the closure of some cap.  
 1164 We call *rogue path* any shortest path in  $S$  whose relative interior is disjoint from the closures  
 1165 of the caps. Every rogue path intersects every edge of  $T'^1$  at most  $O(\log(n) \log^2(r))$  times,  
 1166 because the segment-happiness of  $T_1$  is  $O(\log(n) \log^2(r))$ . Also every cap path intersects  
 1167 every edge of  $T'^1$  at most once. Now consider a shortest path  $p$  in  $S$ . Then  $p$  uniquely  
 1168 writes as a sequence  $X$  of alternatively cap paths and rogue paths. Also, there cannot be  
 1169 two distinct cap paths  $q_0$  and  $q_1$  in  $X$  that both lie in the same cap  $C$ . For otherwise any  
 1170 point of  $q_0$  would be at distance at most  $d/3$  from any point of  $q_1$ . Also the subpath of  $p$   
 1171 between  $q_0$  and  $q_1$  contains a rogue path that must leave the protected region around the  
 1172 central vertex of  $C$ , and is thus longer than  $d/2 - d/6 = d/3$ . That contradicts the fact that  
 1173  $p$  is a shortest path. We proved that there are at most  $O(n)$  paths in  $X$ , each intersecting at  
 1174 most  $O(\log(n) \log^2(r))$  times any given edge of  $T'^1$ . This proves the second claim, and the  
 1175 proposition. ◀

## 1176 H Appendix: proof of Theorem 2

1177 In this section, we detail our construction for the lower bound, and we prove Theorem 2,  
 1178 which we restate for convenience:

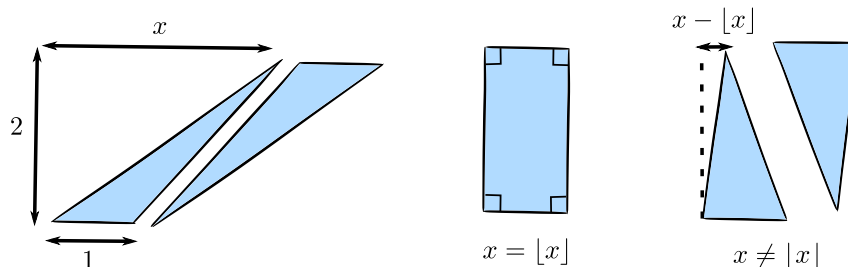
1179 ▶ **Theorem 2.** *Let  $c \in (0, 1)$ . There are a flat torus  $S$ , and for every  $x \in (1, \infty)$ , a*  
 1180 *representation of a portalgon  $T_x$ , with two triangles, whose aspect ratio is  $O(x^2)$ , whose*  
 1181 *surface is  $S$ , that satisfy the following. There is no real RAM algorithm computing a*  
 1182 *representation of the portalgon of the Delaunay tessellation of  $S$  from  $T_x$  in  $O((\log x)^c)$  time.*

1183 Recall that we obtain our results within the real RAM model of computation described  
 1184 by Erickson, van der Hoog, and Miltzow [12]. It is an extension of the standard integer word  
 1185 RAM, with an additional memory array storing reals, and with additional instructions. The  
 1186 available instructions are described in [12, Table 1]. The arithmetic operations that can be  
 1187 performed by the machine on real numbers are addition, subtraction, multiplication, division,  
 1188 and square root.

1192 Recall also that, when modifying a portalgon  $T$ , we actually modify our representation  
 1193 of  $T$ , using elementary operations that are easily seen to be achievable by a real RAM. For  
 1194 example, consider, in the Euclidean plane, two triangles  $\Delta$  and  $\Delta'$ , given by the coordinates  
 1195 of their vertices. Assuming that  $\Delta$  and  $\Delta'$  have respective sides  $s$  and  $s'$  of the same length,

## XX:30 Computing the Intrinsic Delaunay Triangulation of a Closed Polyhedral Surface

1196 we consider the operation of displacing  $\Delta$  in the plane so that afterward  $\Delta$  and  $\Delta'$  are side by  
 1197 side along  $s = s'$ , and we compute the coordinates of the vertices of  $\Delta$  after the displacement.  
 1198 This operation can be achieved by a real RAM.<sup>3</sup>



1199 **Figure 7** (Left) The polygons in the portalgon  $T_x$ . (Right) The polygons in the portalgon  $D_x$ ,  
 1200 depending on whether  $x = \lfloor x \rfloor$  or not.

1201 To obtain our lower bound, we consider, for every  $x \in (1, \infty)$ , a particular representation  
 1202 of a portalgon  $T_x$ . See Figure 7. It has exactly two triangles. The first triangle has vertices  
 1203  $(0, 0)$ ,  $(1, 0)$  and  $(x, 2)$ . The second triangle is isometric to the first triangle, its vertices  
 1204 are  $(1, 0)$ ,  $(x, 2)$ , and  $(x + 1, 2)$ . In  $T_x$  the sides of the first triangle are matched with the  
 1205 corresponding sides of the second triangle. The surface  $\mathcal{S}(T_x)$  is a flat torus  $S$ , independent  
 1206 of  $x$ . We denote by  $D_x$  the portalgon of the Delaunay tessellation of  $S$ .

1207 To obtain Theorem 2, we use the fact that, on a real RAM, the floor of a positive real  
 1208 number cannot be computed in (strongly) sub-logarithmic time (Lemma 39 below), and  
 1209 we reduce the problem of computing the floor of a positive real number to the problem of  
 1210 computing a Delaunay tessellation, in order to transpose the lower bound. More formally,  
 1211 we use the following:

1212 **► Lemma 39.** *Let  $c \in (0, 1)$ . There is no real RAM program computing  $\lfloor x \rfloor$  from  $x \in (1, \infty)$   
 1213 in  $O((\log x)^c)$  time.*

1214 The proof of Lemma 39 is deferred to Appendix H.1. A result similar to Lemma 39  
 1215 was proved by Blum, Shub, and Smale [3, Section 4, Proposition 3] on a different machine,  
 1216 excluding the square root operation. We adapt their arguments to the machine described by  
 1217 Erickson, van der Hoog, and Miltzow [12], including the square root operation.

1218 Theorem 2 is almost immediate from Lemma 39:

1219 **Proof of Theorem 2.** The aspect ratio of  $T_x$  is  $O(x^2)$  because the triangles of  $T_x$  have  
 1220 maximum side length  $O(x)$  and minimum height  $\Omega(1/(1+x))$ . We now prove that there is no  
 1221 real RAM program computing a representation of  $D_x$  from  $x \in (1, \infty)$  in  $O((\log x)^c)$  time for  
 1222 some  $c \in (0, 1)$ . To do so we describe a real RAM program that, given  $x$  and a representation  
 1223 of  $D_x$ , computes  $\lfloor x \rfloor$  in constant time. This will prove the theorem by Lemma 39. There  
 1224 are two cases. See Figure 7. Either  $D_x$  has a unique polygon (in fact a rectangle), in which  
 1225 case  $\lfloor x \rfloor = x$ , so we return  $x$ . Otherwise  $D$  has two triangles. In this case let  $\Delta$  be any of  
 1226 these two triangles in our representation of  $D_x$ . Our triangle  $\Delta$  has a unique side of length  
 1227 one. An orientation-preserving isometry of the plane displaces this unit length side to the  
 1228 segment between  $(0, 0)$  and  $(1, 0)$ . The same isometry displaces the third vertex of  $\Delta$  to a

1189 <sup>3</sup> In fact, this can be done without even using the square root operation. To see that, think of the two  
 1190 initial vertices  $s_0$  and  $s_1$  of  $s$  and the vertices  $s'_0$  and  $s'_1$  of  $s'$  as complex numbers. The displacement of  
 1191  $\Delta$  is then described by the map  $z \rightarrow (z - s_0) \cdot (s'_1 - s'_0)/(s_1 - s_0) + s'_0$ .

1229 point  $(u, v)$  such that  $u = x - \lfloor x \rfloor$ . We compute  $u$  and return  $x - u$ . This can be done using  
 1230 only the basic arithmetic operations of the real RAM on the coordinates of the vertices of  $\Delta$ .  
 1231 The theorem is proved.  $\blacktriangleleft$

## 1232 H.1 Proof of Lemma 39

1233 In this section we prove Lemma 39, which we restate for convenience:

1234 **► Lemma 39.** *Let  $c \in (0, 1)$ . There is no real RAM program computing  $\lfloor x \rfloor$  from  $x \in (1, \infty)$   
 1235 in  $O((\log x)^c)$  time.*

1236 As already mentioned, a result similar to Lemma 39 was proved by Blum, Shub, and  
 1237 Smale [3, Section 4, Proposition 3] on a different machine, excluding the square root opera-  
 1238 tion. We adapt their arguments to the machine described by Erickson, van der Hoog, and  
 1239 Miltzow [12], including the square root operation. This requires a few additional arguments.

1240 As a preliminary, note that the real number operations available to the machine have  
 1241 domains of definition. Indeed, dividing by zero is undefined. Moreover, it is convenient for  
 1242 us to define the square root operation on  $(0, \infty)$ , thus excluding 0. This way square root is  
 1243 real analytic on its domain, and more generally all real number operations available to the  
 1244 machine are real analytic on their domain, so their combinations too, a fact we will use in  
 1245 our proof. Having the square root of 0 undefined does not change the computational power  
 1246 of the machine anyway.

1247 Informally, the core of the proof consists in separating the complexity of a computation  
 1248 induced by the flow control instructions from the complexity induced by the operations on  
 1249 real numbers. So first, we consider a program in which there is no flow control instruction,  
 1250 in other words which instructions are executed does not depend on the input. We formalize  
 1251 that with a simpler model of computation. A **straight-line program** is a sequence of  
 1252  $n \geq 1$  instructions  $I_1, \dots, I_n$  where for each  $i \in [n]$  the instruction  $I_i$  is either  $x_i \leftarrow c$  for  
 1253 some constant  $c \in \mathbb{R}$ ,  $x_i \leftarrow x_j \oplus x_k$  for some  $j, k \in \{0, \dots, i-1\}$  and  $\oplus \in \{+, -, \times, /\}$ , or  
 1254  $x_i \leftarrow \sqrt{x_j}$ . We compute in the natural way. The input is the initial value of the variable  $x_0$ .  
 1255 For each  $i \in [n]$  the instruction  $I_i$  computes the value of the variable  $x_i$ , and the output is  
 1256 the value of  $x_n$  computed by the last instruction  $I_n$ . The computation fails if at some point  
 1257 we divide by zero, or if we take the square root of a non-positive number. This defines a  
 1258 function  $f : D \subset \mathbb{R} \rightarrow \mathbb{R}$ , where  $D$  contains the input values for which the computation does  
 1259 not fail, and where  $f$  maps each input value to the corresponding output value. We say that  
 1260  $f$  is the function **associated to** the straight-line program.

1261 The key argument is to show that the function associated to a straight-line program is  
 1262 “nice”. Formally, given  $y \in \mathbb{R}$ , we say that  $f$  **flattens at**  $y$  if there is an open set  $O \subset \mathbb{R}$  such  
 1263 that  $O \subseteq D$  and  $f(O) = \{y\}$ . Then:

1264 **► Lemma 40.** *If  $f : D \subset \mathbb{R} \rightarrow \mathbb{R}$  is associated to some straight-line program with  $n$   
 1265 instructions then  $f$  flattens at less than  $(7n)^{3n}$  values.*

1266 Note that without the square root operation, every function associated to a straight-line  
 1267 program would be rational, so it would flatten at at most one value. When including the  
 1268 square root operation however, such functions can flatten at several values: consider, for  
 1269 example, the function that maps each  $x \in \mathbb{R} \setminus \{0\}$  to  $\sqrt{x^2}/x$ . This is why we need extra  
 1270 arguments compared to Blum, Shub, and Smale [3, Section 4, Proposition 3].

1271 **Proof of Lemma 40.** The function  $f$  is real analytic. Therefore if  $f$  is constant on some  
 1272 open set  $O \subset \mathbb{R}$  included in  $D$ , then  $f$  is constant on the entire connected component of

## XX:32 Computing the Intrinsic Delaunay Triangulation of a Closed Polyhedral Surface

1273  $D$  that contains  $O$ . We will now prove that  $D$  has less than  $(7n)^{3n}$  connected components.  
1274 This will prove the lemma.

1275 By assumption  $f$  is associated to a straight-line program  $I_1, \dots, I_n$ . For each  $i \in [n]$  we  
1276 associate to the instruction  $I_i$  some polynomial equation(s). For example each instruction  
1277 of the form  $x_i \leftarrow x_j \times x_k$  is associated to the single equation  $x_i - x_j x_k = 0$ . And each  
1278 instruction of the form  $x_i \leftarrow \sqrt{x_j}$  is associated to the three equations  $x_i^2 - x_j = 0$ ,  $x_i > 0$ ,  
1279 and  $x_j > 0$ . The other instructions are handled the same way. This defines at most  $3n$   
1280 polynomial equations, each of degree at most two. The corresponding semi-algebraic subset  
1281  $X \subset \mathbb{R}^{n+1}$  contains the possible values of the variables  $(x_0, \dots, x_n)$  during an execution  
1282 of the straight-line program. By definition the first co-coordinate projection maps  $X$  to  
1283  $D$  in a one-to-one manner, and this projection is continuous, so the number of connected  
1284 components of  $D$  is smaller than or equal to the number of connected components of  $X$ .  
1285 And the latter is smaller than  $(7n)^{3n}$  by a result of Milnor [24, Theorem 3]. ◀

1286 **Proof of Lemma 39.** We consider a program  $P$  that satisfies each of the following for every  
1287  $x \in (1, \infty)$ . Initialize all word and real registers with 0, except the first real register initialized  
1288 with  $x$ , and run the machine with program  $P$ . Then  $P$  is such that 1) the machine never  
1289 tries to perform an undefined operation (dividing by zero, or taking the square root of a  
1290 non-positive number), 2) at some point the machine halts, and 3) afterward the first real  
1291 register contains the value  $\lfloor x \rfloor$ . Assume by contradiction that there are  $c \in (0, 1)$  and  $n \in \mathbb{N}$   
1292 such that  $n > 1$ , and such that for every  $x \geq n$ , when executed with program  $P$  on input  $x$ ,  
1293 the machine halts after at most  $(\log x)^c$  instructions. We will derive a contradiction, which  
1294 will prove the lemma.

1295 Consider an integer  $m \geq n + 1$ . By assumption, when executed with program  $P$  on  
1296 some input  $x \in [n, m]$ , the machine halts after at most  $\alpha = (\log m)^c$  instructions. Which  
1297 instructions are executed depends on  $x$ , and more precisely on the outcomes of the flow  
1298 control instructions. Because at most  $\alpha$  flow control instructions are executed, there are  
1299 at most  $2^\alpha$  possibilities for the outcomes of the flow control instructions. For each such  
1300 possibility, the output (value of the first real register once the machine halts) is a function of  
1301 the input (initial value of the first real register) that is associated to a straight-line program  
1302 with at most  $\alpha$  instructions. In particular, this function flattens at less than  $(7\alpha)^{3\alpha}$  values by  
1303 Lemma 40, we will use this fact. Let  $F$  contain all these functions, over all the possibilities  
1304 for the outcomes of the flow control instructions. Now consider an integer  $k \in [n, m - 1]$ .  
1305 There is a non-empty open subset  $O_k$  of the open interval  $(k, k + 1)$  such that the outcomes  
1306 of the flow control instructions are the same for all inputs in  $O_k$ . So there is  $f_k \in F$ , whose  
1307 domain contains  $O_k$ , such that  $f_k(O_k) = \{k\}$ . In other words,  $f_k$  flattens at  $k$ . Now recall  
1308 that each  $f_k$  flattens at less than  $(7\alpha)^{3\alpha}$  values, so  $(m - n) \leq 2^\alpha \cdot (7\alpha)^{3\alpha}$ . As  $m$  goes to  $\infty$   
1309 this inequality becomes false, because  $\alpha = (\log m)^c$  and  $c < 1$ , a contradiction. ◀

## 1310 **I Appendix: Voronoi diagrams and Delaunay tessellations**

1311 In this section we provide elementary definitions and properties of Delaunay tessellations  
1312 and Voronoi diagrams, for use in Appendix J. This is all folklore, but we could not find all  
1313 the exact statements in the literature, so we provide proofs for completeness.

### 1314 **1.1 Delaunay tessellations**

1315 Consider a closed polyhedral surface  $S$ , and a finite non-empty  $V \subset S$  containing all  
1316 singularities of  $S$ . We consider the definition of Bobenko and Springborn [4, Section 2] of

1317 the Delaunay tessellation of  $(S, V)$ . First, they define an **immersed empty disk** as a pair  
 1318  $(D, \varphi)$  where  $D$  is an open metric disk of  $\mathbb{R}^2$ , and  $\varphi : \overline{D} \rightarrow S$  is a map defined on the closure  
 1319  $\overline{D}$  of  $D$  that satisfies the following: the restriction of  $\varphi$  to  $D$  is an isometric immersion,  
 1320 and  $\varphi(D) \cap V = \emptyset$ . Note that  $\varphi$  is not necessarily injective. Bobenko and Springborn [4,  
 1321 Proposition 4] proved:

1322 ► **Lemma 41** (Bobenko and Springborn). *There is a unique tessellation  $\mathcal{D}$  of  $S$  such that for*  
 1323 *every immersed empty disk  $(D, \varphi)$ , if  $\varphi^{-1}(V)$  is not empty, then the convex hull of  $\varphi^{-1}(V)$*   
 1324 *projects via  $\varphi$  to either a vertex, an edge, or the closure of a face of  $\mathcal{D}$ , and such that every*  
 1325 *vertex, edge, and face of  $\mathcal{D}$  can be obtained this way.*

1326 The tessellation  $\mathcal{D}$  given by Lemma 41 is the **Delaunay tessellation** of  $(S, V)$ . It is “in  
 1327 general” a triangulation, but not always.

1328 We will also use the following definition. For every point  $x \in S$  there is an immersed  
 1329 empty disk  $(D, \varphi)$  such that  $\varphi$  maps the center of  $D$  to  $x$ , and such that  $\varphi^{-1}(V) \neq \emptyset$ . And  
 1330  $(D, \varphi)$  is unique to  $x$  in the sense that if  $(D', \varphi')$  is another such immersed empty disk then  
 1331 there is a plane isometry  $\psi : \mathbb{R}^2 \rightarrow \mathbb{R}^2$  satisfying  $D' = \psi(D)$  and  $\varphi = \varphi' \circ \psi$ . We say that  
 1332  $(D, \varphi)$  is the **maxi-disk** of the point  $x$ .

## 1333 1.2 Voronoi diagrams

1334 Again, consider a closed polyhedral surface  $S$ , and a finite non-empty  $V \subset S$  containing all  
 1335 singularities of  $S$ . The **Voronoi diagram** of  $(S, V)$  contains the points  $x \in S$  such that the  
 1336 distance between  $x$  and  $V$  is realized by at least two distinct paths in  $S$ . Note that it is  
 1337 possible for the Voronoi diagram of  $(S, V)$  to contain a point  $x$  such that all the shortest  
 1338 paths between  $x$  and  $V$  end at the same point of  $V$ . This is for example the case if  $S$  is a  
 1339 flat torus and  $V$  contains exactly one point of  $S$ . In this section we prove the following:

1340 ► **Lemma 42.** *Let  $S$  be a closed polyhedral surface. Let  $V \subset S$  be finite, non-empty, and*  
 1341 *containing all singularities of  $S$ . The Voronoi diagram of  $(S, V)$  is a graph with finitely many*  
 1342 *vertices in which every vertex has degree greater than or equal to three, every edge is geodesic,*  
 1343 *every face is homeomorphic to an open disk and contains exactly one point of  $V$ , and every*  
 1344 *angle at a corner of a face is smaller than or equal to  $\pi$ .*

1345 Note that without the assumption that  $V$  contains all the singularities of  $S$ , it would be  
 1346 possible for the Voronoi diagram of  $(S, V)$  to not be a graph with geodesic edges.

1347 **Proof of Lemma 42.** Consider the Voronoi diagram  $\mathcal{V}$  of  $(S, V)$ . We have three claims that  
 1348 immediately imply the lemma. Our first claim is that  $\mathcal{V}$  is a graph with finitely many vertices,  
 1349 in which every vertex has degree greater than or equal to three, and in which every edge  
 1350 is geodesic. To prove the first claim consider a point  $x \in S$ , and the maxi-disk  $(D, \varphi)$  of  $x$ .  
 1351 Let  $x^*$  be the center of  $D$ . The geodesic paths between  $x^*$  and  $\varphi^{-1}(V)$  in  $\mathbb{R}^2$  correspond  
 1352 via  $\varphi$  to the shortest paths between  $x$  and  $V$  in  $S$ . So  $x$  belongs to  $\mathcal{V}$  if and only if  $\varphi^{-1}(V)$   
 1353 contains several points. Assume that  $x$  belongs to  $\mathcal{V}$ , and let  $m \geq 2$  be the number of points  
 1354 in  $\varphi^{-1}(V)$ . Consider, in  $\mathbb{R}^2$ , the Voronoi diagram of  $\varphi^{-1}(V)$ , which we denote by  $X$ . Then  
 1355  $X$  consists in  $m$  geodesic rays emanating from  $x^*$ . There is an open ball  $O \subset D$  on which  
 1356  $\varphi$  is injective, containing  $x^*$ , and such that  $\varphi(X \cap O) = \mathcal{V} \cap \varphi(O)$ . There are two cases. If  
 1357  $m = 2$  then  $\mathcal{V}$  is locally a geodesic path around  $x$ . If  $m \geq 3$  then  $\mathcal{V}$  is locally a geodesic star  
 1358 whose central vertex is  $x$ . In particular  $\mathcal{V}$  is a graph whose minimum degree is greater than  
 1359 or equal to three, and whose edges are geodesic segments. And  $\mathcal{V}$  has finitely many vertices  
 1360 because  $S$  is compact. That proves the first claim.

## XX:34 Computing the Intrinsic Delaunay Triangulation of a Closed Polyhedral Surface

1361 Now consider a face  $F$  of  $\mathcal{V}$ . Our second claim is that  $F$  is simply connected, and that  
1362  $F$  contains exactly one point of  $V$ . This implies that  $F$  is homeomorphic to an open disk  
1363 because  $F$  is not homeomorphic to a sphere. To prove the second claim first consider a point  
1364  $x \in F$ . There is a unique shortest path  $p$  from  $x$  to  $V$ . Then  $p$  is disjoint from  $\mathcal{V}$ . So the  
1365 endpoint of  $p$  belongs to  $F$ . That proves  $F \cap V \neq \emptyset$ . Now consider the universal covering  
1366 space  $\tilde{F}$  of  $F$ . Then  $\tilde{F}$  does not contain two distinct lifts of points of  $V$ . For otherwise let  
1367  $\tilde{V}$  contain the lifts of the points of  $V$  in  $\tilde{F}$ . There is a point  $\tilde{x} \in \tilde{F}$  whose distance to  $\tilde{V}$  is  
1368 realized by two distinct paths. And  $\tilde{x}$  lifts a point of  $V$ , a contradiction. That proves the  
1369 second claim.

1370 Finally, consider a vertex  $v$  of  $\mathcal{V}$ . Our third claim is that around  $v$  the angles between  
1371 consecutive edges of  $\mathcal{V}$  are all smaller than or equal to  $\pi$ . To prove the claim consider the  
1372 maxi-disk  $(D, \varphi)$  of  $v$ . Let  $v^*$  be the center of  $D$ . Let  $X$  be the Voronoi diagram of  $\varphi^{-1}(V)$   
1373 in the plane. The faces of  $X$  are all convex, being intersections of half-planes. So the angles  
1374 between consecutive rays of  $X$  around  $v^*$  are all smaller than or equal to  $\pi$ . There is an  
1375 open disk  $O$  on which  $\varphi$  is injective, containing  $v^*$ , such that  $\varphi(X \cap O) = \mathcal{V} \cap \varphi(O)$ . That  
1376 proves the third claim, and the lemma. ◀

### 1377 I.3 Voronoi diagram and Delaunay tessellation

1378 A graph  $G$  is **cellularly** embedded on a surface  $S$  if the faces of the embedding are  
1379 all homeomorphic to open disks. In this section, given two graphs  $G$  and  $H$  cellularly  
1380 embedded on  $S$ , we say that  $G$  and  $H$  are **isomorphic** if there is an orientation-preserving  
1381 homeomorphism of  $S$  that maps  $G$  to  $H$ , for some orientation of  $S$ . This does not depend  
1382 on the orientation of  $S$ . We prove the following:

1383 ▶ **Lemma 43.** *Let  $S$  be a closed polyhedral surface. Let  $V \subset S$  be finite, non-empty, and*  
1384 *containing all singularities of  $S$ . The Voronoi diagram of  $(S, V)$  is isomorphic to the dual of*  
1385 *the Delaunay tessellation of  $(S, V)$ .*

1386 (Recall that in Lemma 43 the Voronoi diagram of  $(S, V)$  is a graph cellularly embedded  
1387 on  $S$  by Lemma 42.)

1388 **Proof of Lemma 43.** Consider the Voronoi diagram  $\mathcal{V}$  of  $(S, V)$ , and the Delaunay tessella-  
1389 tion  $\mathcal{D}$  of  $(S, V)$ . Consider a point  $x$  of  $S$ , and its maxi-disk  $(D, \varphi)$ . We already proved that  
1390  $x$  is a vertex of  $\mathcal{V}$  if and only if  $\varphi^{-1}(V)$  contains at least three points. This is the case if and  
1391 only if the convex hull of  $\varphi^{-1}(V)$  projects via  $\varphi$  to the closure of a face  $f$  of  $\mathcal{D}$  (Lemma 41).  
1392 Every face of  $\mathcal{D}$  can be obtained this way (Lemma 41), and distinct vertices of  $\mathcal{V}$  are clearly  
1393 mapped to distinct faces of  $\mathcal{D}$ . So this defines a one-to-one correspondence between the  
1394 vertices of  $\mathcal{V}$  and the faces of  $\mathcal{D}$ . When a vertex  $v$  of  $\mathcal{V}$  corresponds to a face  $f$  of  $\mathcal{D}$  this way  
1395 we say that  $v$  is **dual** to  $f$ .

1396 Now fix a vertex  $v$  of  $\mathcal{V}$ , and its dual face  $f$  of  $\mathcal{D}$ . We call **side** of  $f$  any directed edge of  
1397  $\mathcal{D}$  that sees  $f$  on its left. We now relate the directed edges based at  $v$  in  $\mathcal{V}$  to the sides of  $f$ .  
1398 Again, let  $(D, \varphi)$  be the maxi-disk of  $v$ . Let  $v^*$  be the center of  $D$ , and let  $y_0, \dots, y_{m-1}$  be  
1399 the  $m \geq 3$  points of  $\varphi^{-1}(V)$ . In  $\mathbb{R}^2$  the Voronoi diagram of  $\varphi^{-1}(V)$  consists in  $m$  geodesic  
1400 rays  $r_0, \dots, r_{m-1}$  emanating from  $v^*$ , so that  $r_0, y_0, \dots, r_{m-1}, y_{m-1}$  are in clockwise order  
1401 around  $v^*$ . There is an open ball  $O \subset D$  on which  $\varphi$  is injective, containing  $v^*$ , such that  
1402 within  $O$  the rays  $r_0, \dots, r_{m-1}$  correspond via  $\varphi$  to the directed edges  $e_0, \dots, e_{m-1}$  emanating  
1403 from  $v$  in  $\mathcal{V}$ . For every  $i$  the geodesic path from  $y_i$  to  $y_{i+1}$  corresponds via  $\varphi$  to a side  $e'_i$   
1404 of  $f$ , indices are modulo  $m$ . We say that  $e_i$  and  $e'_i$  are **dual**. This duality is a one-to-one  
1405 correspondence between the directed edges based at  $v$  and the sides of  $f$ . The former are

1406 cyclically ordered around  $v$ , the latter are cyclically ordered along the boundary of  $f$ , and  
 1407 the duality correspondence respects these cyclic orders.

1408 We claim that if a directed edge  $e_0$  of  $\mathcal{V}$  is dual to a directed edge  $e'_0$  of  $\mathcal{D}$ , then the  
 1409 reversal of  $e_0$  is dual to the reversal of  $e'_0$ . The claim immediately implies the lemma, for  
 1410 then the duality correspondences define the desired graph isomorphism between  $V$  and  $\mathcal{D}$ .  
 1411 Let us prove the claim. Let  $e'_1$  be the reversal of  $e'_0$ , and let  $e_1$  be the dual of  $e'_1$ . We shall  
 1412 prove that  $e_1$  is the reversal of  $e_0$ . We consider the maxi-disks  $(D_0, \varphi_0)$  and  $(D_1, \varphi_1)$  of the  
 1413 base vertices of  $e_0$  and  $e_1$ , and we realize them so that they agree on the geodesic segment  $p$   
 1414 that is the pre-image of the common edge of  $e'_0$  and  $e'_1$ . Then  $\varphi_0$  and  $\varphi_1$  agree on  $\overline{D_0} \cap \overline{D_1}$ ,  
 1415 so they agree with a common map  $\varphi_0 \cup \varphi_1 : \overline{D_0} \cup \overline{D_1} \rightarrow S$ . Let  $q$  be the geodesic segment  
 1416 between the centers of  $D_0$  and  $D_1$ . Then  $q$  is contained in  $\overline{D_0} \cup \overline{D_1}$ , and projects via  $\varphi_0 \cup \varphi_1$   
 1417 to the common edge of  $e_0$  and  $e_1$  in  $\mathcal{V}$ . Indeed for every point  $x^*$  in the relative interior of  $q$   
 1418 the maxi-disk  $(D, \varphi)$  of  $\varphi(x^*)$  can be realized so that  $x^*$  is the center of  $D$ , and so that  $\varphi$   
 1419 agrees with  $\varphi_0 \cup \varphi_1$  on  $\overline{D} \cap (\overline{D_0} \cup \overline{D_1})$ . Then  $\varphi^{-1}(V)$  contains exactly the two endpoints of  
 1420  $p$ , and so  $\varphi(x^*)$  belongs to the relative interior of an edge of  $\mathcal{V}$ . This proves the claim, and  
 1421 the lemma. ◀

## 1422 **J** Appendix: proof of Proposition 5

1423 See Appendix I for basic definitions and properties of Delaunay tessellations and Voronoi  
 1424 diagrams. In this section we prove Proposition 5, which we restate for convenience:

1425 ▶ **Proposition 5.** *Let  $T$  be a portalgon of  $n$  triangles, of happiness  $h$ , such that  $\mathcal{S}(T)$  is closed.*  
 1426 *One can compute the portalgon of the Delaunay tessellation of  $\mathcal{S}(T)$  in  $O(n^2 h \log(nh))$  time.*

1427 Proposition 5 slightly extends known results, and is not surprising at all, but we provide  
 1428 proofs for completeness. Our strategy for computing the Delaunay tessellation is, classically,  
 1429 to first compute the Voronoi diagram:

1430 ▶ **Proposition 44.** *Let  $T$  be a portalgon of  $n$  triangles, of happiness  $h$ . Let  $V$  be a set of*  
 1431 *vertices of  $T^1$ . Assume that  $V$  is not empty and contains all singularities of  $\mathcal{S}(T)$ . We can*  
 1432 *compute in  $O(n^2 h \log(nh))$  time a portalgon  $T'$  of  $O(n^2 h)$  triangles, whose surface is  $\mathcal{S}(T)$ ,*  
 1433 *and a subgraph  $\mathcal{V}$  of  $T^1$ , such that  $\mathcal{V}$  is the Voronoi diagram of  $(\mathcal{S}(T), V)$ .*

1434 We will then derive the Delaunay tessellation of from the Voronoi diagram:

1435 ▶ **Proposition 45.** *Let  $T$  be a portalgon of  $n$  triangles. Let  $V$  be a set of vertices of  $T^1$ .*  
 1436 *Let  $\mathcal{V}$  be a subgraph of  $T^1$ . Assume that  $V$  is not empty and contains all singularities of*  
 1437  *$\mathcal{S}(T)$ , and that  $\mathcal{V}$  is the Voronoi diagram of  $(\mathcal{S}(T), V)$ . We can compute the portalgon of the*  
 1438 *Delaunay tessellation of  $(\mathcal{S}(T), V)$  in  $O(n)$  time.*

1439 Proposition 44 and Proposition 45 will immediately imply Proposition 5:

1440 **Proof of Proposition 5, assuming Propositions 44 and 45.** Let  $V$  contain the singularities  
 1441 of  $\mathcal{S}(T)$ , except if  $\mathcal{S}(T)$  is a flat torus in which case let  $V$  contain a single arbitrary vertex of  
 1442  $T^1$ . Apply Proposition 44 to replace  $T$  by a portalgon  $T'$  of  $O(n^2 h)$  triangles, and to compute  
 1443 a subgraph  $\mathcal{V}$  of  $T^1$  that is also the Voronoi diagram of  $(\mathcal{S}(T), V)$ , all in  $O(n^2 h \log(nh))$  time.  
 1444 Apply Proposition 45 to derive from  $T'$  and  $\mathcal{V}$  the portalgon of the Delaunay tessellation of  
 1445  $(\mathcal{S}(T), V)$  in  $O(n^2 h)$  time. ◀

1446 All there remains to do is to prove Proposition 44 and Proposition 45. We prove  
 1447 Proposition 45 in Section J.1, and we prove Proposition 44 in Section J.2.

1448 **J.1 Computing the Delaunay tessellation from the Voronoi diagram**

1449 In this section we prove Proposition 45, which we restate for convenience:

1450 ► **Proposition 45.** *Let  $T$  be a portalgon of  $n$  triangles. Let  $V$  be a set of vertices of  $T^1$ .*  
 1451 *Let  $\mathcal{V}$  be a subgraph of  $T^1$ . Assume that  $V$  is not empty and contains all singularities of*  
 1452  *$\mathcal{S}(T)$ , and that  $\mathcal{V}$  is the Voronoi diagram of  $(\mathcal{S}(T), V)$ . We can compute the portalgon of the*  
 1453 *Delaunay tessellation of  $(\mathcal{S}(T), V)$  in  $O(n)$  time.*

1454 In the setting of Proposition 45, our goal is to compute the portalgon of the Delaunay  
 1455 tessellation  $\mathcal{D}$  of  $(\mathcal{S}(T), V)$ . If we do not care about the shapes of the polygons in the  
 1456 portalgon, then we can easily compute this portalgon from the embedded graph  $\mathcal{V}$ , due  
 1457 to the duality between  $\mathcal{D}$  and  $\mathcal{V}$  (Lemma 43). All there remains to do is to compute the  
 1458 shape of each polygon in the portalgon. First we need a definition and a lemma. Consider  
 1459 a walk  $W$  in the dual of  $T^1$ . To ease the reading assume that every edge of  $T^1$  is incident  
 1460 to two distinct faces of  $T^1$ ; the following definition extends in a straightforward manner to  
 1461 general triangulations. In the plane  $\mathbb{R}^2$  realize the  $k \geq 1$  faces visited by  $W$  isometrically,  
 1462 and respecting their orientation, by respective triangles  $\Delta_1, \dots, \Delta_k$ . Make sure that for every  
 1463  $1 \leq i < k$  the triangles  $\Delta_i$  and  $\Delta_{i+1}$  agree on the placement of the  $i$ -th edge of  $T^1$  crossed by  
 1464  $W$ . The resulting sequence  $\Delta = (\Delta_1, \dots, \Delta_k)$  is an **unfolding** of  $W$ . In general a vertex  $w$   
 1465 of  $T^1$  may occur several times among the vertices of the triangles in  $\Delta$ , and those occurrences  
 1466 may be at distinct points in the plane. Nevertheless:

1467 ► **Lemma 46.** *If the faces of  $T^1$  visited by  $W$  are all included in the same face of  $\mathcal{V}$ , and if*  
 1468  *$w \in V$ , then all the occurrences of  $w$  in  $\Delta$  are at the same point of  $\mathbb{R}^2$ .*

1469 **Proof.** Let  $F$  be the face of  $\mathcal{V}$  containing the faces of  $T^1$  visited by  $W$ . By Lemma 42 the  
 1470 face  $F$  is homeomorphic to an open disk, and  $w$  is the unique point of  $V \cap F$ . Let  $\widehat{F}$  be  
 1471 the surface homeomorphic to a closed disk obtained by cutting the closure of  $F$  along the  
 1472 boundary of  $F$ . The angles at the corners of  $\widehat{F}$  are smaller than or equal to  $\pi$  by Lemma 42.  
 1473 So the shortest paths between those corners and  $w$  are, together with the boundary edges of  
 1474  $\widehat{F}$ , the edges of a triangulation  $Y$  of  $\widehat{F}$ . The dual of  $Y$  is a cycle, and  $w$  is the central vertex  
 1475 of  $Y$ . If  $\Delta$  is an unfolding of a walk in the dual of  $Y$ , then all occurrences of  $w$  in  $\Delta$  are at  
 1476 the same point in the plane. This easily extends to every other triangulation  $Y'$  of  $\widehat{F}$ , by  
 1477 considering a triangulation of  $\widehat{F}$  that contains both  $Y$  and  $Y'$ . ◀

1478 In the portalgon of  $\mathcal{D}$ , consider a polygon  $P$ . We describe how to compute the positions  
 1479 of the vertices of  $P$ . Note that these positions are only defined up to translating and rotating  
 1480  $P$  in the plane. As a preliminary, consider the vertex  $v$  of the Voronoi diagram  $\mathcal{V}$  that is  
 1481 dual to  $P$ . Embed a neighborhood of  $v$  in the plane  $\mathbb{R}^2$ , isometrically and respecting the  
 1482 orientation, by embedding the faces of  $T^1$  incident to  $v$ . This is possible because  $v$  is flat.

1483 Assign to each vertex  $x$  of  $P$  a point  $\pi_P(x) \in \mathbb{R}^2$  as follows. The vertex  $x$  of  $P$  is dual to  
 1484 an incidence  $c$  between the vertex  $v$  of  $\mathcal{V}$  and some face  $F$  of  $\mathcal{V}$ . In this incidence  $c$ , consider  
 1485 one of the faces  $W_0$  of  $T^1$  that we embedded in the plane, and its embedding  $W_0^*$ . Consider  
 1486 the unique point  $w \in V \cap F$  (Lemma 42). Consider a walk  $W$  in the dual of  $T^1$  that starts  
 1487 with  $W_0$ , remains in  $F$ , and visits at least one face of  $T^1$  incident to  $w$ . Unfold the faces  
 1488 visited by  $W$  in the plane, starting from  $W_0^*$ . Let  $\pi_P(x)$  be any occurrence of  $w$  in the  
 1489 unfolding.

1490 ► **Lemma 47.** *Up to translating and rotating  $P$ , the assignment  $\pi_P$  maps each vertex of  $P$*   
 1491 *to its position.*

1492 **Proof of Lemma 47.** Consider the maxi-disk  $(D, \varphi)$  of  $v$ . Without loss of generality  $\varphi$  agrees  
 1493 with the embedding of the neighborhood of  $v$  that we fixed as a preliminary. Recall from the  
 1494 definition of the Delaunay tessellation that  $P$  is the convex hull of  $\varphi^{-1}(V)$ . Let  $v^*$  be the  
 1495 middle point of  $D$  (the embedding of  $v$ ). The points in  $\varphi^{-1}(V)$  correspond to the incidences  
 1496 between  $v$  and the faces of  $\mathcal{V}$  around  $v$ . Consider such an incidence  $c$ , and its corresponding  
 1497 point  $y \in \varphi^{-1}(V)$ . Consider also the face  $F$  of  $\mathcal{V}$  that contains  $c$ . The geodesic path  $p$  from  
 1498  $v^*$  to  $y$  projects via  $\varphi$  to a shortest path  $\varphi \circ p$  from  $v$  to  $V$ . And  $\varphi \circ p$  immediately enters  $F$   
 1499 after leaving  $v$ . So the relative interior of  $\varphi \circ p$  is included in  $F$ , and thus ends at the unique  
 1500 point  $w \in V \cap F$ . By slightly perturbing  $p$  without changing its endpoints we may ensure  
 1501 that  $\varphi \circ p$  corresponds to a walk in the dual of  $T^1$ . Then  $y = \pi_P(x)$  by Lemma 46. This  
 1502 proves the lemma. ◀

1503 **Proof of Proposition 45.** We must compute the portalgon of the Delaunay tessellation  $\mathcal{D}$  of  
 1504  $(S, V)$ . We immediately compute the combinatorics of the portalgon from  $\mathcal{V}$ , because  $\mathcal{V}$  is  
 1505 isomorphic to the dual of  $\mathcal{D}$  by Lemma 43.

1506 Now, by Lemma 47, all there remains to do is to compute, for each polygon  $P$  of the  
 1507 portalgon, the assignment  $\pi_P$  of positions for the vertices of  $P$ . Achieving the claimed linear  
 1508 running time when doing so requires a slight technicality. Consider a face  $F$  of  $\mathcal{V}$ , and the  
 1509 point  $w \in V \cap F$ . Recall that for some faces  $W_0$  of  $T^1$  included in  $F$  we need to construct  
 1510 a walk  $W$  from  $W_0$  to  $w$  in the dual of  $T^1$ , unfold  $W$ , and retain the relative positions of  
 1511 some occurrences of  $W_0$  and  $w$  in the unfolding. Doing so independently for every face  $W_0$   
 1512 may take too long as we would visit faces of  $T^1$  several times. Instead we consider a single  
 1513 spanning tree  $Y$  in the dual of  $T^1$  within  $F$ , we unfold the faces of  $T^1$  that are included in  
 1514  $F$  along  $Y$ , and we retrieve all the required information from this unfolding. Note that the  
 1515 choice of  $Y$  does not matter, and that the unfolding may overlap. Doing so for all faces  $F$  of  
 1516  $\mathcal{V}$  takes linear time. ◀

## 1517 J.2 Computing the Voronoi diagram

1518 In this section we prove Proposition 44, which we restate for convenience:

1519 ▶ **Proposition 44.** *Let  $T$  be a portalgon of  $n$  triangles, of happiness  $h$ . Let  $V$  be a set of*  
 1520 *vertices of  $T^1$ . Assume that  $V$  is not empty and contains all singularities of  $\mathcal{S}(T)$ . We can*  
 1521 *compute in  $O(n^2 h \log(nh))$  time a portalgon  $T'$  of  $O(n^2 h)$  triangles, whose surface is  $\mathcal{S}(T)$ ,*  
 1522 *and a subgraph  $\mathcal{V}$  of  $T^1$ , such that  $\mathcal{V}$  is the Voronoi diagram of  $(\mathcal{S}(T), V)$ .*

1523 To prove Proposition 44 we revisit the single source shortest path algorithm described  
 1524 by Löffler, Ophelders, Silveira, and Staals [22]. In particular we extend their algorithm to  
 1525 multiple sources (we let the sources be the points in  $V$ ). The authors consider a triangulated  
 1526 surface, and compute the shortest paths emanating from a point  $x_0$  on the surface by  
 1527 decomposing the surface according to how those paths visit the faces of the triangulation.  
 1528 They describe a discrete process that simulates the propagation of some waves on the surface.  
 1529 Their waves all start from the point  $x_0$ . In the setting of Proposition 44, we adapt this  
 1530 strategy to simulate waves on  $\mathcal{S}(T)$  that start from all the points in  $V$ , so that the waves  
 1531 meet along the Voronoi diagram  $\mathcal{V}$  of  $(\mathcal{S}(T), V)$ . That simplifies the algorithm because waves  
 1532 now meet along a graph with geodesic edges (Lemma 42) and do not go through singularities.  
 1533 We now provide a formalization of this *wave algorithm*. The continuous propagation of  
 1534 waves is discretized by a propagation of *events*. A crucial feature of our formalization of the  
 1535 algorithm is that it operates on triangles, point sets, and Voronoi diagrams *in the plane*  $\mathbb{R}^2$ ,

## XX:38 Computing the Intrinsic Delaunay Triangulation of a Closed Polyhedral Surface

1536 never in the surface  $\mathcal{S}(T)$ . Only the proofs of correctness will argue on the surface  $\mathcal{S}(T)$ . We  
1537 will insist on that.

1538 Recall that the triangles of the input portalgon  $T$  lie in the Euclidean plane  $\mathbb{R}^2$ , and they  
1539 are disjoint. The reader can think of them as being far away from each other if this helps  
1540 the reading. The data structure maintains, for every triangle  $\Delta$  of  $T$ , a set  $X_\Delta$  of points in  
1541  $\mathbb{R}^2$ . We insist, again, that all these objects lie *in the plane*  $\mathbb{R}^2$ , not in the surface  $\mathcal{S}(T)$ .

1542 We need a definition. Given  $X \subset \mathbb{R}^2$  finite and  $x \in X$  we denote by  $\text{Vor}(x, X)$  the closed  
1543 cell of  $x$  in the Voronoi diagram of  $X$  in  $\mathbb{R}^2$ . Formally,  $\text{Vor}(x, X)$  contains the points  $y \in \mathbb{R}^2$   
1544 such that the distance between  $x$  and  $y$  is smaller than or equal to the distance between  $x'$   
1545 and  $y$  for every  $x' \in X$ .

1546 Central to the wave algorithm is the notion of candidate event that we now define.  
1547 Consider a triangle  $\Delta$  of  $T$ , a side  $s$  of  $\Delta$ , a point  $x \in \mathbb{R}^2$ , and some  $t > 0$ . The surface  
1548  $\mathcal{S}(T)$  being closed, there are a triangle  $\Delta'$  of  $T$  and a side  $s'$  of  $\Delta'$  such that  $s$  is matched  
1549 to  $s'$ . Consider the orientation-preserving isometry of  $\mathbb{R}^2$  that maps  $s$  to  $s'$  and puts  $\Delta$   
1550 side-by-side with  $\Delta'$ , apply this isometry to  $x$ , and consider the resulting point  $x' \in \mathbb{R}^2$ . The  
1551 tuple  $(t, \Delta, s, x)$  is a **candidate event** if it satisfies each of the following. First,  $x \notin X_\Delta$   
1552 and  $x' \in X_{\Delta'}$ . Second, the intersection between  $\text{Vor}(x', X_{\Delta'})$  and  $s'$  is not empty, and its  
1553 distance to  $x'$  is equal to  $t$ . In other words,  $t$  is equal to the smallest distance between  $x'$  and  
1554 a point of  $\text{Vor}(x', X_{\Delta'}) \cap s'$ . We say that  $t$  is the **date** of the candidate event  $(t, \Delta, s, x)$ .

1555 The data structure additionally maintains a list of the candidate events sorted by date.

1556 **Wave algorithm.** Initialize for each triangle  $\Delta$  of  $T$  the set  $X_\Delta$  with the vertices of  $\Delta$  that  
1557 correspond to points in  $V$ , if any. Then, as long as possible, consider any candidate event  
1558  $(t, \Delta, s, x)$  of smallest date  $t$ , add  $x$  to  $X_\Delta$ , and repeat. In the end return the sets  $(X_\Delta)_\Delta$ .

1559 Again, we insist that the wave algorithm operates *in the plane*  $\mathbb{R}^2$ . In particular the  
1560 sets  $X_\Delta$  are subsets of  $\mathbb{R}^2$ . Nevertheless, their Voronoi diagrams are related to the Voronoi  
1561 diagram of  $V$  on the surface  $\mathcal{S}(T)$ , and more strongly:

1562 ► **Proposition 48.** *The wave algorithm terminates after  $O(n^2h)$  iterations. In the end, for*  
1563 *every triangle  $\Delta$  of  $T$ , the intersection with  $\Delta$  of the Voronoi diagram of  $X_\Delta$  in  $\mathbb{R}^2$  is the*  
1564 *pre-image in  $\Delta$  of the Voronoi diagram of  $V$  in  $\mathcal{S}(T)$ .*

1565 It is easy to compute the list of the candidate events from the sets  $(X_\Delta)_\Delta$  in polynomial  
1566 time. More strongly:

1567 ► **Proposition 49.** *We can maintain the list of candidate events sorted by date through  $k$*   
1568 *insertions of points in the sets  $(X_\Delta)_\Delta$  in  $O(k \log k)$  total time.*

1569 Proposition 44 is immediate from Proposition 48 and Proposition 49:

1570 **Proof of Proposition 44.** Proposition 48 and Proposition 49 imply that the wave algorithm  
1571 can be performed in  $O(n^2 \cdot h \cdot \log(nh))$  time. Consider the returned sets  $(X_\Delta)_\Delta$ . The sum  
1572 of the cardinalities of the sets  $X_\Delta$ , summed over all the triangles  $\Delta$  of  $T$ , is  $O(n^2h)$  by  
1573 Proposition 48. Also, for every triangle  $\Delta$ , the intersection with  $\Delta$  of the Voronoi diagram of  
1574  $X_\Delta$  in  $\mathbb{R}^2$  is the pre-image in  $\Delta$  of the Voronoi diagram of  $V$  in  $\mathcal{S}(T)$ , by Proposition 48.  
1575 Cutting each triangle  $\Delta$  along the Voronoi diagram of  $X_\Delta$ , and cutting the resulting polygons  
1576 into triangles along vertex-to-vertex arcs, provides the desired triangular portalgon  $T'$ , along  
1577 with  $\mathcal{V}$ . ◀

1578 The rest of this section is dedicated to the proofs of Proposition 48 and Proposition 49.

1579 **J.2.1 Proof of Proposition 48**

1580 In this section we prove Proposition 48. Recall that the triangles of the portalgon  $T$  are  
 1581 realized dis-jointly in the Euclidean plane  $\mathbb{R}^2$ , and that we think of these triangles as being  
 1582 far away from each other, this will help the reading. It is now convenient to introduce a  
 1583 notation for the projection of this disjoint union of triangles onto the surface  $\mathcal{S}(T)$ , so we let  
 1584  $\rho$  be this projection.

1585 Given a triangle  $\Delta$  of  $T$ , we consider the immersed empty disks  $(D, \varphi)$  such that the  
 1586 center of  $D$  belongs to  $\Delta$ , and such that  $\varphi$  agrees with  $\rho$  on  $\overline{D} \cap \Delta$ . We say that  $(D, \varphi)$  is an  
 1587 immersed empty disk **attached to  $\Delta$** . We further consider the union of the sets  $\varphi^{-1}(V)$  over  
 1588 the immersed empty disks  $(D, \varphi)$  attached to  $\Delta$ . We call this union the **constellation** of  $\Delta$ ,  
 1589 and we denote it by  $V_\Delta$ . We will show that the sets  $X_\Delta$  computed by the wave algorithm are  
 1590 exactly the constellations  $V_\Delta$ . Before that, we have two preliminary lemmas on constellations.

1591 First, the constellations, while lying *in the plane*  $\mathbb{R}^2$ , are related to the Voronoi diagram  
 1592 of  $V$  *in the surface*  $\mathcal{S}(T)$ :

1593 **► Lemma 50.** *For every triangle  $\Delta$  of  $T$  the intersection with  $\Delta$  of the Voronoi diagram of*  
 1594 *the constellation  $V_\Delta$  is the pre-image in  $\Delta$  of the Voronoi diagram of  $V$  in  $\mathcal{S}(T)$ .*

1595 The proof of Lemma 50 relies on the following, which will be used again:

1596 **► Lemma 51.** *Let  $(D, \varphi)$  be an immersed empty disk attached to a triangle  $\Delta$  of  $T$ . Then*  
 1597  *$V_\Delta \cap \overline{D} = \varphi^{-1}(V)$ . In particular  $V_\Delta \cap D = \emptyset$ .*

1598 **Proof.** We have  $V_\Delta \cap \overline{D} \supseteq \varphi^{-1}(V)$  by definition of the constellation  $V_\Delta$ . The other inclusion  
 1599 is immediate from the fact that if two immersed empty disks  $(D, \varphi)$  and  $(D', \varphi')$  are attached  
 1600 to  $\Delta$  then  $\varphi$  and  $\varphi'$  agree on  $\overline{D} \cap \overline{D}'$ . Finally  $\varphi^{-1}(V) \cap D = \emptyset$  by definition of an immersed  
 1601 empty disk (recall that  $D$  is open). ◀

1602 **Proof of Lemma 50.** Consider a point  $x \in \Delta$ . There is a unique immersed empty disk  $(D, \varphi)$   
 1603 attached to  $\Delta$  such that the center of  $D$  is  $x$ , and such that the radius of  $D$  is maximum.  
 1604 Then  $\varphi^{-1}(V) \neq \emptyset$  because the radius of  $D$  is maximum. And  $\varphi^{-1}(V) = V_\Delta \cap \overline{D}$  by Lemma 51.  
 1605 The geodesic path(s) between  $x$  and the point(s) in  $\varphi^{-1}(V)$  corresponds via  $\varphi$  to the shortest  
 1606 path(s) between  $\rho(x)$  and  $V$ . So  $\rho(x)$  belongs to the Voronoi diagram of  $V$  in  $\mathcal{S}(T)$  if and  
 1607 only if  $\varphi^{-1}(V)$  contains several points, equivalently  $V_\Delta \cap \overline{D}$ , which is the case if and only if  
 1608  $x$  belongs to the Voronoi diagram of  $V_\Delta$  in  $\mathbb{R}^2$ . ◀

1609 Second, the cardinalities of the constellations are bounded by the number  $n$  of triangles  
 1610 and the happiness  $h$  of the portalgon  $T$ :

1611 **► Lemma 52.** *For every triangle  $\Delta$  of  $T$  the constellation  $V_\Delta$  has cardinality  $O(nh)$ .*

1612 **Proof.** Given a triangle  $\Delta$  of  $T$ , and a point  $x$  in the constellation  $V_\Delta$ , there is by definition  
 1613 an immersed empty disk  $(D, \varphi)$  attached to  $\Delta$  such that  $x \in \varphi^{-1}(V)$ . And the center  $y$   
 1614 of  $D$  belongs to  $\Delta$ . Then the geodesic segment between  $y$  and  $x$  projects via  $\rho$  to a path  
 1615 between  $\rho(y)$  and  $\rho(x)$ , and the length of this path is the smallest possible among all the  
 1616 paths between  $\rho(y)$  and a point of  $V$  (possibly another point of  $V$  than  $\rho(x)$ ). We will argue  
 1617 on such shortest paths between a point of  $\mathcal{S}(T)$  and the set  $V$ .

1618 We call regions the following subsets of  $\mathcal{S}(T)$ : a vertex of  $T^1$ , the relative interior of an  
 1619 edge of  $T^1$ , and a face of  $T^1$ . The regions partition  $\mathcal{S}(T)$ . For every shortest path  $p$  between  
 1620 a point  $x \in \mathcal{S}(T)$  and the set  $V$ , record the sequence of regions intersected by  $p$  when directed  
 1621 from  $V$  to  $x$ . If two such paths  $p$  and  $p'$  end in  $\rho(\Delta)$  and have the same sequence then they

## XX:40 Computing the Intrinsic Delaunay Triangulation of a Closed Polyhedral Surface

1622 correspond to the same point in the constellation  $V_\Delta$ . We claim that for every region  $R$  there  
1623 are  $O(nh)$  sequences ending with  $R$ . This claim implies the lemma. Let us prove the claim.  
1624 We say that a sequence is maximal if it is not a strict prefix of another sequence. And we  
1625 say that a sequence is critical if it is the maximal common prefix of two distinct maximal  
1626 sequences. Every critical sequence ends with a face of  $T^1$ . For every face  $R'$  of  $T^1$  there is at  
1627 most one critical sequence ending with  $R'$ . Indeed every critical sequence is realized by two  
1628 distinct paths. If two distinct critical sequences were to end with  $R'$ , then at least two of the  
1629 four associated paths would cross, and thus could be shortened, a contradiction. We proved  
1630 that there are  $O(n)$  critical sequences. So there are  $O(n)$  maximal sequences. And every  
1631 sequence contains  $O(h)$  occurrences of  $R$  because the happiness of  $T$  is equal to  $h$ . This  
1632 proves the claim, and the lemma.  $\blacktriangleleft$

1633 We will now show that the wave algorithm computes the constellations. To do so, we  
1634 introduce an invariant. We need a definition. Fix a point  $x \in V_\Delta$ , and consider all the  
1635 immersed empty disks  $(D, \varphi)$  attached to  $\Delta$  such that  $x \in \varphi^{-1}(V)$ . Among all these immersed  
1636 empty disks  $(D, \varphi)$ , the smallest radius of  $D$  is the **depth** of  $x$  in  $V_\Delta$ .

1637 **invariant.** There is  $\tau > 0$  such that both of the following hold for every triangle  $\Delta$  of  $T$ .  
1638 Every point of  $X_\Delta$  belongs to the constellation  $V_\Delta$ . And every point of  $V_\Delta \setminus X_\Delta$  has depth  
1639 greater than or equal to  $\tau$  in  $V_\Delta$ .

1640 It is not clear a priori that the invariant is maintained by the wave algorithm, and this  
1641 will be proved only at the end, when proving Proposition 48. Before that we need some  
1642 lemmas.

1643  $\blacktriangleright$  **Lemma 53.** *Assume that the invariant holds for some  $\tau > 0$ , and that there is a candidate*  
1644 *event  $(t, \Delta, s, x)$  such that  $t \leq \tau$ . Then  $t = \tau$ ,  $x$  belongs to  $V_\Delta$ , and the depth of  $x$  in  $V_\Delta$*   
1645 *is equal to  $\tau$ .*

1646 **Proof.** We claim that  $x \in V_\Delta$ , and that the depth of  $x$  in  $V_\Delta$  is smaller than or equal to  
1647  $t$ . The claim implies the lemma. Indeed we assumed  $t \leq \tau$ . And, if  $x \in V_\Delta$ , then the  
1648 depth of  $x$  in  $V_\Delta$  cannot be smaller than  $\tau$ , for otherwise the invariant would imply  $x \in X_\Delta$ ,  
1649 contradicting the fact that  $(t, \Delta, s, x)$  is a candidate event. All there remains to do is to  
1650 prove the claim.

1651 To do so consider the triangle  $\Delta'$  of  $T$  and the side  $s'$  of  $\Delta'$  such that  $s$  is matched to  $s'$ .  
1652 Consider the orientation-preserving isometry of  $\mathbb{R}^2$  that maps  $s$  to  $s'$  and puts  $\Delta$  side-by-side  
1653 with  $\Delta'$ , apply this isometry to  $x$ , and consider the resulting point  $x' \in \mathbb{R}^2$ . Using the  
1654 assumption that  $(t, \Delta, s, x)$  is a candidate event, the point  $x'$  belongs to  $X_{\Delta'}$ , while  $x$  does  
1655 not belong to  $X_\Delta$ . Moreover there is a point  $z'$  along  $s'$  such that  $x'$  is at distance  $t$  from  $z'$ ,  
1656 and such that no point of  $X_{\Delta'}$  is closer to  $z'$  than  $x'$ . Consider the immersed empty disk  
1657  $(D', \varphi')$  attached to  $\Delta'$  such that the center of  $D'$  is  $z'$ , and such that the radius of  $D'$  is  
1658 maximum.

1659 By contradiction, assume that the radius of  $D'$  is smaller than  $t$ . There is a point  
1660  $v \in \varphi'^{-1}(V)$  because the radius of  $D'$  is maximum. We have  $v \in V_{\Delta'}$ , and the depth of  $v$  in  
1661  $V_{\Delta'}$  is smaller than or equal to the radius of  $D'$ , which is smaller than  $\tau$ . So  $v$  belongs to  
1662  $X_{\Delta'}$  by the invariant. But then  $v$  is a point of  $X_{\Delta'}$  closer to  $z'$  than  $x'$ , a contradiction.

1663 We proved that the radius of  $D'$  is greater than or equal to  $t$ . Then  $x'$  belongs to  $\bar{D}$ .  
1664 Moreover  $x'$  belongs to  $X_{\Delta'}$ , and thus to  $V_{\Delta'}$  by the invariant. Therefore  $x'$  belongs to  
1665  $\varphi'^{-1}(V)$  by Lemma 51. In particular the radius of  $D'$  is equal to  $t$ .

1666 It is now convenient to name the orientation-preserving isometry of  $\mathbb{R}^2$  that maps  $s$  to  $s'$   
1667 and puts  $\Delta$  side-by-side with  $\Delta'$ , so let  $\lambda : \mathbb{R}^2 \rightarrow \mathbb{R}^2$  be this isometry. Consider the point

1668  $z = \lambda^{-1}(z')$ , and the immersed empty disk  $(D, \varphi)$  attached to  $\Delta$  such that the center of  $D$  is  
 1669  $z$ , and such that the radius of  $D$  is maximum. Observe that  $\lambda(D) = D'$ , and that  $\varphi' \circ \lambda = \varphi$ .  
 1670 In particular the radius of  $D$  is also  $t$ . And, crucially,  $x \in \varphi^{-1}(V)$ , because we already proved  
 1671  $x' \in \varphi'^{-1}(V)$ . This proves that  $x \in V_\Delta$ . And the depth of  $x$  in  $V_\Delta$  is smaller than or equal  
 1672 to the radius of  $D$ , which is  $t$ . The claim is proved, along with the lemma. ◀

1673 ▶ **Lemma 54.** *Assume that the invariant holds for some  $\tau > 0$ . Further assume that there is*  
 1674 *a triangle  $\Delta$  of  $T$  such that  $V_\Delta \setminus X_\Delta$  contains a point whose depth in  $V_\Delta$  is  $\tau$ . Then there is*  
 1675 *a candidate event whose date is smaller than or equal to  $\tau$ .*

1676 The proof of Lemma 54 relies on the following:

1677 ▶ **Lemma 55.** *Let  $(D, \varphi)$  be an immersed empty disk attached to a triangle  $\Delta$  of  $T$ . Assume*  
 1678 *that there is  $x \in \varphi^{-1}(V)$ , and let  $y$  be the center of  $D$ . If the geodesic segment between  $x$*   
 1679 *and  $y$  intersect  $\Delta$  in any other point than  $y$  then the depth of  $x$  in  $V_\Delta$  is smaller than the*  
 1680 *radius of  $D$ .*

1681 **Proof.** Assuming that the geodesic segment between  $x$  and  $y$  intersects  $\Delta$  in a point  $y' \neq y$   
 1682 (at least), consider the open disk  $D'$  whose center is  $y'$  and whose boundary circle contains  
 1683  $x'$ . Then  $D' \subset D$ . Let  $\varphi'$  be the restriction of  $\varphi$  to  $\overline{D'}$ . Then  $(D', \varphi')$  is an immersed empty  
 1684 disk,  $\varphi'$  agrees with  $\rho$  on  $\Delta \cap \overline{D'}$ , and  $x \in \varphi'^{-1}(V)$ . So the depth of  $x$  in  $V_\Delta$  is smaller than  
 1685 or equal to the radius of  $D'$ , which is smaller than the radius of  $D$ . ◀

1686 **Proof of Lemma 54.** Consider a point  $x \in V_\Delta \setminus X_\Delta$  that has depth  $\tau$  in  $V_\Delta$ . There is an  
 1687 immersed empty disk  $(D, \varphi)$  that satisfies each of the following. Let  $y$  be the center of  $D$ .  
 1688 Then  $y$  belongs to  $\Delta$ , the radius of  $D$  is  $\tau$ ,  $\varphi$  agrees with  $\rho$  on  $\overline{D} \cap \Delta$ , and  $x \in \varphi^{-1}(V)$ . In  
 1689 top of that we can add that  $y$  belongs to the boundary of  $\Delta$ , for otherwise the depth of  $x$  in  
 1690  $V_\Delta$  would be smaller than  $\tau$  by Lemma 55, a contradiction. There are two cases: either  $y$   
 1691 lies in the relative interior of a side of  $\Delta$ , or  $y$  is a vertex of  $\Delta$ .

### 1692 J.2.1.1 First case

1693 First consider the case where  $y$  lies in the relative interior of a side  $s$  of  $\Delta$ . In this case we  
 1694 shall prove that there is  $t \leq \tau$  such that  $(t, \Delta, s, x)$  is a candidate event. The surface  $\mathcal{S}(T)$   
 1695 being closed, there are a triangle  $\Delta'$  of  $T$ , and a side  $s'$  of  $\Delta'$ , such that  $s$  is matched to  
 1696  $s'$ . Consider the orientation-preserving isometry  $\lambda : \mathbb{R}^2 \rightarrow \mathbb{R}^2$  that maps  $s$  to  $s'$  and puts  
 1697  $\Delta$  side-by-side with  $\Delta'$ . We consider the points  $x' = \lambda(x)$  and  $y' = \lambda(y)$ , the open disk  
 1698  $D' = \lambda(D)$ , and the map  $\varphi' = \varphi \circ \lambda^{-1}$ . Observe that  $(D', \varphi')$  is an immersed empty disk  
 1699 attached to  $\Delta'$ , that the center of  $D'$  is  $y'$ , and that  $x'$  belongs to the boundary circle of  $D'$ .  
 1700 Informally,  $x'$ ,  $y'$ , and  $(D', \varphi')$  correspond to  $x$ ,  $y$ , and  $(D, \varphi)$ , but in the reference frame of  
 1701  $\Delta'$ .

1702 We claim that  $x'$  belongs to  $X_{\Delta'}$ . To prove the claim consider the geodesic line  $L$   
 1703 supported by  $s$ , and direct  $L$  so that  $\Delta$  is on the *right* of  $L$ . Similarly, consider the geodesic  
 1704 line  $L' = \lambda(L)$ . Then  $L'$  is supported by  $s'$ , and  $\Delta'$  is on the *left* of  $L'$ . We have that  $x$   
 1705 lies strictly on the left of  $L$ , for otherwise the depth of  $x$  in  $V_\Delta$  would be smaller than  $\tau$  by  
 1706 Lemma 55, a contradiction. So  $x'$  lies (strictly) on the left of  $L'$ . And so the depth of  $x'$   
 1707 in  $V_{\Delta'}$  is smaller than  $\tau$  by Lemma 55. Therefore  $x' \in X_{\Delta'}$  by the invariant. The claim is  
 1708 proved.

1709 We use the claim immediately,  $x'$  belongs to  $X_{\Delta'}$ . No point of  $X_{\Delta'}$  is closer to  $y'$  than  $x'$ ,  
 1710 because  $X_{\Delta'} \subseteq V_{\Delta'}$  by the invariant, and because  $D' \cap V_{\Delta'} = \emptyset$  by Lemma 51. So  $\text{Vor}(x', X_{\Delta'})$   
 1711 intersects  $s'$  (at least in  $y'$ ), and its intersection with  $s'$  is at distance a distance  $t \leq \tau$  from

## XX:42 Computing the Intrinsic Delaunay Triangulation of a Closed Polyhedral Surface

1712  $x'$  (because the distance between  $y'$  and  $x'$  is  $\tau$ ). The tuple  $(t, \Delta, s, x)$  is a candidate event.  
1713 We are done in this case.

### 1714 Second case.

1715 Now consider the case where  $y$  is a vertex of  $\Delta$ . Then  $\rho(y)$  is a vertex of the graph  $T^1$   
1716 embedded on  $\mathcal{S}(T)$ . Note also that  $\rho(y)$  lies in the interior of  $\mathcal{S}(T)$  because  $\mathcal{S}(T)$  has no  
1717 boundary. And  $\rho(y)$  is flat as it does not belong to  $V$ . We assume that no face of  $T^1$  appears  
1718 twice around  $y$ , for this eases the reading, and the proof trivially extends to the general case.  
1719 Consider the  $k \geq 3$  faces of  $T^1$  incident to  $\rho(y)$ , in order around  $\rho(y)$  (clockwise say, but  
1720 counter-clockwise would do too), and the corresponding triangles  $\Delta_0, \dots, \Delta_{k-1}$  of  $T$ , with  
1721  $\Delta_0 = \Delta$ . We fix  $\Delta_0$ , and we place copies of the triangles  $\Delta_1, \dots, \Delta_{k-1}$  around  $y$ , in order.  
1722 This is possible because  $\rho(y)$  is flat. For each  $i$  we record the orientation-preserving isometry  
1723  $\lambda_i : \mathbb{R}^2 \rightarrow \mathbb{R}^2$  that maps the copy of  $\Delta_i$  around  $y$  to the original triangle  $\Delta_i$ . We consider  
1724 the points  $x_i = \lambda_i(x)$  and  $y_i = \lambda_i(y)$ . Also we consider the open disk  $D_i = \lambda_i(D)$  and the  
1725 map  $\varphi_i = \varphi \circ \lambda_i^{-1}$ . Observe that  $(D_i, \varphi_i)$  is an immersed empty disk attached to  $\Delta_i$ , that  
1726 the center of  $D_i$  is  $y_i$ , and that  $x_i$  belongs to the boundary circle of  $D_i$ . Informally,  $x_i, y_i$ ,  
1727 and  $(D_i, \varphi_i)$  correspond to  $x, y$ , and  $(D, \varphi)$ , but in the reference frame of  $\Delta_i$ .

1728 We claim that there is  $i$  such that  $x_i \in X_{\Delta_i}$ . Indeed there is  $i$  such that the geodesic  
1729 segment between  $y$  and  $x$  intersects the copied triangle  $\lambda_i^{-1}(\Delta_i)$  in another point than  $y$ .  
1730 Then the geodesic segment between  $y_i$  and  $x_i$  intersects  $\Delta_i$  in another point than  $y$ . So  $x_i$   
1731 belongs to  $V_{\Delta_i}$  and has depth smaller than  $\tau$  in  $V_{\Delta_i}$ , by Lemma 55 applied to  $\Delta_i, (D_i, \varphi_i)$ ,  
1732  $x_i$ , and  $y_i$ . And so  $x_i \in X_{\Delta_i}$  by the invariant. The claim is proved.

1733 Using the claim immediately, and because  $x_0 \notin X_{\Delta_0}$ , there is  $i$  such that  $x_i \in X_{\Delta_i}$  and  
1734  $x_{i+1} \notin X_{\Delta_{i+1}}$ , indices are modulo  $k$ . Consider the side  $s_i$  of  $\Delta_i$  that is matched to a side of  
1735  $\Delta_{i+1}$ . We shall prove that there is  $t \leq \tau$  such that  $(t, \Delta_i, s_i, x_i)$  is a candidate event. To  
1736 do so first observe that no point of  $X_{\Delta_i}$  is closer to  $y_i$  than  $x_i$  because  $X_{\Delta_i} \subseteq V_{\Delta_i}$  by the  
1737 invariant, and because  $D_i \cap V_{\Delta_i} = \emptyset$  by Lemma 51. So  $\text{Vor}(x_i, X_{\Delta_i})$  intersects  $s_i$  (at least in  
1738  $y_i$ ), and its intersection with  $s_i$  is at a distance  $t \leq \tau$  from  $x_i$  (because the distance between  
1739  $y_i$  and  $x_i$  is  $\tau$ ). The tuple  $(t, \Delta_i, s_i, x)$  is a candidate event. We are done in this case. The  
1740 lemma is proved. ◀

1741 **Proposition 48.** First we prove that the invariant holds throughout the execution of the wave  
1742 algorithm. To prove the claim first observe that the invariant holds after the initialization  
1743 phase. Now assume that it holds at the beginning of an iteration of the loop, for some  $\tau > 0$ ,  
1744 and that there is a candidate event  $(t, \Delta, s, x)$ , of smallest date  $t$ . If every triangle  $\Delta$  of  $T$   
1745 satisfies  $X_\Delta = V_\Delta$  then the invariant holds for every  $\tau > 0$  anyway. Otherwise there are  
1746 without loss of generality a triangle  $\Delta$  and a point in  $V_\Delta \setminus X_\Delta$  whose depth in  $V_\Delta$  is  $\tau$ , so  
1747 there is a candidate event whose date is smaller than or equal to  $\tau$  by Lemma 54. In any  
1748 case  $t \leq \tau$  holds without loss of generality. Then  $t = \tau$ ,  $x$  belongs to  $V_\Delta$ , and the depth of  $x$   
1749 in  $V_\Delta$  is equal to  $\tau$  by Lemma 53. So, after adding  $x$  to  $X_\Delta$ , the invariant still holds. This  
1750 proves that the invariant holds throughout the execution of the wave algorithm.

1751 The wave algorithm never adds twice the same point in a set  $X_\Delta$  of a triangle  $\Delta$  of  $T$ .  
1752 Moreover  $X_\Delta \subseteq V_\Delta$  by the invariant. And the cardinality of  $V_\Delta$  is  $O(nh)$  by Lemma 52. So  
1753 the wave algorithm terminates after  $O(n^2h)$  iterations. The algorithm does not stop until  
1754  $X_\Delta = V_\Delta$  for every triangle  $\Delta$  of  $T$ , by Lemma 54. And the sets  $(V_\Delta)_\Delta$  are as desired by  
1755 Lemma 50. The lemma is proved. ◀

1756 **J.2.2 Proof of Proposition 49**

1757 In this section we prove Proposition 49, that during the wave algorithm the list of the candidate  
 1758 events sorted by date can be maintained in amortized  $O(\log(nh))$  time per insertion of a  
 1759 point in the set  $X_\Delta$  of a triangle  $\Delta$ .

1760 The crux of the matter is to maintain the intersection of a Voronoi diagram in  $\mathbb{R}^2$  with  
 1761 a closed segment of  $\mathbb{R}^2$  in a dynamic manner while adding the sources one-by-one to the  
 1762 Voronoi diagram. To do that we consider a game that we play with Alice. Informally, Alice  
 1763 sends us the sources of the Voronoi diagram one-by-one, and we tell her what is changed  
 1764 after each insertion of a source. Formally, Alice initially sends us a closed segment  $I$  of  $\mathbb{R}^2$ .  
 1765 Then Alice sends us  $k \geq 1$  pairwise distinct points  $z_1, \dots, z_k \in \mathbb{R}^2$  in this order. We do not  
 1766 know the points before they are sent to us by Alice, nor the number of points to be sent. For  
 1767 each  $i \in [k]$ , after the  $i$ -th point  $z_i$  is sent to us by Alice, and before  $i + 1$ -th point  $z_{i+1}$  is  
 1768 sent to us, we must send two things to Alice. First, we must send the set  $U_i \subseteq [i]$  containing  
 1769 the index  $i$  together with the indices  $j \in [i - 1]$  such that  $\text{Vor}(z_j, Z_i) \cap I \neq \text{Vor}(z_j, Z_{i-1}) \cap I$ .  
 1770 Second, for each index  $j \in U_i$ , we must send the (possibly empty) set  $\text{Vor}(z_j, Z_i) \cap I$ . Note  
 1771 that each set  $\text{Vor}(z_j, Z_i) \cap I$  is a closed segment of  $\mathbb{R}^2$ , so it is either empty, a single point,  
 1772 or has two distinct endpoints by which it is uniquely determined. We have two lemmas:

1773 **► Lemma 56.** *The sum over  $1 \leq i \leq k$  of the cardinality of the set  $U_i$  is smaller than or*  
 1774 *equal to  $5k$ .*

1775 **Proof.** Consider  $i \in [k]$ . We claim that at most four indices  $j \in U_i$  are such that  $\text{Vor}(z_j, Z_i)$   
 1776 intersects  $I$ . The claim immediately implies the lemma.

1777 To prove the claim we consider the subset  $Y$  of  $I$  that contains the points that are strictly  
 1778 closer to  $z_i$  than to any point of  $Z_{i-1}$ . And we consider the closure  $X$  of  $Y$ . Then  $X$  is a  
 1779 closed segment of  $\mathbb{R}^2$  and, assuming that  $U_i$  is not empty, we have that  $Y$  is not empty, so  $X$   
 1780 is not empty, and  $X$  is not a single point either. Informally, we now consider the two “ends”  
 1781 of  $X$ . Formally, we consider the two endpoints  $x_0$  and  $x_1$  of  $X$ , and for each  $\varepsilon \in \{0, 1\}$ ,  
 1782 we consider an arbitrarily short closed segment  $X_\varepsilon \subset X$ , not a single point, that contains  
 1783  $x_\varepsilon$ . Provided  $X_\varepsilon$  is short enough, there are no more than two indices  $j \in U_i$  such that the  
 1784 relative interior of  $X_\varepsilon$  is included in  $\text{Vor}(z_j, Z_{i-1})$ .

1785 On the other hand if  $j \in U_i$  is such that  $\text{Vor}(z_j, Z_i)$  intersects  $I$ , then not only  $\text{Vor}(z_j, Z_{i-1})$   
 1786 also intersects  $I$ , but  $\text{Vor}(z_j, Z_{i-1}) \cap I$  contains a point in  $Y$  and a point not in  $Y$ , so it  
 1787 contains the relative interior of  $X_\varepsilon$  for some  $\varepsilon \in \{0, 1\}$ . This proves the claim, and the  
 1788 lemma. ◀

1789 **► Lemma 57.** *There is an algorithm that receives  $I$  and  $z_1, \dots, z_k$  in this order, and that,*  
 1790 *after receiving  $z_i$ ,  $i \in [k]$ , returns  $U_i$  together with the closed segments  $\text{Vor}(z_j, Z_i) \cap I$  for all*  
 1791  *$j \in U_i$ , and runs in  $O(k \log k)$  total time.*

1792 **Proof.** Consider  $i \in [k]$ , and assume that the point  $z_i$  has just been sent by Alice. We  
 1793 must return to Alice. The crux of the matter is to have maintained at this point the list  
 1794 of tuples  $(j, \text{Vor}(z_j, Z_{i-1}) \cap I)$  over  $j \in [i - 1]$ , ordered by the position of  $\text{Vor}(z_j, Z_{i-1}) \cap I$   
 1795 along  $I$  (for some direction of  $I$ , and resolving any ambiguity arbitrarily). Now we can use  
 1796 the list to answer Alice, and update the list, as follows. Given a tuple  $(j, \text{Vor}(z_j, Z_{i-1}) \cap I)$   
 1797 we can determine in constant time whether  $j \in U_i$  by checking whether there is a point of  
 1798  $\text{Vor}(j, Z_{i-1}) \cap I$  that is strictly closer to  $z_i$  than to  $z_j$ . If  $j \notin U_i$ , then either all the tuples  
 1799  $(j', \text{Vor}(z_{j'}, Z_{i-1}) \cap I)$  before  $(j, \text{Vor}(z_j, Z_{i-1}) \cap I)$  in the list are such that  $j' \notin U_i$ , or all the  
 1800 tuples after  $(j, \text{Vor}(z_j, Z_{i-1}) \cap I)$  are like that, and we can find out which case it is in constant  
 1801 time. So we can list by dichotomy the  $k' \geq 0$  tuples  $(j, \text{Vor}(z_j, Z_{i-1}) \cap I)$  such that  $j \in U_i$

## XX:44 Computing the Intrinsic Delaunay Triangulation of a Closed Polyhedral Surface

1802 in  $O(k' + \log k)$  time. For each such tuple  $(j, \text{Vor}(z_j, Z_{i-1}) \cap I)$ , we derive  $\text{Vor}(z_j, Z_i) \cap I$   
1803 from  $\text{Vor}(z_j, Z_{i-1})$ ,  $z_j$ , and  $z_i$  in constant time. In the end we compute  $\text{Vor}(z_i, Z_i) \cap I$  in  
1804  $O(\log k)$  time by finding by dichotomy the first and last tuples  $(j, \text{Vor}(z_j, Z_{i-1})$  such that  
1805  $\text{Vor}(z_j, Z_{i-1}) \cap I$  contains a point that is at least as close to  $z_i$  than to  $z_j$ , if any. This way  
1806 we can return to Alice, and update the list of tuples, in  $O(k' + \log k)$  total time. Lemma 56  
1807 concludes. ◀

1808 In the following, when maintaining the list of candidate events, we also maintain appro-  
1809 priate search trees in which we store the candidate events, so that the candidate events can  
1810 be accessed by date or position in logarithmic time.

1811 **Proof of Proposition 49.** When inserting a point  $x$  in the set  $X_\Delta$  of a triangle  $\Delta$ , we  
1812 maintain the list of candidate events sorted by date as follows. First, we find the candidate  
1813 events of the form  $(\cdot, \Delta, \cdot, x)$ , and we remove these candidate events from the list. All but  
1814  $O(\log k)$  of the time spent here is amortized by the fact that every event deleted here was  
1815 created earlier in the execution of the algorithm.

1816 Second, for every side  $s$  of  $\Delta$ , we consider the triangle  $\Delta'$  and the side  $s'$  of  $\Delta'$  such  
1817 that  $s$  is matched to  $s'$ , along with the orientation-preserving isometry  $\lambda : \mathbb{R}^2 \rightarrow \mathbb{R}^2$  that  
1818 maps  $s$  to  $s'$  and puts  $\lambda(\Delta)$  and  $\Delta'$  side by side. Among the candidate events of the form  
1819  $(\cdot, \Delta', s', \lambda(y))$ ,  $y \in X_\Delta$ , those for which  $\text{Vor}(y, X_\Delta \cup \{x\}) \cap s \neq \text{Vor}(y, X_\Delta) \cap s$  may have to  
1820 be updated. If  $\text{Vor}(y, X_\Delta \cup \{x\}) \cap s = \emptyset$ , then the event must be deleted. Otherwise, only the  
1821 date of the event may change. This is done in amortized  $O(\log k)$  time using Lemma 57.

1822 Finally, Lemma 57 also provides us with the set  $\text{Vor}(x, X_\Delta \cup \{x\}) \cap s$ . If this set is not  
1823 empty, and if  $\lambda(x) \notin X_{\Delta'}$ , then we consider the distance  $t$  between  $x$  and  $\text{Vor}(x, X_\Delta \cup \{x\}) \cap s$ ,  
1824 and we create the event  $(t, s', \Delta', \lambda(x))$ , in  $O(\log k)$  time. ◀

### 1825 **K Appendix: applications of Theorem 1**

1826 Theorem 1 has two interesting applications. First, recall that Delaunay triangulations have  
1827 bounded happiness [22, Section 4]. Combined with Theorem 1 we obtain:

1828 ▶ **Corollary 58.** *Let  $T$  be a portalgon of  $n$  triangles, of aspect ratio  $r$ , whose surface  $\mathcal{S}(T)$   
1829 is closed. One can compute in  $O(n^3 \log^2(n) \cdot \log^4(r))$  time a portalgon  $T'$  of  $O(n)$  triangles,  
1830 whose surface is  $\mathcal{S}(T)$ , and whose happiness is  $O(1)$ .*

1831 **Proof of Corollary 58.** Apply Theorem 1 to compute the portalgon  $T'$  of the Delaunay  
1832 tessellation of  $\mathcal{S}(T)$  in  $O(n^3 \log^2(n) \cdot \log^4(r))$  time. Some polygons of  $T'$  may not be triangles.  
1833 Cut the polygons of  $T'$  that are not triangles (if any) along vertex-to-vertex arcs to obtain  
1834 a triangular portalgon  $T''$ . Then  $T''$  is the portalgon of a Delaunay triangulation of  $\mathcal{S}(T)$ ,  
1835 so  $T''$  has bounded happiness by the result of Löffler, Ophelders, Silveira, and Staals [22,  
1836 Section 4]. Moreover the vertex set of its 1-skeleton  $T''^1$  is exactly the set of singularities of  
1837  $\mathcal{S}(T)$ , except if  $\mathcal{S}(T)$  is a flat torus in which case  $T''^1$  has exactly one vertex, so in any case  
1838  $T''$  has  $O(n)$  triangles. ◀

1839 On the portalgon  $T'$  returned by Corollary 58 the single-source shortest path algorithm  
1840 of Löffler, Ophelders, Silveira, and Staals [22, Section 3] would run in time  $O(n^2 \log^{O(1)}(n))$ ,  
1841 so that:

1842 ▶ **Observation 59.** *On the portalgon  $T'$ , one can compute a shortest path between two given  
1843 points in time  $O(n^2 \log^{O(1)}(n))$ .*

1844        Second, Theorem 1 enables us to test whether the surfaces of two given portalgons are  
 1845 isometric, simply by computing and comparing the portalgons of the associated Delaunay  
 1846 tessellations:

1847   ► **Corollary 60.** *Let  $T$  and  $T'$  be portalgons of less than  $n$  triangles, whose aspect ratios are*  
 1848 *smaller than  $r$ , and whose surfaces  $\mathcal{S}(T)$  and  $\mathcal{S}(T')$  are closed. One can determine whether*  
 1849  *$\mathcal{S}(T)$  and  $\mathcal{S}(T')$  are isometric in  $O(n^3 \log^2(n) \cdot \log^4(r))$  time.*

1850   **Proof.** Theorem 1 computes the portalgons  $\mathcal{T}$  and  $\mathcal{T}'$  of the Delaunay tessellations of  
 1851 respectively  $\mathcal{S}(T)$  and  $\mathcal{S}(T')$  in  $O(n^3 \log^2(n) \cdot \log^4(r))$  time. We claim that we can determine  
 1852 whether  $\mathcal{T}$  and  $\mathcal{T}'$  are equal in  $O(n^2)$  time. The claim immediately implies the corollary.

1853        Let us prove the claim. We consider the sides of the polygons of  $\mathcal{T}$  and  $\mathcal{T}'$ . There are  $O(n)$   
 1854 such sides. Fix a side  $s$  of a polygon of  $\mathcal{T}$ . For every side  $s'$  of a polygon of  $\mathcal{T}'$ , determine in  
 1855  $O(n)$  time whether there exists a one-to-one correspondence  $\varphi$  from the sides of the polygons  
 1856 of  $\mathcal{T}$  to the sides of the polygons of  $\mathcal{T}'$  that maps  $s$  to  $s'$ , the boundary closed walks of the  
 1857 polygons of  $\mathcal{T}$  to the boundary closed walks of the polygons of  $\mathcal{T}'$ , and the matching of  $\mathcal{T}$   
 1858 to the matching of  $\mathcal{T}'$ . If  $\varphi$  exists then  $\varphi$  is unique since  $\mathcal{S}(T)$  and  $\mathcal{S}(T')$  are connected:  
 1859 construct  $\varphi$  in  $O(n)$  time. Then determine in  $O(n)$  time if for every polygon  $P$  of  $\mathcal{T}$  there is  
 1860 an orientation-preserving isometry  $\tau_P : \mathbb{R}^2 \rightarrow \mathbb{R}^2$  such that  $\varphi(s) = \tau_P(s)$  for every side  $s$  of  
 1861  $P$ . In which case return correctly that  $\mathcal{T}$  and  $\mathcal{T}'$  are equal. In the end, if every polygon side  
 1862  $s'$  of  $\mathcal{T}'$  has been looped upon, and if no equality has been found, return correctly that  $\mathcal{T}$   
 1863 and  $\mathcal{T}'$  are distinct. This proves the claim, and the corollary. ◀